

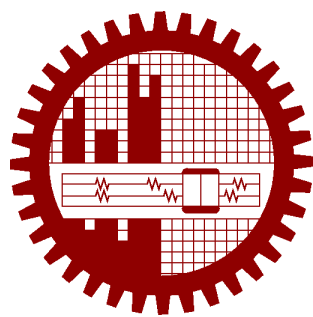
EXPERIMENTAL INVESTIGATION OF HIGH VACUUM DENSIFICATION METHOD

by

Ripon Chandra Malo

1017042229

MASTER OF SCIENCE
IN
CIVIL ENGINEERING (GEOTECHNICAL)



Department of Civil Engineering
Bangladesh University of Engineering and Technology
Dhaka, Bangladesh

January 2023

This thesis titled, “**Experimental Investigation of High Vacuum Densification Method**”, submitted by Ripon Chandra Malo, Roll No.: 1017042229, Session: October 2017, has been accepted as satisfactory in partial fulfillment of the requirement for the degree of MASTER OF SCIENCE in CIVIL ENGINEERING (Geotechnical) on 28th January 2023.

BOARD OF EXAMINERS

Dr. Mehedi Ahmed Ansary Professor Department of Civil Engineering, BUET, Dhaka	Chairman (Supervisor)
Dr. Abu Siddique Head and Professor Department of Civil Engineering, BUET, Dhaka	Member (Ex-Officio)
Dr. Abu Siddique Professor Department of Civil Engineering, BUET, Dhaka	Member
Dr. Jibon Kumar Sarker, PEng Superintending Engineer Bangladesh Water Development Board, Dhaka	Member (External)

Candidate's Declaration

This is to certify that the work presented in this thesis entitled, "Experimental Investigation of High Vacuum Densification Method", is the outcome of the research carried out by Ripon Chandra Malo under the supervision of Dr. Mehedi Ahmed Ansary, Professor, Department of Civil Engineering, Bangladesh University of Engineering and Technology (BUET), Dhaka-1000, Bangladesh.

It is also declared that neither this thesis nor any part thereof has been submitted anywhere else for the award of any degree, diploma, or other qualifications (except for publication) .

Signature of the Candidate

Ripon Chandra Malo

1017042229

Dedication

This thesis is humbly dedicated to my parents, who always give me support and love for inspiring me to accomplish this research. This work is also dedicated to all aspiring students and future researchers.

Acknowledgement

First, I would like to express my sincere gratitude to the Almighty God for his mercy and blessing and for allowing me to complete this research peacefully.

I would like to express my sincere gratitude to my thesis supervisor Dr. Mehedi Ahmed Ansary, Professor, Department of Civil Engineering, BUET; for providing me with excellent guidance and continuous assistance throughout the research. His constant advice, assertions, and appreciation were very vital and irrevocable. Without his motivation, it would not have been possible for me to finish my paper. I am indebted to him for his constant motivation during the study.

I'm writing to impart my gratitude and appreciation to Dr. Sarwar Jahan Md. Yasin, Professor, Department of Civil Engineering, BUET, for his significant time, dynamic direction, and recommendations.

Sincere appreciation goes to the members of my M.Sc. defense committee: Dr. Abu Siddique, Professor and Head of the Department of Civil Engineering, BUET; and Dr. Jiban Kumar Sarker, Superintending Engineer, Bangladesh Water Development Board, Dhaka; for their thoughtful questions, valuable comments, and suggestions.

I would like to acknowledge the grant received from Geoharbour Bangladesh Engineering & Construction Limited, Dhaka, Bangladesh, and the Committee for Advanced Studies and Research (CASR) of BUET, Dhaka.

I am very much grateful to the laboratory assistants and staff of the Geotechnical Engineering Laboratory of the Civil Engineering Department, Bangladesh University of Engineering and Technology, for their cooperation and assistance throughout my research. A special thanks go to Laboratory assistant Pomel Barua who mostly assist me in conducting this research.

Finally, an exceptional debt of deepest gratitude and appreciation is offered to my family members for their continuous support, without which this thesis work would not have come to reality.

Abstract

Bangladesh is a densely populated country with a 32% coastal area. Many coastal regions of Bangladesh have very soft to soft soil with poor geotechnical properties such as very low bearing capacity, high compressibility, great susceptibility to volumetric change, and a very long time of consolidation. Soft soils are categorized as problematic soils, and Geotechnical Engineers have always struggled with Construction on soft soils. In order to use soft soils for engineering applications, it is necessary to treat them first. Construction on problematic soils is possible by applying suitable ground improvement techniques.

High Vacuum Densification Method (HVDM) is an innovative ground improvement technique to treat saturated soft soil in a cost-effective and time-efficient manner. It is based on the combination of the two processes of Vacuum Consolidation and Dynamic Compaction to improve saturated soft cohesive soil. In the HVDM technique, the vacuum helps to generate negative pore pressure, and dynamic compaction helps to generate positive pore pressure in the soil. The negative and positive pore pressure in the soil creates a lateral pressure gradient, and this pressure gradient helps to accelerate the consolidation process.

In this research, an experimental investigation of HVDM was carried out in a physical model. In this model, all associated arrangements of field execution of HVDM were simulated. The experiment was carried out on the collected sample after numerous trials on the physical model. Also, the pore pressure and settlement were measured during the investigation and compared with field results. After the successful execution of the HVDM experiment in the physical model, undisturbed samples were collected by Core Cutter Method for conducting consolidation, Direct shear, Triaxial CD, and UCS test. Also, remoulded samples were made at the same density and moisture content to compare with HVDM-treated samples.

After the successful execution of HVDM, it was found that 94 % compaction was achieved in the physical model. The UCS test shows that the HVDM-treated sample achieved 37 % greater unconfined compressive strength than the remoulded sample. Also, the Triaxial CD test shows that HVDM treated samples have 38 % greater deviator stress and 66 % greater cohesion than the remoulded sample. Comparing Consolidation, Triaxial CD, Direct shear, and UCS test results of HVDM treated with remoulded samples, it is seen that the HVDM treated samples were stiffer and achieved greater strength than remoulded samples. The visual evidence, settlement, and pore pressure curve of the HVDM experiment are proof of rapid consolidation, maximum density, and a remarkable change in the stiffness of HVDM-treated soil.

Finally, it can be concluded that the HVDM is a cost and time-effective ground improvement method. The desired stiffness can be achieved within a short time run of HVDM.

Table of Contents

	Page
Certification	ii
Candidate's Declaration	iii
Dedication	iv
Acknowledgement	v
Abstract	vi
List of Figures	xi
List of Tables	xiv
1 Introduction	1
1.1 General	1
1.2 Objectives with Specific Aims and Possible Outcomes	2
1.3 Thesis Layout	3
2 Literature Review	4
2.1 General	4
2.2 Ground Improvement in Bangladesh	4
2.2.1 Dynamic Compaction	5
2.2.2 Prefabricated Vertical Drains (PVD)	5
2.2.3 Vacuum Consolidation	5
2.2.4 Vibroflotation	6
2.2.5 Stone Columns	6
2.2.6 Lime Stabilization	6
2.2.7 Geosynthetics	6
2.2.8 Deep Cement Mixing (DCM)	7
2.3 Vacuum Consolidation	7
2.3.1 History of Vacuum Consolidation	8
2.3.2 Principles And Mechanism of Vacuum Consolidation	9
2.3.3 Advantages and Disadvantages of Vacuum Consolidation	10
2.3.4 Applications of Vacuum Consolidation	10
2.3.5 Design Parameters of Vacuum Consolidation	11

2.3.6	Parameters Influencing Vertical Drain Behaviour	12
2.3.7	Reviews of Previous Practices on Vacuum Consolidation	12
2.4	Dynamic Compaction	16
2.4.1	History of Dynamic Compaction	17
2.4.2	Suitability	17
2.4.3	Adverse Situations for Dynamic Compaction	18
2.4.4	Design Principles	20
2.4.5	Design Considerations	20
2.4.6	Quality Control and Assurance	23
2.4.7	Reviews of Previous Practices on Dynamic Compaction	24
2.5	High Vacuum Densification Method (HVDM)	26
2.5.1	Mechanisms of Gain in Undrained Strength	26
2.5.2	Working Principles of HVDM	28
2.5.3	Distinguishing Features of HVDM	33
2.5.4	Advantages and Limitations	33
2.5.5	Design Considerations of HVDM	34
2.5.6	Quality Control and Assurance	34
2.5.7	Reviews of Previous Practices on HVDM	34
2.6	Summary	39
3	Field and Laboratory Investigation	40
3.1	General	40
3.2	Site Selection	40
3.3	Reclamation Area	41
3.4	In-situ Investigations	42
3.4.1	Site Characteristics	42
3.4.2	Soil Profile	42
3.4.3	Site Visit and sample collection	44
3.4.4	Disturbed Sample Collection	50
3.5	Laboratory Soil Testing Program	50
3.5.1	Moisture Content test	50
3.5.2	Specific Gravity	51
3.5.3	Index Properties Test	52
3.5.4	Standard Proctor Test	57
3.5.5	Direct Shear Test	58
3.5.6	Unconfined Compressive Strength Test	59
3.5.7	1D Consolidation Test	60
3.5.8	Triaxial Compression Test	61
3.6	Summary	63

4 Experimental Investigation Program	64
4.1 General	64
4.2 Physical Model	64
4.2.1 Model Type	65
4.2.2 Scale Factor	66
4.3 Physical Model Design and Implementation	67
4.3.1 Planning Of 1g Physical Model	67
4.3.2 Test Facility	68
4.3.3 Equipment and Materials	70
4.4 Methodology of Experimental Investigation	79
4.4.1 Trial on Physical Model	79
4.4.2 Procedure of The Experiment	82
4.5 Data Processing with Python	91
4.6 Summary	93
5 Results and Discussion	94
5.1 General	94
5.2 Soil Index Properties	94
5.3 HVDM Investigation Result	96
5.3.1 Visual Witness of HVDM Treated Soil Improvement	96
5.3.2 Evaluation of Settlement and Comparison with Field Data	98
5.3.3 Evaluation of Excess Pore Pressure and Comparison with Field Result	100
5.4 Compaction Percentage Evaluation	101
5.5 Evaluation and Comparison of Shear Strength Properties	102
5.5.1 Evaluation of Shear Strength Properties from Direct Shear Test on HVDM Treated Sample	103
5.5.2 Evaluation and Comparison of Shear Strength Properties from Unconfined Compression Test (UCS) Test on Remoulded and HVDM Treated Sample	104
5.5.3 Evaluation and Comparison of Shear Strength Properties from Triaxial CD Test on Remoulded and HVDM Treated Sample	111
5.6 Evaluation and Comparison of Consolidation Characteristics from 1D Consolidation Test on Remoulded and HVDM Treated Sample	130
6 Conclusions and Recommendation	136
6.1 General	136
6.2 Conclusions	136
6.3 Recommendations for Future Study	137
References	138

List of Figures

FIGURE	Page
2.1 Typical setup of vacuum consolidation method	8
2.2 Principle of Menard Vacuum Method	9
2.3 Loading history and Consolidation settlements result	14
2.4 Results of CPT test before and after vacuum consolidation	15
2.5 Schematic of dynamic compaction	16
2.6 Grouping of soils for dynamic compaction	18
2.7 Schematics of HVDM method	26
2.8 e-log p plot under many times of dynamic impact and vacuum Consolidation	27
2.9 Working Principles of HVDM method	28
2.10 In-situ vacuum pipe arrangement	30
2.11 Vacuum drainage system layout	30
2.12 Vacuum pump in research site	31
2.13 Dynamic compaction Procedure	32
2.14 CPT cone resistance readings between before and after ground improvement	36
2.15 Soil profile of the Ji-hong's research location	37
2.16 CPT and SPT test results between before and after soil improvement	38
3.1 Research site location	40
3.2 Autocad drawing of study area	41
3.3 Field Borelog of HA16 for the research site	43
3.4 Filling work on the research site	44
3.5 Installation process of PVD at the research site	46
3.6 Vacuum Pipe Arrangement in the site	47
3.7 Vacuum arrangement in the site	48
3.8 Dynamic compaction process at the research site	49
3.9 Air drying and pulverization process of collected disturbed sample	50
3.10 Some steps of Specific Gravity Test	51
3.11 Some steps of mechanical sieve analysis test	53
3.12 Some steps of Hydrometer analysis test	54
3.13 Conducting Falling head Permeability test	55
3.14 Conducting Relative Density test	56
3.15 Executing Standard Proctor test	58
3.16 Executing Direct Shear Test	59
3.17 Executing Unconfined Compressive Strength test	60

3.18 Conducting consolidation test-(a) Consolidation test setup and (b) Taking dial reading	60
3.19 Some steps of Triaxial CD test	63
4.1 Beam geotechnical centrifuge in University of California	65
4.2 1g physical model of shaking table	66
4.3 Cork sheet dummy model idea	68
4.4 Schematic view of the experimental setup of 1g physical model	69
4.5 Side view of Physical model	71
4.6 Side view of Physical model along its width	72
4.7 Top View of Physical Model	73
4.8 Dynamic compaction arrangement	74
4.9 Vacuum pipe arrangement	75
4.10 Vacuum pump	76
4.11 Vacuum sealing system	76
4.12 Water Level Monitoring System	77
4.13 Vertical Displacement Measuring setup	78
4.14 Data Acquisition System	79
4.15 Trial-1 experiment with dummy sample	80
4.16 Trial-2 experiment with dummy sample	81
4.17 Checking process in Trial-3	82
4.18 Sample preparation arrangement	84
4.19 Dynamic compaction arrangement-(a) Compaction Location	87
4.20 After 2nd cycle of dynamic compaction	87
4.21 Execution of Field Density Test after levelling of the treated sample in the physical model	88
4.22 Undisturbed sample collection locations from the physical model	90
4.23 HVDM Treated UD samples Collection	91
5.1 Particle size distribution curve of representative sample	95
5.2 Visual proof of soft soil before execution of HVDM	97
5.3 Visual improvement of soft to stiff soil	98
5.4 Time vs recorded settlement of the experiment	99
5.5 Time vs settlement of the research site	99
5.6 Time vs excess pore pressure of the experiment	100
5.7 Time vs excess pore pressure of the research site	101
5.8 Relationship between dry density and moisture content of representative soil	102
5.9 Direct shear Consolidated Drained Test result	104
5.10 Some Strain vs Stress curve and Mohr circle of HVDM treated sample . . .	108
5.11 Combined Mohr circles of HVDM treated samples	108

5.12 Combined Stress vs Strain Relationship of HVDM treated samples	109
5.13 Comparative strain vs stress curve of HVDM treated and remoulded samples	111
5.14 Time Vs. B-Value relationship in saturation stage	112
5.15 Time vs back volume relationship in Consolidation stage for HVDM treated and remoulded sample	115
5.16 Time vs. cell volume relationship in consolidation stage for HVDM treated and remolded sample	118
5.17 Time vs. pore pressure relationship in consolidation stage for HVDM treated and remolded sample	121
5.18 Axial strain vs. back volume change relationship of the shear stage of remolded and HVDM-treated samples	123
5.19 Axial strain vs. deviator stress relationship in the shear stage of HVDM treated and remolded samples	124
5.20 Mohr circle obtained from the drained triaxial test results of HVDM treated and remoulded sample	125
5.21 Evaluation of Young's modulus from strain vs. stress curve of HVDM treated samples	127
5.22 Evaluation of Young's modulus from strain vs. stress curve of remoulded samples	129
5.23 Illustration of the comparative result of Confining pressure vs Young's modulus	130
5.24 e vs log p curve for HVDM treated and remoulded sample	131
5.25 Evaluation of preconsolidation pressure from e vs log p curve-(a) HVDM Treated Sample and (b) Remoulded Sample	132
5.26 Time vs vertical displacement curves of entire consolidation test duration for both sample	133
5.27 e vs P curves for HVDM treated and remoulded sample	134
5.28 Comparison of C_v values from Taylor's T_{90} method for HVDM treated and remoulded samples.	135
A.1 Square-root of time vs Dial reading plot for both HVDM treated and remoulded sample	147

List of Tables

TABLE	Page
2.1 Soil suitability based on permeability	17
2.2 Suitability of Dynamic Compaction with soil type along with Degree of Saturation (After Martin Larisch and Tim Pervan)	19
2.3 Adverse condition with possible difficulties	19
2.4 n_c value depend on different soil types	22
3.1 Reclamation areas of research site	41
4.1 Scaling factors in physical model testing	67
5.1 Summary of grain size analysis result	94
5.2 Summary of permeability test result	95
5.3 Summary of UCS test result	105
5.4 General Relationship of Consistency and Unconfined Compression Strength of Cohesive Soil	105
5.5 Summary of peak deviator stress at maximum axial strain for both remoulded and HVDM-treated samples.	123
5.6 Triaxial test result summary	125
5.7 Summary of the evaluated result of Young's modulus and Secant modulus .	129
5.8 Summary of consolidation test results of HVDM treated and remoulded sample	133
5.9 Summary of comparative results of Coefficient of Consolidation of HVDM treated and remoulded sample	135

List of Abbreviations and Notations

Abbreviations

ASTM	American Society for Testing and Materials
CD	Consolidated Drained
CPT	Cone Penetration Test
EPWP	Excess Pore Water Pressure
HEDC	High Energy Dynamic Compaction
HVDM	High Vacuum Densification Method
PI	Plasticity Index
PL	Plastic Limit
PMT	Pressuremeter Test
PVC	Polyvinyl Chloride
PVD	Prefabricated Vertical Drains
SL	Shrinkage Limit
SPT	Standard Penetration Test
UCS	Unconfirmed Compressive Strength

Notations

C_v	Coefficient of Consolidation
a_v	Coefficient of Compressibility
C_c	Compression Index
m_v	Coefficient of Volume Compressibility
C_r	Recompression Index
k	Coefficient of Permeability
e_0	Initial Void Ratio
e_f	Final Void Ratio
E_{50}	Young's Modulus
E_{100}	Secant Modulus
ϕ°	Angle of Internal Friction
C	Cohesion
S_u	Undrained Shear Strength
q_u	Unconfined Compression Strength
D_{10}	Effective Grain Size
C_u	Coefficient of Uniformity

Chapter 1

Introduction

1.1 General

The availability of suitable land has decreased due to the rapid urbanization, population growth, numerous infrastructure expansions, and the ever-increasing economic activities in the developed countries such as Bangladesh. In order to find suitable land for Construction, reclaiming land from the coastal area has often been the preferred solution. Bangladesh is a densely populated country with a 32% coastal area (Islam and Ahmad, 2004). Many coastal areas in Bangladesh have very soft to soft soil with poor geotechnical properties such as very low bearing capacity, high compressibility, great susceptibility to volumetric change, and a very long time of consolidation. Soft soils are categorized as problematic soils, and Geotechnical Engineers have always struggled with Construction on soft soils. In order to use soft soils for engineering applications, it is necessary to treat them first. Construction on problematic soils is possible by applying suitable ground improvement techniques.

Ground improvement is the most imaginative field of geotechnical engineering. Ground improvement helps to modify the soil in the foundation by changing the soil characteristics (density, swelling, shear strength, shrinkage characteristics, bearing capacity, etc.) to allow the utilization of sites with poor subsurface conditions. It not only saves construction cost but also reduce implementation time. Several techniques are available for improving the mechanical and engineering properties of soft soils. The widely used current improvement techniques are sand drains, PVD, granular piles, deep mixing method, rammed aggregate piers, reinforced soil foundations, Dynamic compaction, HVDM, etc. Among them, HVDM is one of the best salutatory soft soil improvement methods.

High Vacuum Densification Method (HVDM) is an innovative ground improvement technique to treat the saturated soft soil in a cost-effective and time-efficient manner (Yin et al., 2013). HVDM is based on the combination of the two processes of Vacuum Consolidation and Dynamic Compaction to improve saturated soft cohesive soil. One of the earliest experiments with high vacuum density methods began in 2000 when the Shanghai Geoharbour Group first began trying out the notion of the High Vacuum Densification Method and applying it on big-scale projects around Shanghai (Liang and Xu, 2012). After being implemented in the Shanghai area with great success, HVDM has been expanded to other parts of China

Chapter 1. Introduction

as well as other parts of the Asian continent, such as Bangladesh, Malaysia, and Vietnam. HVDM is a technique for compacting soil to its maximum dry density or the most densified state (Chang et al., 2010). In HVDM technique, the vacuum helps to generate negative pore pressure and dynamic compaction helps to generate positive pore pressure in the soil. The negative and positive pore pressure in the soil creates a lateral pressure gradient. Because of this pressure gradient, it is possible to achieve both consolidation and densification effects, resulting in a decrease in water content while simultaneously increasing the density of the soil. The High Vacuum Densification Method is considered as a green technology due to no sign of chemical additives uses.

This research is aimed to investigate the HVDM in a 1g physical model at laboratory. Physical modeling in geotechnical engineering refers to the representation of a real-life geotechnical system or structure using a physical model. The aim of physical modeling is to study the behavior of the real-life system under various conditions and understand the physical processes involved. The physical model is usually a smaller-scale replica of the actual system, constructed using materials that closely resemble the properties of the real-life system. A 1g model refers to a physical model that operates under normal gravity (1g), which is equal to 9.8 m/s^2 . This is in contrast to a centrifuge model, where the model is spun to produce high gravity and simulate the effects of high gravitational loads. The advantage of a 1g model is that it can be easily observed and measured, and the behavior of the model can be directly compared to the real-life system.

1.2 Objectives with Specific Aims and Possible Outcomes

The main objectives of this research are as follows:

- i) To develop a 1g physical model to simulate High Vacuum Densification Method in small scale at laboratory.
- ii) To simulate the vacuum consolidation and dynamic compaction at laboratory.
- iii) To measure the vacuum applied settlement and excess pore pressure from the physical model.
- iv) To compare and evaluate the shear strength properties of HVDM Treated sample and remoulded sample from different shear strength tests of soil (Triaxial, UCS, Direct shear).
- v) To compare and evaluate the consolidation properties of HVDM Treated sample and remoulded sample.
- vi) To compare the experimental results obtained from the physical model with field HVDM investigation results.

1.3 Thesis Layout

This thesis is comprised of six chapters. A brief outline of the material covered in each chapter is summarized below,

Chapter One gives an overview of the whole research work. It includes the background, objectives of this research.

Chapter Two has been devoted to the review of past researches. This chapter starts with a brief introduction of the High Vacuum Densification Method (HVDM). As HVDM is based on the combination of the two ground improvement method named Vacuum Consolidation and Dynamic Compaction. this chapter describes the mechanism, applications, design parameters, and review of past researches on Vacuum Consolidation, Dynamic Compaction, and HVDM respectively.

Chapter Three is dedicated to the field and laboratory investigation programs. In this chapter, selected study areas have been presented with the geological conditions. This chapter includes field visits, In-situ HVDM procedure investigation, sample collection, and laboratory test program.

The experimental program of HVDM in the physical model has been presented in Chapter Four. In this chapter physical model design, scaling, trial on the model, sample preparation, experiment procedures, Undisturbed sample collection, and big data processing with python are described.

Chapter Five presents the experimental results of the HVDM investigation and Laboratory test results of HVDM treated and remoulded sample. Also, some comparisons are presented to verify the work efficiency of the High Vacuum Densification Method.

Chapter Six presents the conclusion chapter where the summary of the research findings has been provided. It also includes recommendations for further study.

Chapter 2

Literature Review

2.1 General

High Vacuum Densification Method is a green ground improvement method due to no sign of chemical additives used in the soil. The present study is aimed to investigate High Vacuum Densification Method on Laboratory. In this chapter, The application of ground improvement techniques in Bangladesh will be reviewed and the review of the literature regarding previous studies on the High Vacuum Densification Method will be presented also.

2.2 Ground Improvement in Bangladesh

Bangladesh is the largest delta of world receiving sediments from three rivers, namely, the Padma, the Meghna, the Jamuna, and numerous tributaries. Based on surficial geology, Bangladesh may be split up into a number of landform patterns that have evolved under relatively uniform geological and climate conditions with similar topographic features. The raised alluvial terrace deposits and the recent deposits constitute more than 80% land of Bangladesh. Soft soils in Bangladesh are mainly available in the alluvial flood plain deposits, depression deposits and estuarine and tidal plain deposits (Siddique et al., 2002). The soft soil, mainly comprise underconsolidated to normally consolidated clays and silts often containing organic. The principal foundation problems in Bangladesh are related to the low shearing resistance and settlement of underlying soil. In Bangladesh, ground improvement techniques have become increasingly important due to the country's geotechnical challenges, including soil liquefaction, settlement, and instability. In recent years, a number of new and innovative ground improvement techniques have been developed and tested in Bangladesh. These techniques are designed to improve the foundation conditions and stability of construction sites, and are being used with increasing frequency in the country. Methods and applications of ground improvement techniques in Bangladesh have been summarised by Ansary and Doulah (1993). Typical methods used to increase the bearing capacity of soft soils of Bangladesh include preloading (or precompression) and vertical drainage in conjunction with precompression. Loading berms, or pressure berms, are being used as counter weights to increase the stability of road and railway embankments in Bangladesh. Fabric reinforced soil, where woven or non-woven fibre materials are placed in road and railway embankments

to improve their overall stability. Vertical drainage methods using three types of drains, namely, sand drain, wick drain, prefabricated vertical drain, dynamic compaction, admixture stabilization, stone columns and electroosmosis are being used. Some of the most recent practices on ground improvement techniques in Bangladesh are described in the following sections,

2.2.1 Dynamic Compaction

Dynamic compaction is a technique in which heavy weights are repeatedly dropped from a height to compact the soil. This method is particularly useful for improving the strength and stability of loose and granular soils, such as sand and gravel. In Bangladesh, dynamic compaction has been used to improve the foundation conditions of construction sites and has been found to be effective in increasing the bearing capacity and stability of the soil as well decrease the potential of liquefaction (Hore and Ansary, 2020).

2.2.2 Prefabricated Vertical Drains (PVD)

Prefabricated Vertical Drains (PVD) are perforated tubes that are inserted into the soil to improve its compressibility and reduce the settlement of construction sites. PVDs work by allowing water to drain from the soil, reducing the effective stress and allowing the soil to compress more easily. A book chapter on Ground Improvement Using Prefabricated Vertical Drains with Preloading was written by Siddique et al. (2023) in Practices and Trends in Ground Improvement Techniques book edited by Hazarika, Hemanta and Nakazawa, Juichi and Nakahara, Iwao based on prospective application of PVDs in Bangladesh. In Bangladesh, PVDs have been used in the construction of buildings, bridges, and other structures to improve the foundation conditions and reduce settlement. From Siddique et al. (2002) and Dhar et al. (2011) researches, it has found that the PVDs can be effective in reducing settlement and improving the stability of the soil.

2.2.3 Vacuum Consolidation

Vacuum Consolidation is a ground improvement technique that involves applying vacuum pressure to the soil to improve its compressibility and reduce the settlement of construction sites. Vacuum consolidation works by reducing the pore water pressure in the soil, allowing the soil to compact more easily and reducing the risk of settlement. This technique has been applied in Bangladesh in recent years to improve the soil conditions and reduce settlement in construction sites. Research has shown that vacuum consolidation can be effective in

reducing settlement and improving the stability of the soil (Chakraborty et al., 2018).

2.2.4 Vibroflotation

Vibroflotation is a ground improvement technique that involves the insertion of a long and thin probe into the soil and the application of high-frequency vibrations. The vibroflotation method for treating foundations will rearrange the soil particles, quickly release extra void water pressure, and create a drainage channel in the gravel pile, all of which significantly increase the foundation's resistance to liquefaction. The magnitude 6.2 earthquake that occurred during the building phase brought attention to the vibroflotation-treated foundation's ability to resist liquefaction. Vibroflotation has been used successfully in Bangladesh such as Karnaphuli river tunnel project , Chattagram .

2.2.5 Stone Columns

Stone columns are cylindrical columns of compacted stones that are placed in the soil to improve its strength and stability. This technique is particularly useful for improving the foundation conditions of soft, compressible soils. In Bangladesh, stone columns have been used in the construction of bridges and other infrastructure projects and have been found to be effective in increasing the bearing capacity of the soil (Jan E Alam et al., 2018).

2.2.6 Lime Stabilization

Lime stabilization is a ground improvement technique that involves adding lime to the soil to improve its physical and engineering properties. Lime reacts with the soil to increase its strength, stability, and compressibility, making it more suitable for construction. Lime stabilization has been used in Bangladesh to improve the foundation conditions of construction sites and has been found to be effective in increasing the strength and stability of the soil (Ansary et al., 2003).

2.2.7 Geosynthetics

Geosynthetics are synthetic materials that are used in ground improvement to reinforce the soil and improve its properties. In Bangladesh, geosynthetics have been used in the construction of retaining walls, embankments, and other structures to improve the stability and strength of the soil (Alam and Kabir, 2000).

2.2.8 Deep Cement Mixing (DCM)

Deep Cement Mixing (DCM) is a ground improvement technique that involves mixing cement with the soil to improve its physical and engineering properties. DCM works by increasing the strength and stability of the soil, making it more suitable for construction. In Bangladesh, DCM has been used in the construction of buildings, bridges, and other structures to improve the foundation conditions and increase the strength and stiffness of soft soil. Research has shown that DCM can be effective in increasing the strength and stiffness of soft soil, reducing settlement, and improving the foundation conditions of construction sites (Rahman et al., 2011).

High vacuum densification method (HVDM) is a new technique for soil improvement that has recently been applied in Bangladesh with great success. This method is particularly useful for soft soil improvement projects and recently used in the construction of the 700-megawatt coal-fired power station in Barishal, Bangladesh which is the study area of this research. As The HVDM is based on the combination of the two ground improvement methods named Vacuum Consolidation and Dynamic Compaction, the following sections describe the mechanism, applications, design parameters, and review of past research on Vacuum Consolidation, Dynamic Compaction, and HVDM, respectively.

2.3 Vacuum Consolidation

Vacuum Consolidation is a ground improvement technique, that accelerates the ground settling by decreasing the air pressure at the earth's surface. A vacuum is supplied to a soil mass, and this decreases the water pressure in the soil mass. In other words, when the overall stress stays the same, the pore pressure decreases, which means effective stress increases in the soil and consolidation. The main concept of vacuum consolidation involves raising effective stress without affecting total stress by applying a negative vacuum pressure into an isolated soil mass.

A diagram of the vacuum consolidation method is shown in Figure 2.1. Theoretically, the highest possible vacuum pressure may be in the range of 100 kPa, although physically possible values are usually found between 60 and 80 kPa when the needed preloading pressure is greater than roughly 60 to 80 kPa, using a vacuum pressure alone will be not enough (Tang and Shang, 2000). It is possible to use a combined vacuum and surcharge fill when a surcharge load greater than 80 kPa is necessary. When treating extremely soft ground, the vacuum preloading method is more efficient than the surcharge fill method because, at a pressure of 80 kPa (kiloPascals), the vacuum may be applied instantly without generating an issue with the stability of the ground. Additionally, the vacuum preloading technique is

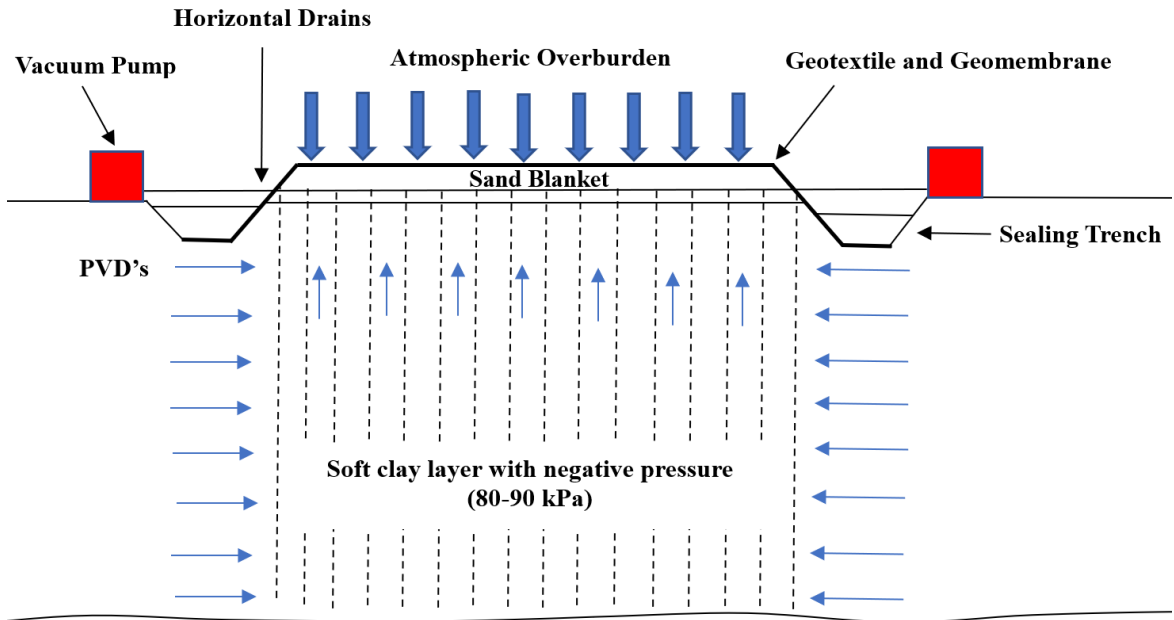


Figure 2.1: Typical setup of vacuum consolidation method (after Koirala et al., 2022)

less expensive than the surcharge fill method for a comparable load (Chu et al., 2000). Also, vacuum-induced consolidation has been shown to enhance the shear strength of soft soils by two to three times, according to several researchers.

2.3.1 History of Vacuum Consolidation

Vacuum Consolidation method was first introduced by Kjellman in 1952. Also, he was the inventor of the pre-fabricated vertical drain. Kjellman proposed the use of vacuum pressure as a surcharge for consolidating soft cohesive soil. Later, this became a method of soft soil improvement employed by the Royal Swedish Geotechnical Institute. The U.S. Army Corps of Engineers has designed the possibility of vacuum consolidation in dredging disposal areas with a view to increasing storage capacity in the 1970s (Johnson, 1977). There have been extensive experimental studies and field trials in China on the vacuum consolidation method since the early 1980s, with work as planned back in the 1960s. It was used in a total of 31 projects (with an aggregated land area of 1.6 million square meters) in the Port of Tianjin alone between 1982 and 1996, primarily for improving foundation soils in warehouses, docking facilities, and storage yards. It was also used in about 20 projects in other parts of China during the same period (mostly in the provinces of Jiangsu and Hebei) (Liu, 1996). Instead of being restricted to port structures, vacuum consolidation has been used since 1996 to improve the foundation of seawalls, airport runways, and expressways, as well as the improvement of the foundation of bridges. More than 2 million m^2 of Chinese land had been treated with the vacuum method by 1996, according to Liu (1996) research. Furthermore,

China has extensively applied the method to a large number of ground improvement projects in other countries. Also, Several field trials conducted in USA (Jacob et al., 1994), France (Cognon, 1991), and Japan (Shinsha, 1991) confirmed the efficiency of vacuum-applied consolidation in combination with Prefabricated Vertical Drains (PVDs) /Wick Drains for soil improvement. In the years thereafter, this technique has emerged as one of the most popular and commonly used methods for dealing with very soft soil deposits.

2.3.2 Principles And Mechanism of Vacuum Consolidation

There is already a significant amount of research in this area, some of which may be found in the literature e.g., Chu et al. (2000); Holtz and Wager (1975); Kjellman (1952) and Indraratna et al. (2004).

Basically, a vacuum consolidation system comprises the following steps:

Drainage system: The drainage system's purpose is to create a pathway for the distribution of vacuum pressure and water movement.

Sealing system: Slurry wall, Geomembrane, and the soft soil itself comprise the sealing system. The sealing mechanism aids in preventing water and air leakage beneath it.

Vacuum pumps: Vacuum pressure generated by vacuum pumps seeps into soils via drainage systems, sucking water out and speeding up the consolidation of the soil.



Figure 2.2: Principle of Menard Vacuum Method (source Menard Vacuum™)

2.3.3 Advantages and Disadvantages of Vacuum Consolidation

Compared to other methods of ground improvement method, Vacuum Consolidation has many advantages as well as some limitations. The advantages of vacuum consolidation are as follows,

- Vacuum Consolidation method helps to speed up the consolidation process.
- It helps to improve the bearing capacity of soil up to 100%.
- Vacuum Consolidation is an environmentally friendly and Green Technology due to no sign of using chemicals or toxic materials.
- For Vacuum Consolidation no stability problem is anticipated.
- The construction period is shorter compared to other methods.
- It does not require any type of fill materials.
- No need for heavy machinery in this method.
- The isotropic condition of Vacuum Consolidation increases the effective stress of soil.
- Due to the inward direction of lateral displacement, there is no risk of shear failure.

The limitations of vacuum consolidation are as follows,

- Vacuum consolidation method costs relatively more than other traditional methods.
- Maintenance and quality control in this method is highly required.
- It is not suitable for deep soft soil improvement.

2.3.4 Applications of Vacuum Consolidation

Vacuum Consolidation has been commonly used in the following areas:

- Construction of embankments and railways
- Construction of runways and airports
- Treating for soft deposits
- Dredging and land reclamation
- Storage tanks
- Buildings
- Mining

2.3.5 Design Parameters of Vacuum Consolidation

Design parameters are highly reliant on the characteristics of the site, such as soil and drainage features, as well as the amount of vacuum and drainage used in the project. Dam et al. (2006) explained design parameters as,

2.3.5.1 Treatment area

The total treatment surface is separated into blocks to be sealed for each vacuum treatment depending on their size. By Dam et al. (2006), the standard size of blocks in China normally varies at $6,000\text{-}10,000\text{ m}^2$ and the standardization of a single vacuum pump is $1,000\text{-}1,500\text{m}^2$. The typical dimension for a Menard vacuum pumping system in Menard design is $5000\text{-}7000\text{m}^2$.

2.3.5.2 Drain spacing

The horizontal coefficient of consolidation of the treated soil and the computational time should be used to determine the vertical drain spacing. In addition, optimal spacing should be chosen based on how long it takes and how much it costs. The PVD spacing depends on the design parameters and different practice methods, such as, for Menard practice, it commonly used 1-1.8m; In Japan, the PVD spacing should not be larger than 1.2m, as well as in China it used 1.2-1.3m and sometimes 0.5-0.85m in cases of restricted time.

2.3.5.3 Effective depth

The treatment depth depends on the soil profiles and the required improvement depth of the soil. The adequate depth for most projects is about 20-30m.

2.3.5.4 Effective vacuum pressure

Menard vacuum systems are designed to have a vacuum pressure of 75 kPa, although China has an 80 kPa value. In addition, a minimum vacuum pressure of 60 kPa was previously recommended for design in Japan.

2.3.5.5 Consolidation degree and vacuum pumping duration

From Terzaghi's 1-D consolidation theory and based on the final settlement, the duration of vacuum pumping is determined. The vacuum loading time is varied around 3-5 months for most vacuum consolidations with or without surcharge.

2.3.6 Parameters Influencing Vertical Drain Behaviour

Indraratna et al. (2007) explained factors affecting vertical drain efficiencies are

- Vertical drain equivalent diameter
- Apparent opening size of drain
- Discharge capacity
- Smear zone
- Drain unsaturation

2.3.7 Reviews of Previous Practices on Vacuum Consolidation

The following case studies were found in the literature of vacuum consolidation,

Menard Vacuum Consolidation (1989) described Vacuum Consolidation is a ground improvement method developed by Menard Sol-Traitment, a French firm with overseas subsidiaries in the United States, Europe, and Asia. MVC was introduced in 1989 and has since garnered extensive expertise in designing and constructing various structures. In this research, a case study was discussed on Kimhae Sewage Treatment Plant in South Korea. The project for the Kimhae Sewage Treatment Plant in South Korea was the worldwide record of a successful vacuum consolidation project with the highest-ever depth and load. In this study surrounded by 25-43m of extremely compressible marine clay, the sewage treatment plant covered an area of $83,580 m^2$. The average settlement across the entire area of 4.5m has been achieved successfully after nine months of sustaining 70 kPa vacuum pressure in conjunction with multi-stage surcharge embankment up to 6.5-15.5m. After 20 months of soil improvement, the plant was able to begin full operation with no evidence of residual settlement.

Sandiford et al. (1996) conducted a study to determine the feasibility of employing Vacuum Consolidation to increase the dewatering of dredging material in order to increase the capacity of a sub-aqueous Confined Disposal Facility (CDF) in the New York and New Jersey metropolitan areas. The settlement of 8.2m induces an increase of $855,000 m^3$ in CDF capacity with vacuum application throughout 2 years. Finally, this research concluded

Chapter 2. Literature Review

that compared to the other technique, vacuum consolidation offers the largest capacity at the lowest possible cost.

Shang et al. (1998) studied the construction of the East Pier of Xingang Port of Tianjin project, which was carried out by the First Navigational Engineering Bureau of China, is the world's largest vacuum consolidation treatment on reclaimed land, covering a total area of 480,000 m^2 and being built on soft clay that is 20 meters thick as described in this research. For the purpose of performing vacuum consolidation on a per-block basis, the treatment area was divided into 70 blocks, each covering 5,000-30,000 m^2 . For the treatment, 4m of soft hydraulic fill is used to cover highly compressible peat and organic clays that extend to a depth of 20m beneath the surface. After 135-175 days of pumping, a total settlement of 1.6-2.3m was achieved using a vacuum consolidation system with PVDs that provided a vacuum pressure efficiency of 70% near the ground surface. This research summarized that the soil strength was increased by up to 1700-2300 percent at the ground and by 30-40 percent at the lowest part of the treated zone, depending on the treatment method.

Tang and Shang (2000) described a case study on the applications of vacuum consolidation at Yaoqiang Airport, China. The project began on June 9, 1990, and ended on August 14, 1991. The total treatment area was 145000 m^2 , including the entire runway and a portion of the road leading to the boarding area. It took over 1000 km to install all 86 970 PVDs in the grid, and each PVD was placed 12 meters deep in a 1.3 m square grid. In the treatment, cut-off walls were excavated to a depth of 1.5 meters, filled with silty sand, and compacted to a degree of 95% compaction. It took 80-90 days to achieve the targeted level of consolidation under the design preloading pressure, with soil settlements ranging from 20 to 30 centimeters.

On very soft ground with unevenly thick clay and peat layers near the Monou Interchange of the Sanriku Motorway, a 12.5-meter experimental embankment with a surface area of 3750 m^2 was built as part of that project on that project (Tohoku, Japan 2003). A 30-day soil improvement could allow for an earlier start to the embankment and also shorten the time required for vacuum maintenance following the construction of the embankment. The 12.5m high embankment was successfully built with 109 days of vacuum support and 33 additional days of maintenance until all excess pore water pressure had dissipated. The combined vacuum and embankment loading resulted in 302 cm total settlement in the embankment's center.

Chu et al. (2008) conducted an investigation of a combined vacuum and surcharge load through PVD in a storage yard at Tianjin Port, China, which was carried out with the aid of finite element analysis. To enhance the soft ground conditions and minimize any instability hazards, 80 kPa vacuum pressure and 40 kPa fill surcharge were used. Since the average excess pore pressure was negative (suction), all possible undrained failures were avoided. The difference in measured and expected lateral movements at the embankment's toe after

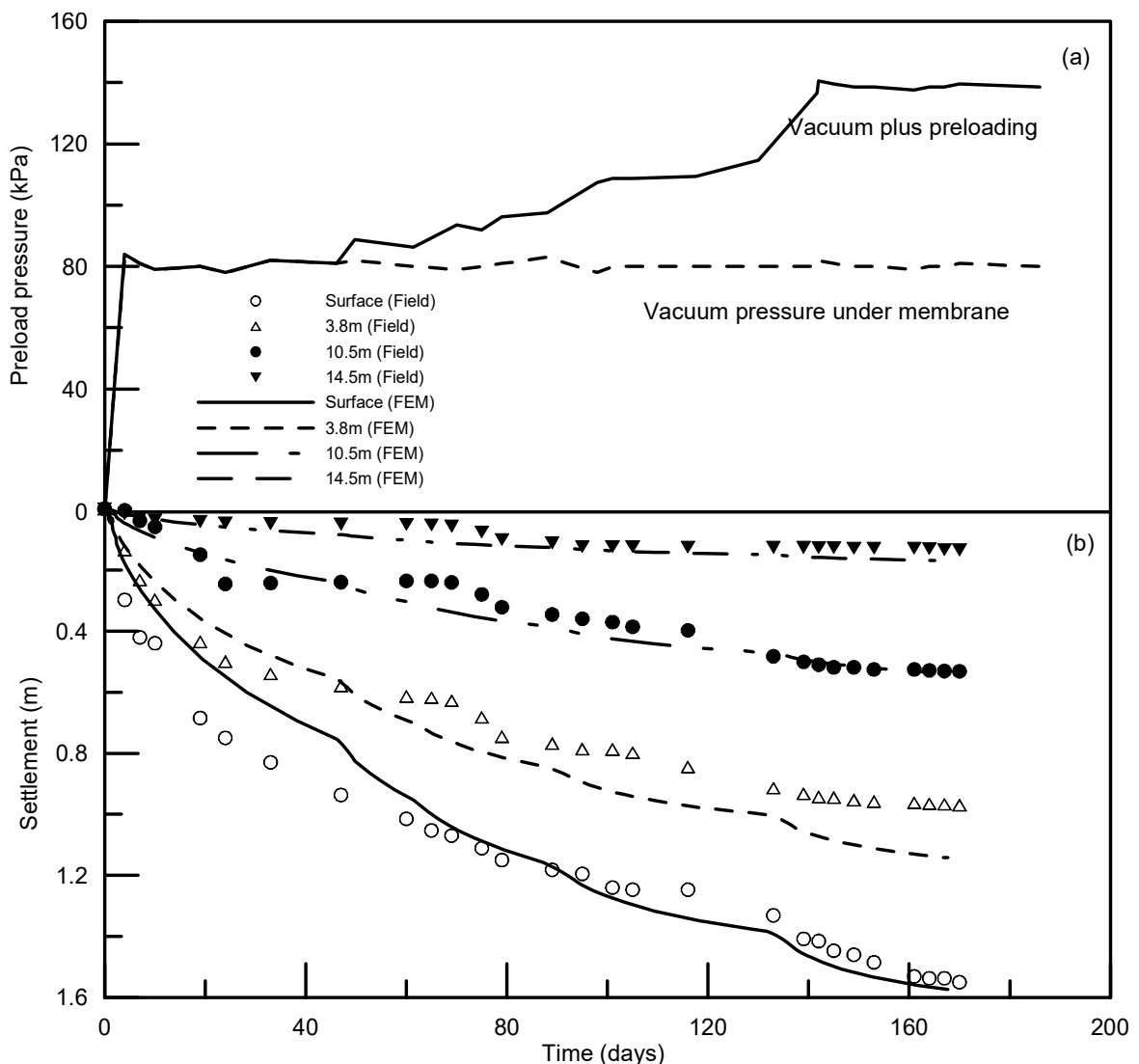


Figure 2.3: a) Loading history and (b) Consolidation settlements result of research site (after Chu et al., 2008)

180 days showed in Figure 2.3. The authors concluded that vacuum consolidation can be considered as a way to reduce lateral outward soil yield and boost the stability of soft clay foundations.

Berthier et al. (2009) conducted a study to test the feasibility of deep soft ground consolidation using the vacuum method along the site border, where any instability would have a severe influence on the nearby Marine Park, the Port of Brisbane Corporation. A difficult set of ground conditions was created by the presence of up to 7m of dredged mud reclamation underlying paleochannels of soft clay that were up to 25m thick. The in-situ compressible clay was even deeper, reaching up to 30m in thickness. The reclamation is being carried out with the assistance of channel maintenance and berth dredging materials, resulting in the deposit of 79 meters of mud on the original seabed and its capitulation with sand. The vacuum method can be combined with a conventional surcharge placed on top of the membrane, in order to

achieve the required degree of consolidation under a given design load and within the allowed time frame. As part of the optimized design, vertical transmission pipes (Menard MCD34, diameter 34mm) were used to transmit the preload (1.2m square grid) and to transmit the sand surcharge (2.2m above vacuum membrane) for 9 months. The ensuing 77 percent degree of condensation was achieved.

Kumar G. et al. (2015) conducted a field trial of vacuum consolidation at the Kakinada port in Andhra Pradesh, India. In this study, a conventional surcharge loading and vacuum pressure were applied to an area of $100 m^2$.

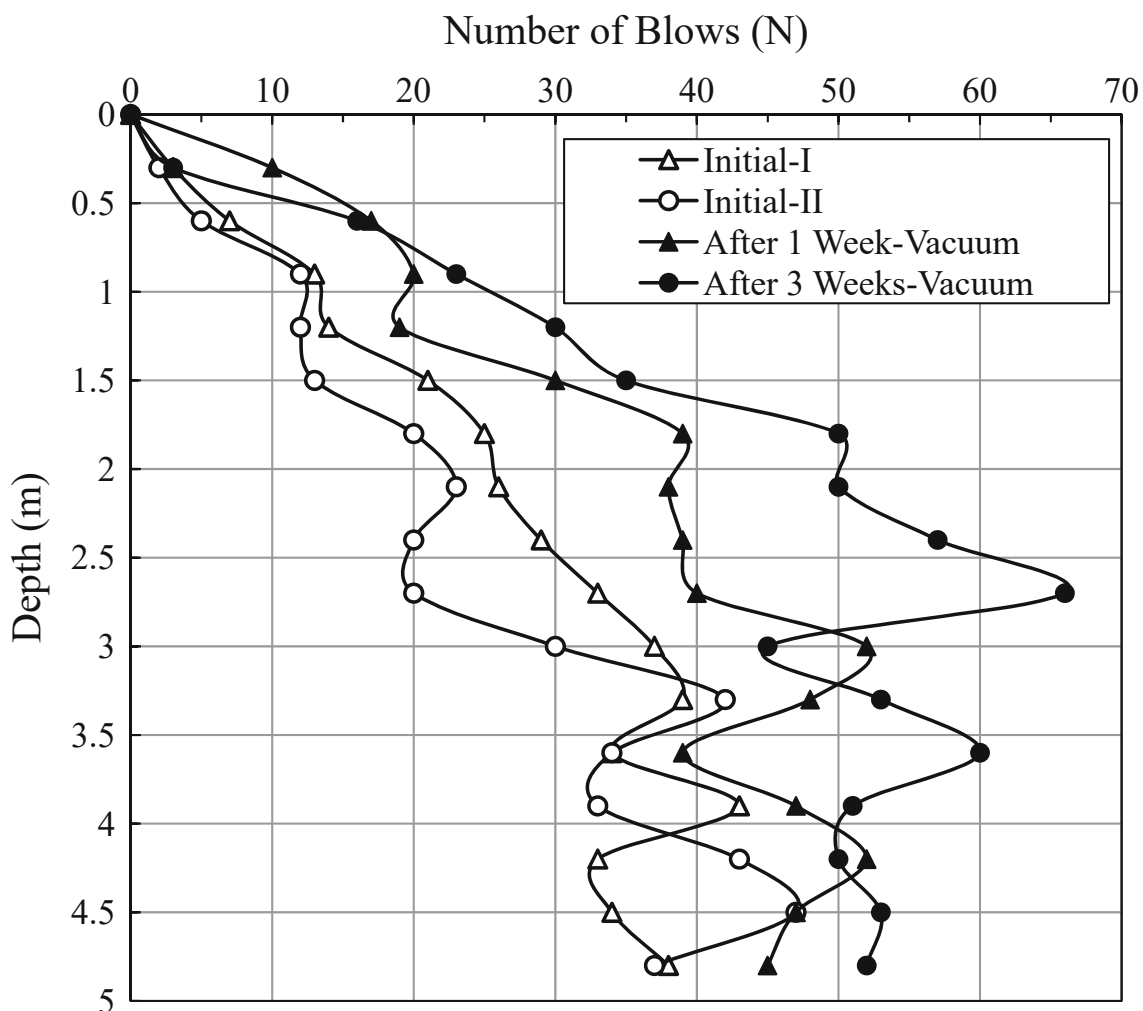


Figure 2.4: Results of CPT test before and after vacuum consolidation (after Kumar G. et al., 2015)

Under a surcharge pressure of 20.9 kPa, a settlement of 143.5 mm was expected. The final settlement was calculated at 149 mm, which is comparable to 143.5 mm for time settlement under a surcharge load. If a vacuum pressure of 86.5 kPa was applied to the earth, the

ground settlement would be calculated to be 734 mm. The projected final settlement for Time-Settlement Under Vacuum Loading was 213 mm, which is significantly less than the computed settlement of 734 mm. The authors presented a comparison of cone resistances before and after vacuum treatment in Figure 2.4. According to the preceding CPT results, the light cone penetration tests revealed a considerable increase in cone penetration resistance during vacuum consolidation, implying an increase in the shear strength of the foundation soil.

2.4 Dynamic Compaction

Dynamic Compaction is a technique for enhancing the ground in situ that uses a drop weight to densify soils and fill materials. The Deep Dynamic Compaction (DDC) technique is based on the principle of dropping a large weight into the ground to be compacted, typically weighing between 10 and 40 tons. The drop height is typically between 10 and 30 meters. A crane hoists the drop weight, which is usually steel, and then drops it repeatedly on the ground. The subsurface conditions, foundation loading, and geometry influence how far apart drop locations should be placed on a grid. The Dynamic Compaction technique has been applied to planned structures in order to increase bearing capacity while simultaneously reducing settlement and liquefaction potential. It has also been used to compact landfills before the construction of parking lots and roadways and stabilize large areas of embankment work.

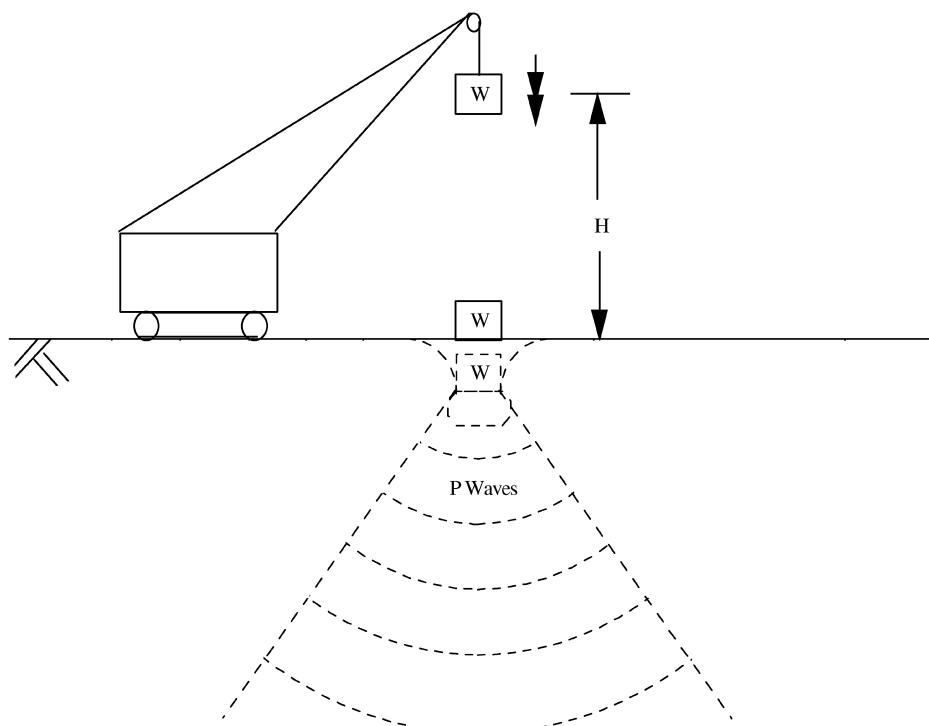


Figure 2.5: Schematic of dynamic compaction (after Selby, 2002)

Among the most often used dynamic compaction techniques are the following:

- Heavy Tamping techniques (Deep Dynamic Compaction)
- The High Energy Impact Compaction (HEIC) techniques
- Dynamic replacement
- The Rapid Impact Compaction (RIC), and
- Rotational dynamic compaction.

2.4.1 History of Dynamic Compaction

In 1975, the French company Menard Techniques Limited came up with the idea of “Dynamic Compaction”, which has been widely adopted due to its cost-effectiveness and simplicity. The approach has been shown to be effective on a wide range of soil types and conditions, notably, sandy materials and granular fills (Mayne et al., 1984), but it’s important to be careful with saturated clay and fine-grained soils(Lukas, 1986). Many civil engineering projects, including buildings, container terminals, highways, airports, and dockyards have used this method during the past 30 years. It has also been used to reduce the liquefaction potential of loose soils in earthquake-prone areas (Han, 1998; Kumar, 2001; Liang and Xu, 2011; Lukas, 1986; Mayne et al., 1984).

2.4.2 Suitability

It has been demonstrated that the dynamic compaction method may be used on granular soils. Also, it should be noted that dynamic compaction can reduce bearing capacity if the excess pore pressure is not properly dissipated during compaction in saturated clay soil deposits.

Table 2.1: Soil suitability based on permeability (after Lukas, 1986)

Soil Category	Permeability (cm/sec)	Plastic Index	Suitability for Deep Compaction
Previous soil deposits	$K > 10^{-3}$	0	Improvements are achievable
Intermediate soil deposit	$10^{-3} - 10^{-6}$	0-8	Dissipation of pore pressure is a necessity
Impervious clayey deposits	$K < 10^{-6}$	$PI > 8$	Not Recommended

Using the grain size distribution, the plasticity index, and the permeability of the material, Lukas came up with a way to figure out if dynamic compaction would work in a certain situation in Table 2.1 and Figure 2.6. Also, there are some recommendations regarding the

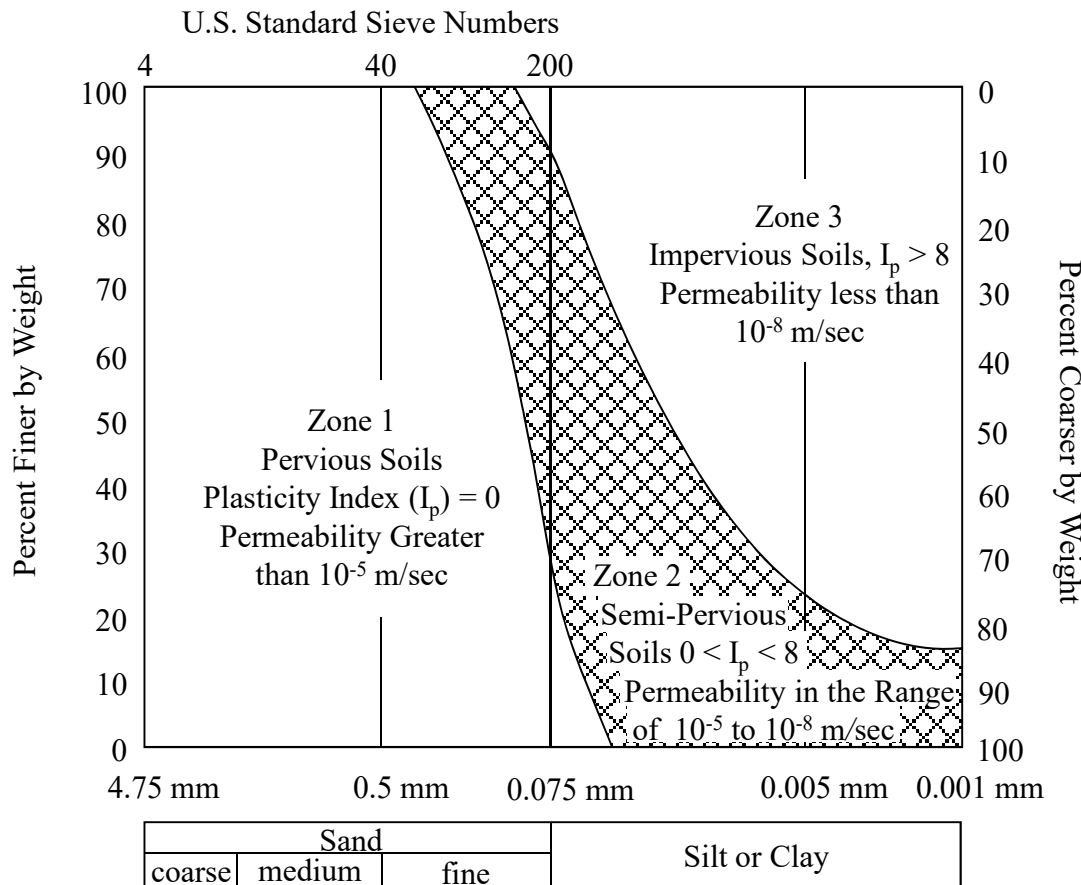


Figure 2.6: Grouping of soils for dynamic compaction. Zone 1 soils are most suitable (after Lukas, 1986)

general soil type with their degree of saturation and the suitability of the dynamic compaction to treat them given by Martin Larisch and Tim Pervan, Fletcher Construction Private Ltd (Table 2.2).

2.4.3 Adverse Situations for Dynamic Compaction

As a result of the application of drainage or dewatering, Deep Dynamic Compaction is generally less effective at improving saturated clayey soils because of the long waiting period for the dissipation of excess pore water pressure. The impact caused by Deep Dynamic Compaction generates noise, vibration, and lateral displacement, all of which can pose problems for neighboring buildings, substructures, and utility lines. Tamping could result in debris flying around, which could be dangerous to workers. Also, Mitchell et al. (2002) introduces the adverse situations for consideration of Dynamic Compaction in the following Table 2.3.

Chapter 2. Literature Review

Table 2.2: Suitability of Dynamic Compaction with soil type along with Degree of Saturation (After Martin Larisch and Tim Pervan)

General Soil type	Degree of Saturation	Suitability of DC
Granular deposits in the grain size range of boulders to sand with 0% passing the 0.075mm sieve	High or Low	Excellent
Granular deposits containing not more than 35% silts	High	Good
	Low	Excellent
Semi-permeable soil deposits, generally silty soils containing some sands but less than 25% clay with $PI < 8$	High	Fair
	Low	Good
Impermeable soil deposits generally clayey soils where $PI > 8$	High	Not Recommended
	Low	Fair-minor improvements water content should be less than plastic limit
Miscellaneous fill including paper, organic deposits, metal, and wood	Low	Fair-long term settlement anticipated due to decomposition. Limit use to embankments
Highly organic deposits peat-organic silts	High	Not recommended unless sufficient energy applied to mix granular with organic soils

Table 2.3: Adverse condition with possible difficulties (after Mitchell et al., 2002)

Adverse situation	Possible difficulties
Soft clays (undrained shear strength less than 30 kPa)	Insufficient resistance to transmit tamper impulse
High groundwater level	Need to dewater and to consider possible effects of subsequent recovery in water level
Vibration effects (may be worse if groundwater level is high)	Distance from closest structure to be of the order of 30 m or more
Clay surface	May be inadequate for heavy cranes and unsuitable for imprint backfilling
Clay fills	May be subject to collapse settlement if inundated later
Voided ground or Karst features below treated ground	Treatment may not reach the voided zone or may make it less stable
Biologically degrading material	Compaction may create anaerobic conditions and regenerate or change the seat of the biological degradation

2.4.4 Design Principles

There are mainly three basic principles of dynamic compaction by which the soil can be treated and get rid of most of the faulty nature of pre-treated unbalanced soil profile. Those are,

- Dynamic densification
- Dynamic consolidation
- Dynamic replacement

Dynamic Densification

In the case of unsaturated granular soil, the impact of heavy tamper quickly displaces the particles to a denser condition, expels air from voids, and increases the density of the soil.

Dynamic Consolidation

Menard and Broise (1975) proposed the notion of dynamic consolidation. It is also possible to enhance saturated fine-grained soils by periodically dropping a heavy tamper. The four primary mechanisms of dynamic consolidation were identified by the researchers.

- Microbubbles in saturated soil increase compressibility.
- The progressive liquefaction caused by repeated impacts.
- The alteration of the soil mass's permeability as a result of the formation of fissures.
- It has a thixotropic nature.

Dynamic Replacement

Densification and consolidation are ineffective when the clayey soil is excessively soft and has low permeability. It is possible to dislodge soil rather than improve it by the use of tamping, backfilling, and subsequent tamping.

2.4.5 Design Considerations

The design of dynamic compaction should consider the following factors,

- Site Investigation.
- Influence Factors.
- Soil Type.

- Depth and Area of Improvement.
- Tamper Geometry and Weight.
- Drop Height and Energy.

Others

2.4.5.1 Site Investigation

A geotechnical research is required prior to the design of deep dynamic compaction in order to evaluate the site conditions, which include,

- Particle size, fine content, saturation level, and Atterberg limits are all included in the geomaterial profile
- Relative density of cohesionless geomaterial
- Groundwater level
- Possible voids
- The depth of improvement may contain hard lenses
- Possible sensitive soil

2.4.5.2 Influence Factors

It is important to consider these factors when designing deep dynamic compaction.

- Particle size, fine content, saturation level, and Atterberg limits are all included in the geomaterial profile.
- Degree of improvement
- Geomaterial type
- Drop height and energy
- Depth of crater
- Depth and area of improvement
- Pattern and spacing of drops
- Number of drops and passes
- High groundwater table
- Elapsed time
- Presence of hard layer
- Presence of soft Layer
- Environmental impact (vibration, noise, and lateral ground movement)

2.4.5.3 Soil Type

According to Lukas et al. (1995), there are three types of soil that are ideal for dynamic compaction:

1. Previous soil deposits—granular soil
2. Semi-pervious deposit—primary silts with plasticity index less than 8
3. Semi-pervious deposit—primary clayey soil with plasticity index more than 8

2.4.5.4 Depth and Area of Improvement

The depth of improvement is determined by the project's requirements for the targeted performance. For example, a layer of loose and saturated sand is prone to liquefaction should be made better to the point where no liquefaction will happen. The following formula, created from field data, can be used to estimate the degree of improvement:

$$D_i = n_c \sqrt{W_t H_d} \quad (2.1)$$

where D_i = depth of improvement (m), W_t = weight of tamper (ton), H_d = height of drop (m), n_c = constant, depending on soil type, degree of saturation, and speed of drop.

It's important to remember that the formula above is unit-dependent. It is recommended that the units defined in the definitions be followed. The values may be found in Table 2.4. Grainy soils can improve up to 10 meters deep, but cohesive soils and clay fills can only improve up to 5 meters deep. A distance equal to the depth of improvement on each side of the improvement area should be maintained.

Table 2.4: n_c value depend on different soil types (after Lukas et al., 1995)

Soil Type	Degree of Saturation	n_c
Pervious Soil deposits -granular soils	High	0.5
	Low	0.5-0.6
Semipervious deposits-primary silts with PI< 8	High	0.35-0.4
	Low	0.4-0.5
Semipervious deposits-primary clay soil with PI> 8	High	Not Recommended
	Low(w<PL)	0.35-0.4

2.4.5.5 Tamper Geometry and Weight

To get the job done, tampers are often fashioned out of steel or steel shells that are filled with concrete and have an area of 3–6 square meters in size. Cohesive soils require tampers with

large base areas (more than 6 m^2), whereas granular soils require tampers with smaller base areas ($3\text{--}4\text{ m}^2$). Tampers can weight anywhere from 5 to 40 tons.

2.4.5.6 Drop Height and Energy

Tamper drop heights commonly range from 10–40 meters. In fact, the energy per drop is often between 800 and 8000 kN/m, according to Mayne et al. (1984). Based on field data, Mayne et al. (1984) produced a graph showing the link between tamper weight and drop height. It is possible to express this relationship in terms of the following:

$$H_d = (W_t H_d)^{0.45} \quad (2.2)$$

where $W_t H_d$ = energy per drop of tamper (ton-m), which is determined from Equation (2.1) based on the required depth of improvement. The drop height computed may be changed in accordance with the contractor's available tamper.

Other following design considerations should be considered, example as pattern, spacing of drops, depth of crater, number of drops, and degree of improvement, etc.

2.4.6 Quality Control and Assurance

Ensure that the drop height and drop points are accurate before beginning any tamping activity. During field tamping operations, it is critical to keep an eye on things and keep an eye on things. Observations and monitoring can lead to adjustments. To put it another way, it's a signal that the geomaterial at one site is weaker than the geomaterial at other locations.

Over-excavation and replacement may be essential to improve this area. To prevent future densification failure, stop or reduce the amount of subsequent tamping around the crater if it causes substantial amounts of heave.

It's common to use piezometers to monitor saturated fine-grained soil, inclinometer cabling to track horizontal movement, and accelerometer sensors to measure ground vibration.

After the tamping job is completed, field excursions should be done to verify or evaluate the improvement in the degree and depth. After tamping, the field evaluation should be conducted at least once every two weeks for coarse-grained geomaterial and once every three to four weeks for fine-grained geomaterial, depending on groundwater level and geomaterial type. Sampling for laboratory testing, SPT, CPT, or PMT are all examples of field excursions. The test's depth should be less than the improvement's design depth.

A big project site can accommodate static plate load tests. It's a good idea to use PMT and

plate load tests because they're more sensitive to changes in soil stiffness than SPT and CPT, respectively.

2.4.7 Reviews of Previous Practices on Dynamic Compaction

Wang et al. (2000) study area was a big commercial storage facility, which was a low marshland near a tropical beach in southern China. Work began in August 1997, and fill material was dispersed across the site without engineering compaction. The site was located around 4.5 meters above sea level and had colluvial material ranging from 2 to 6 meters deep. The site is approximately 350,000 m^2 in size. A 15,000-kilogram steel tamper with a 2.5-meter diameter was employed. As a result, it was concluded that the dynamic compaction program had been successful in densifying the higher colluvial fills. There was an average settlement of 500 mm across the whole project site. In 180 days, they were able to achieve an 80 percent consolidation rate, compared to a non-treatment projection of 15 years. The surface fill layer's shear strength was instantly increased.

Liu et al. (2008) conducted a study based on the Hunan province's Yizhang — Fengtouling expressway. Embankment height ranged from 4 m to 8 m, the subgrade top was 17 m wide, and the infill soil was red clay. The first 4 compactations have the heaviest compacting settlement, with each compacting settlement measuring around 10cm and accounting for about 80% of the overall compacting settlement. The Yizhang—Fengtouling expressway red clay embankment can be treated with dynamic compaction in situ. The physical and mechanical properties of soils can be improved via dynamic compaction treatment. In its plastic or hard plastic condition prior to compacting, embankment soil is transformed into a hard plastic or hard state, which results in a decrease in water content, and an increase in densities (an overall decrease in void ratios). The anti-shear strength of embankment fills was improved following dynamic compaction treatment.

Feng et al. (2010) selected Mabianzhou Island, in Huizhou City, Guangdong Province, China, as the proposed location for the project. From 5 to 11 meters of water surrounds this island. The coastal reclamation area has a lift thickness of approximately 12 meters. The design parameters for ground bearing capacity and improvement depth following HEDC treatment were not less than 160 kPa and 14 m, respectively. Following HEDC, the average elevation of the test zone was 10.32m, which was in line with the design specifications. The allowable bearing capacity at this location has been increased to more than 160 kPa following HEDC therapy. Higher ground carrying capacities and deeper improvements can be achieved using this method.

The existing Nice airport was expanded by building two additional, 3200-meter-long runways parallel to the shoreline on reclaimed land near the city. Loose fill, stiff marls, and soft sand

Chapter 2. Literature Review

silt deposits were the predominant soil types. Thus, the runway needed to be compacted with severe dynamic compaction. On reclaimed ground, two new 3200-meter runways were built parallel to the shoreline to expand the current Nice airport. Loose fill, stiff marls, and soft sand silt deposits were the predominant soil types. A substantial dynamic compaction was therefore required surrounding the runway. In order to establish a reclaimed platform of 200 hectares, around 20,000,000 m^3 of fill had to be placed. The borrow pit was 13 kilometers away from the main site of the project.. A fleet of 38 dumper trucks with a combined weight of 145 tons transported the goods. During DC, the change in pore water pressure was tracked over time and depth. In order to avoid building up excessive pore pressure, work has been carried out in multiple stages with enough rest periods. The intensity of the treatment was determined by the volume vs DC energy ratio. Numerous CPT and PMT have been done during Dynamic Compaction and after treatment to manage fill characteristics.

The Shuaiba Independent Water Power Project (IWPP) was designed to fulfil the growing need for water and energy in Saudi Arabia's Shuaiba district, which is 110 kilometres from the capital, Jeddah. The project is expected to be completed by 2015. There were two distinct soil types on the site. Silty sand was found in both the upper and lower portions of the first profile, ranging from fine to coarse. The bedrock was placed on top of this. Twelve evaporators, three water tanks, and several other buildings were part of the project. The tank had a diameter of 106.6 meters and a height of 20 meters. The tanks were to have a bearing capacity and a maximum settlement of 200 kPa and 75 mm, respectively, according to the design standards. The same 150 kPa and 25 mm requirements were applied to the other structures. In order to get the best foundation solution possible, the project team opted to use dynamic compaction and dynamic replacement. The properties of the soil influenced the decision to use this approach. 75 pressure meter tests (PMT) and a zone load test were used to show that the acceptance criteria had been met following the conclusion of soil improvement work. The tests' outcomes showed that the ground improvement project was a success and that the foundations could safely handle the design loads they were designed to carry.

Reclamation of 900000 m^2 utilizing dredged sand for a depth ranging from 4m to 12m extended the New Corniche road to 200m. In order to stabilize this 4750 meters long structure, anchored by sheet piles, it was required to use a well-compacted undersea backfill to provide the necessary horizontal reaction. High Energy DC and Dynamic Compaction (with 15 and 25T pounders, respectively) were used for the majority of fill, with special attention paid to sections with silt pockets. The same procedure was for the sea wall region, with a denser grid on an initially enlarged and raised platform, then excavated following soil improvement completion in order to obtain the final shape of the structure. Also, The researchers used PMT and finite element analysis to get the measurements.

2.5 High Vacuum Densification Method (HVDM)

In order to improve saturated soft cohesive soil, High Vacuum Densification Method (HVDM) combines the two procedures of **Vacuum Consolidation or Vacuum dewatering with Dynamic Compaction**. This approach employs a series of vacuum dewatering and deep dynamic compaction runs to generate negative and positive pore pressures, respectively, which aid in pore pressure dissipation and achieve both consolidation and densification effects, lowering water content and increasing density. **Because of this, soil stiffness and strength are enhanced.**

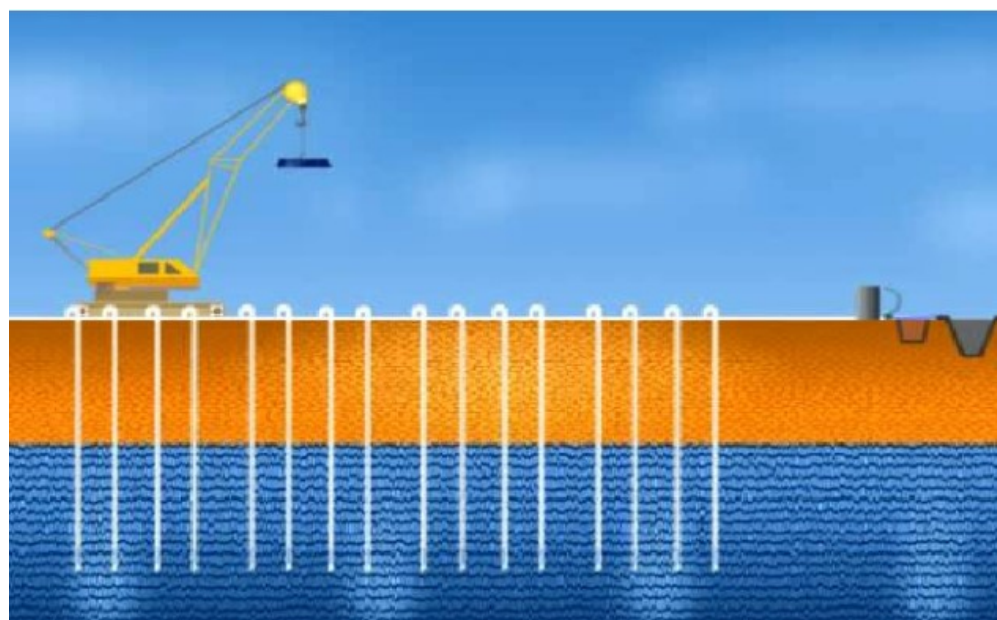


Figure 2.7: Schematics of HVDM method (after Liang and Xu, 2011).

Since its inception in early 2000, Shanghai Geoharbour Group has been testing the concept of High Vacuum Densification Method and applying it on a large scale to many well-known projects around Shanghai, such as Shanghai Pudong Airport Runway No. 2, Shanghai Formula F1 Race Track, Shanghai port expansion. China and other Asian countries such as Vietnam, Malaysia, and Indonesia were then added to the HVDM system after early success in Shanghai. **In China and other nations, HVDM is the most used approach for land reclamation and soft soil improvement.**

2.5.1 Mechanisms of Gain in Undrained Strength

e-log P' plot in Figure 2.10 shows the processes of vacuum consolidation and dynamic compaction work together to improve soil strength and reduce water content increasing soil strength and decreasing water content respectively. Assume normal consolidation of fine-grained soil and point A's pre-improvement state. Positively in the excess pore pressure

is generated by dynamic compaction and is responsible for changing the soil condition from A to B_1 (despite the apparent drop in the void ratio caused by dynamic compaction). After the soil has been compacted dynamically, high vacuum is employed to quickly remove the extra pore pressure and move the soil from condition B_1 to D_1 .

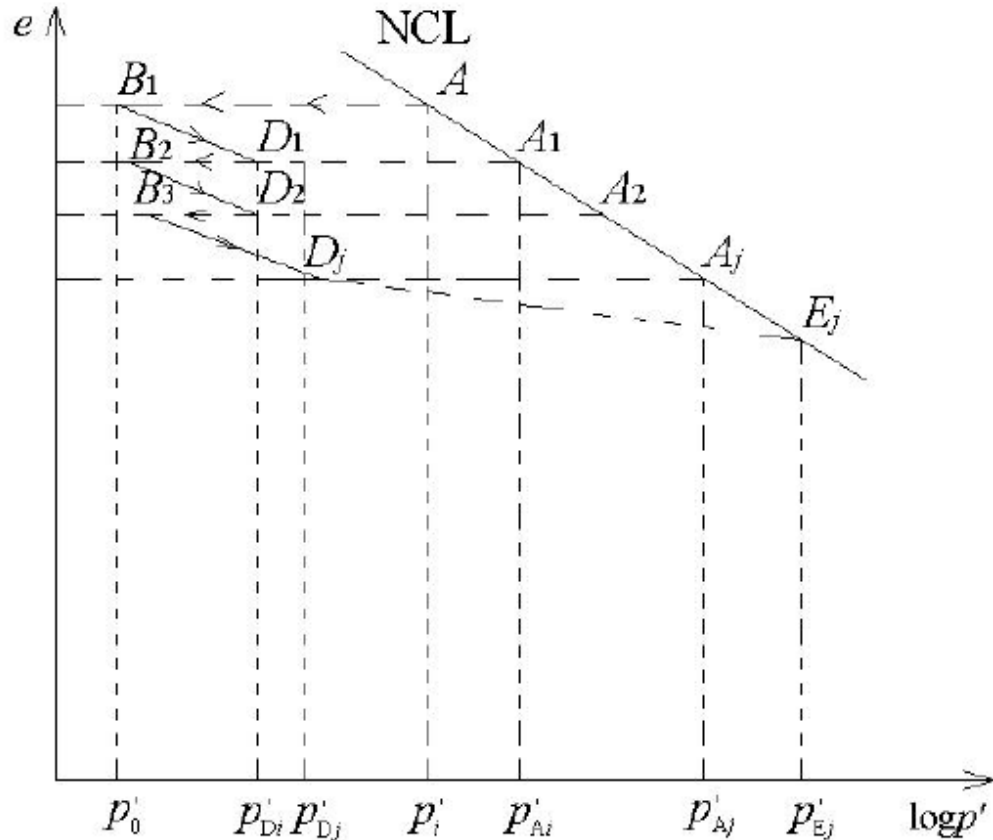


Figure 2.8: e-log p plot under many times of dynamic impact and vacuum Consolidation (after Liang and Xu, 2012).

As more pressure is dissipated during rapid consolidation, the void ratio is decreased. **Improved soil strength can be achieved through repeated cycles of vacuum and dynamic compaction on fine-grained materials.** The following relationship between undrained shear strength and apparent over-consolidation ratio (OCR) can be used to evaluate the undrained shear strength of the improved fine-grained soils.

$$OCR = \frac{P_{Ei}'}{P_{Ai}'} \quad (2.3)$$

$$\frac{(S_u)_{OCR}}{(S_u)_{NC}} = OCR^A \quad (2.4)$$

2.5.2 Working Principles of HVDM

HVDM run consists of a combination of Vacuum Dewatering and Dynamic Compaction. A vacuum effort is used to remove soil moisture while standard dynamic compaction methods are used to compact the soil. A negative pore pressure is caused by a vacuum effort, while a positive pore pressure is caused by dynamic compaction.

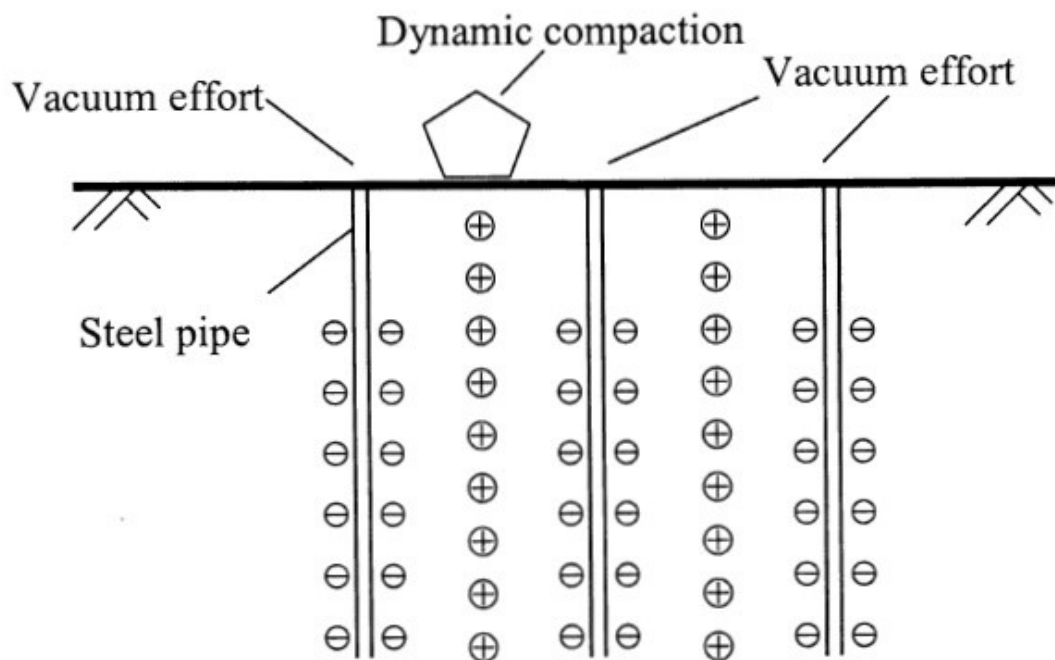


Figure 2.9: Working Principles of HVDM method (after Deng and Xu, 2010).

There will be two opposite pore pressures from a lateral pressure gradient in soil that has been vacuumed and compacted on the construction site if these things are done well. The pressure gradient is created in order to accelerate the dissipation of pore pressure and the discharge of moisture.

The following steps comprise the HVDM:

Step 1: An in-depth soil investigation is required to determine the site's soil profile. A number of fundamental soil parameters, such as gradation curves, **Atterberg Limits, water content, Permeability, compressibility, and the coefficient of consolidation**, should be evaluated and determined. Additionally, some in-situ tests, such as CPT or SPT, should be performed to establish baseline values prior to initiating HVDM in the field. Begin by **doing a rough sketch to figure out the best spacing and depth of vacuum pipes, the amount of power needed for Deep Dynamic Compaction, the number of drops and grid spacing of a tamper, how long it will take for Vacuum Consolidation between cycles of Dynamic Compaction, and more.**

Chapter 2. Literature Review

Step 2: A vibratory hammer with a mandrel, or a hydraulic system that directly pushes vacuum pipes into the ground, can be used to install vertical vacuum pipes and horizontal drainage pipes.



(a)



(b)

Chapter 2. Literature Review



(c)

Figure 2.10: In-situ vacuum pipe arrangement-(a) Vertical Perforated vacuum pipe, (b) Using geotextile fabric around the outside of the vacuum pipes and (c) Preparation of installation of vacuum pipe by water pressure



Figure 2.11: Vacuum drainage system layout

Vacuum pipes are commonly made of steel with an exterior diameter of 1 to 1.25 inches and thickness of 1/8 inch. A geotextile fabric is stretched around the outside of the vacuum

pipes to provide filtration. Elbow connectors connect the steel vacuum pipes to the horizontal drainage pipes, commonly PVCs.

Step 3: Reduce water content and early saturation by using the first cycle of vacuuming. This will also increase the soil's load-bearing capacity, making it more tolerant of the weight of workers and equipment for the following phase of work (Deep Dynamic Compaction). Soil dewatering is a process that takes place during this period. A week normally suffices to complete this phase before moving on to the next.



Figure 2.12: Vacuum pump in research site

Step 4: Soil densification and positive pore water pressure can be achieved through Deep Dynamic Compaction. Using heavy tamping creates craters that displace dirt and reduce the void ratio (direct densification), all while increasing the pressure inside the zone of influence (positive pore pressure).

Even if the vacuum pipes aren't removed during dynamic compaction, the soil can benefit greatly from the "pressure gradient" created by vacuum pressure and dynamic compaction energy. The weight, dimension, drop height, grid spacing, and number of tamper drops per spot are the most critical control factors for dynamic compaction. To ensure that the bottom of the crater does not suffer undrained shear failure or the so-called "rubber soil" phenomenon, these characteristics must be determined from site monitoring findings. Typically, this phase takes one week to complete on a $10,000 \text{ m}^2$.



Figure 2.13: Dynamic compaction Procedure

Step 5: For dissipating EPWP generated during DC attempts, minimizing saturation and void ratio of soil mass, perform an additional vacuum cycle. Because of this large pore pressure gradient, water content is lowered as a result of a combination of vacuum and dynamic compaction generating positive pore water pressures, both of which generate negative pore water pressure. This stage usually lasts no more than a week.

Step 6: After completing Step 5, conduct an evaluation of the soil's qualities. This initial cycle (steps 4 and 5) of the HVDM process must be evaluated to identify the water content, pore water pressures, water elevation, ground subsidence, and in-situ test findings such as CPT cone resistance or N values of SPT. In the following cycle of HVDM, the operating settings (vacuum pipe spacing and depth, dynamic compaction energy level, grid spacing of tamping points, etc.) can be adjusted based on ground improvement results.

Step 7: Steps 4 through 6 should be repeated until the desired results have been achieved. According to CPT or SPT and post-treatment settlement, two cycles of the HVDM procedure are often adequate to satisfy the required performance parameters.

2.5.3 Distinguishing Features of HVDM

There are two ways to make the soil less watery: by using a high vacuum system and by changing how the soil is combed. In saturated soft soils, customary reluctance to apply dynamic compaction is effectively addressed by this innovative use of high vacuum. Also, by employing a series of sequential and repeated cycles of vacuum dewatering and deep dynamic compaction, HVDM may successfully treat soils with low permeability in a substantially shorter amount of time than other methods. An impenetrable seepage barrier and excellent load-bearing layer are provided by a hard shell of up to 5 to 8 meters thick on the surface of the treated ground after HVDM treatment. If any post-treatment consolidation occurs, the hardened and impermeable shell acts as a buffer to reduce the post-treatment total and differential settlements by diffusing the surface loads and preventing water from draining from soils beneath the hardened surface layer.

2.5.4 Advantages and Limitations

High Vacuum Densification Method has several advantages over other ground improvement methods, but also comes with some limitations.

The advantages of HVDM are as follows,

- The vertical vacuum pipes can be used more than once and are easy to connect to the horizontal PVC pipes and vacuum pumps to make a closed vacuum system for dewatering.
- As dynamic compaction supplies the means to generate positive pore water pressure and mechanical densification of the soft soils, there is no need to bring in surcharge load.
- The combined negative pore pressure from vacuum and positive pore pressure from dynamic compaction facilitate expeditious dissipation of pore pressure and resulting in fast consolidation of the cohesive soil deposit.
- There is no need for a special construction requirement to carry out the work in the field, which is in contrast to the necessity of special equipment to install PVDs.
- Compared to PVD, vacuum pipes perform more effectively as a conduit for vacuum and dewatering processes.

The limitations of HVDM are as follows,

- The treatment depth can't be more than 10 meters because the zone of deep dynamic compaction and the efficiency of vacuum dewatering decreases when the depth goes below that.
- Cohesive soils with a high percentage of organic matter may also be incompatible with HVDM.
- Fine-grained soils with a hydraulic conductivity of not less than 5×10^{-7} cm/sec are suitable for HVDM.

2.5.5 Design Considerations of HVDM

The following design considerations should be considered ,

- | | |
|--------------------------|------------------------------|
| • Soil Type | • Pore pressure monitoring |
| • Improvement Depth | • Groundwater observation |
| • PVD Installation | • Water content |
| • Hydraulic Conductivity | • Vacuum pressure monitoring |
| • Surface settlement | |

2.5.6 Quality Control and Assurance

Heavy tamping energy (mass of tamper, drop height and drop spacing and number of drops per spot) and vacuum consolidation parameters such as pipe spacing and depth are among the parameters that must be optimized for HVDM success through the intelligent use of field monitoring of relevant information. The most common types of field monitoring include pore water pressure, crater depth, ground water level, ground subsidence, water content, and CPT (or SPT).

2.5.7 Reviews of Previous Practices on HVDM

Deng and Xu (2010) conducted a study on East China's Yangtze River port. The site was made up of farmland that had been reclaimed and soil that had been dredged. The water's depth was roughly 6 inches below the surface of the earth. The site's top layer was silty fine sand that had been drained (1-3 m thick), mixture of sand, silt, and clay (1-2 m thick), Mucky

Chapter 2. Literature Review

and sludgey soil (0-6 m thick), and the finest sand. The interlayers of soft and sandy soil were found beneath the surface. HVDM performed a pilot treatment on a 20 X 20 m piece of the skin. An array of 3.5x4.5 m vacuum pipes was set up. The first Vacuum drainage lasted for 11 days. The 1st compaction was 3000 kN-m at 7 x 7m spacing and 8 blows per site with 8 blows per location for the 1st time. After that, second vacuum drainage was done, followed by a second compaction at an energy level of 1800 kN-m after a drainage period of 10 days had passed. After the first, second, and third runs of HVDM, the settlement was 65.8 centimeters. The bearing capacity of the shallow deposit was increased from 80-100 kPa to 160 kPa based on CPT test data, which met the design requirement.

From Liang and Xu (2010) study, it was found that about 740,000 m^2 of land has been improved for storage yards and transportation routes in the Ningbo Zhenhai Harbor District as part of the project. SPT-N values for the site's soil profile range from 2.75 to 1.7 meters thick, with loose sand at the top and hydraulic fly ash fill at the bottom. (a) improve the bearing capacity of the silty sand layer to 80 to 100 kPa, (b) improve cone penetration resistance of the fly ash layer by a factor of 2.5, and (c) increase cone penetration resistance of soft clay mud by a factor of 1.5 were achieved by using the HVDM method. Three phases of high vacuum dewatering and three stages of dynamic compaction are used in the HVDM treatment of the site. The first stage of tamping uses 800 kN-m energy with three consecutive tamper drops at each tamping position, followed by the second stage of tamping utilizing 1200 kN-m energy and two consecutive tamper drops. When compared with conventional PVD and surcharge preloading procedures, the HVDM technology has met its performance goals while saving time and money.

In Liang and Xu (2011) study, approximately 110 hectares of land had to be cleared in order to build Runway No.2 at Pudong International Airport. It was very soft bay mud with a thickness of between 20 and 30 meters. Limiting post-treatment settlement to 10 cm and 1/1000, respectively, were the ground improvement standards. The ground sank by 55.7 cm as a result of HVDM. The observed settlement was in the 10 cm range after the runway had been in service for approximately six years. It took just four months to complete the ground enhancement work on Runway No 2. In comparison to the usual ground enhancement procedure including PVDs and fill charges, the Pudong Airport Authority saved around 100 million RMB by using HVDM.

Liang and Xu (2012) studied on Ningbo Port, which was a land reclamation project underway with the goal of creating an area large enough to store 5 million tons of coke per hectare. It was composed of a 2 m layer of clay, a 2.0 m layer of hydraulically filled fly ash, a 2.0 m layer of hydraulically filled mud clay, and then a silty sand layer. According to its name, B11 was the first of four subdivisions to be tested. For the third stage of dynamic compaction, impact energy of 800 to 1000 kN-m was used in all subdivisions, with two drops and no spacing between the drop spots. For Sub-divisions B11 and B12, the settlement at the end of

the three stages of dynamic compaction was 42 cm, 17 cm, and 6 cm. Also, 35.3 cm, 29.5 cm, and 8.9 cm were the settlements for subdivisions B13 and B14. 90% of the generated pore pressure was dissipated in 7 to 8 days for the first and second DC/vacuum runs. A 3.37 improvement ratio was achieved in layer-2's cone resistance, which was raised from 0.74 MPa to 2.51 MPa. With an improvement ratio of 1.66, the cone resistance was raised from 0.21 MPa to 0.35 MPa in layer 3. The enhanced cone resistance in PVD zones can be as much as 10% to 20% greater on average than in non-PVD zones when comparing B13 to B11 or B14 to B12 (i.e., PVD zones and non-PVD zones).

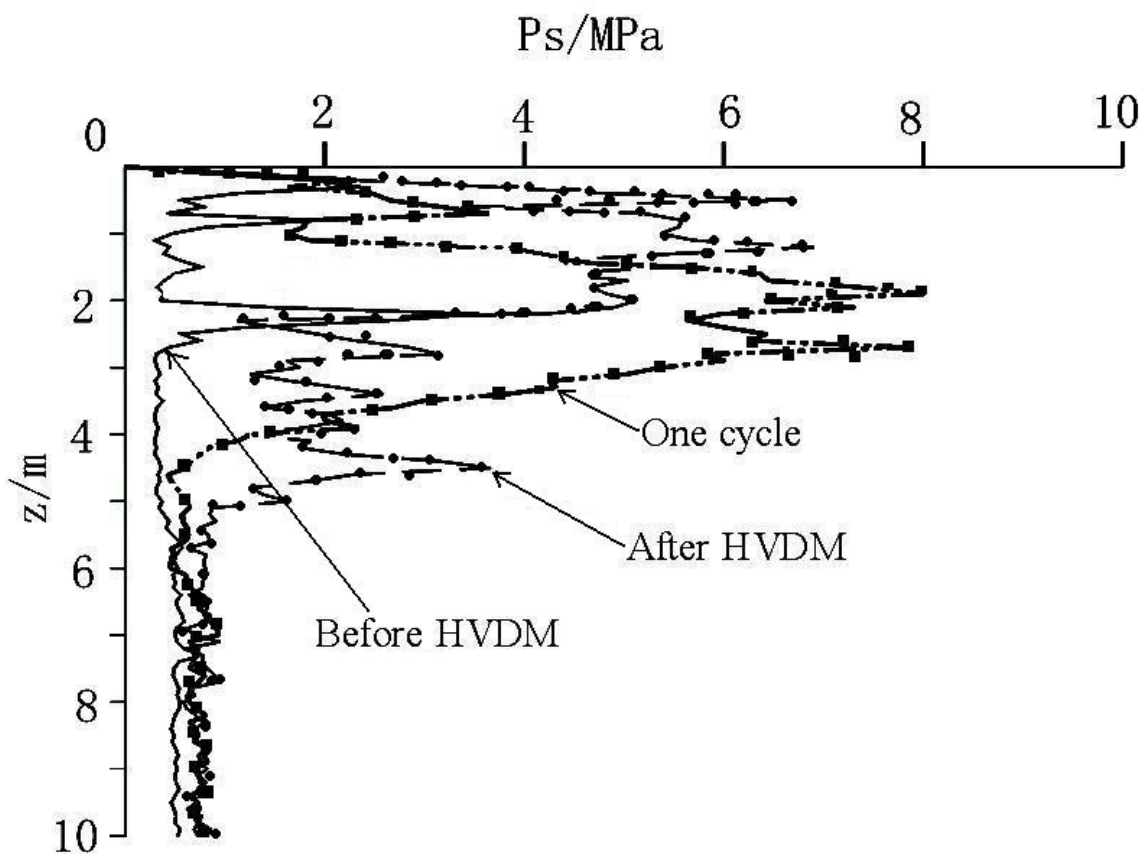


Figure 2.14: CPT cone resistance readings between before and after ground improvement (after Liang and Xu, 2012)

Yin et al. (2013) conducted a study on the amber bay foundation treatment project, which covered an area of approximately $94700\ m^2$, and due to the high subterranean water level, the common dynamic compaction phenomena known as rubber soil might occur, which does not provide reinforcement. High Vacuum Densification was used as a treatment approach for the project. The first time high vacuum construction employing hierarchical intubation was used, the primary goal was to control soil moisture and saturation. By using the company's proprietary high vacuum technology, the device can quickly drop the subsurface water level. After the process design value is met, the initial densification tamping will begin. It's more cost-effective and time-efficient than traditional processes, and it also protects the

environment while allowing for precise control over the final product's quality.

Ji-hong (2014) suggested the location was an estuary, near the mouth of a river, with a groundwater level of 0.5-0.7 m. The soil profile of the location is depicted in the illustration below.

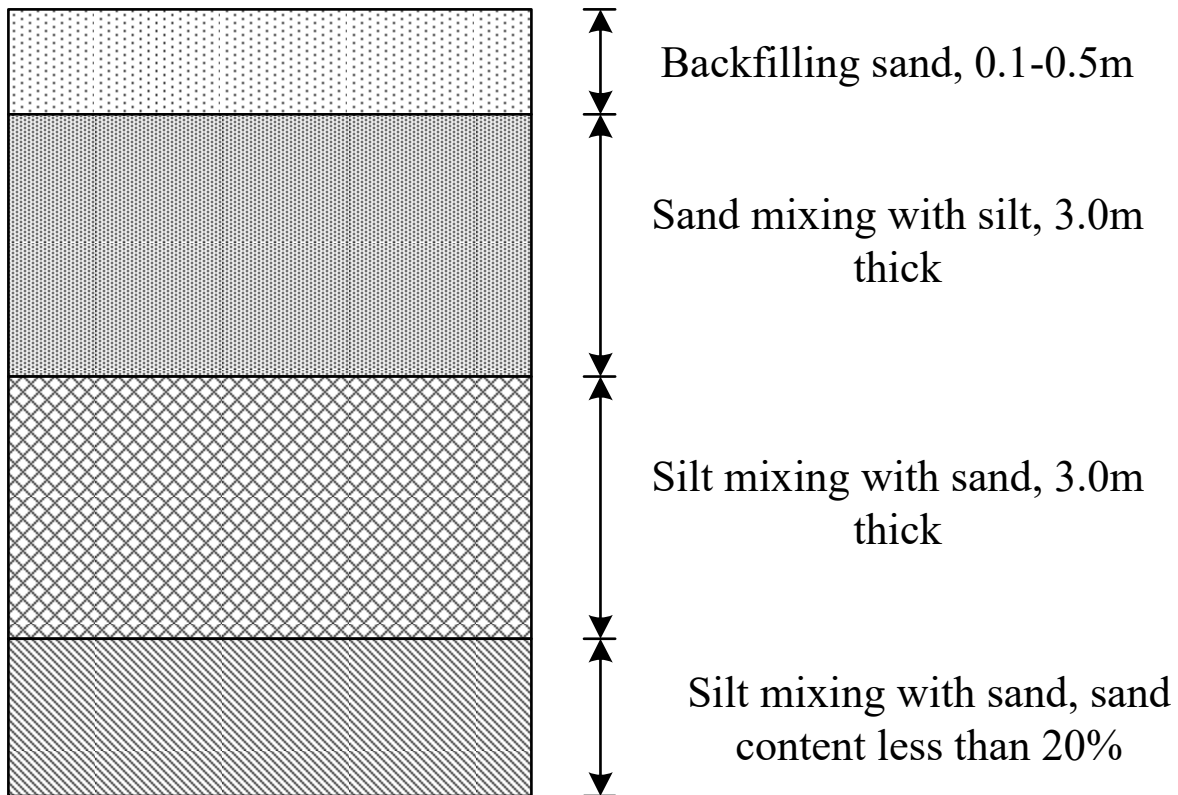


Figure 2.15: Soil profile of the Ji-hong's research location (after Ji-hong, 2014).

There are three typical test plots of 7500 m^2 that will be used in this project. A, B, and C test plots, each $50\text{m} \times 50\text{m}$ in size, were created from the whole test area. Vacuum dewatering and dynamic compaction cycles will be used twice in each zone, according to the plan. This suggests that the 7-day gap between each ramming is suitable in the HVDM building technique, as the excess water pressure dissipation rate has reached above 85 percent at the time of each ramming. To account for the lag effect of increased strength following HVDM, the SPT test was conducted seven days after HVDM and the CPT test was conducted fourteen days after HVDM. The P_s values of CPT in the range of 0m to 6m depth rise significantly after soil improvement by HVDM (Figure 2.16.a). Overcoming design constraints, the average P_s value increased from 0.94 MPa to 4.31 MPa for the silt and fine sand layers, and from 4.33 MPa to 6.91 MPa for the latter two. The SPT results also reveal that HVDM has a significant impact on soft soil (Figure 2.16.b). Silt combined with fine sand enhanced the average value of N from 3.5 to 6.5, whereas fine sand mixed with silt improved it from 7 to 10.5.

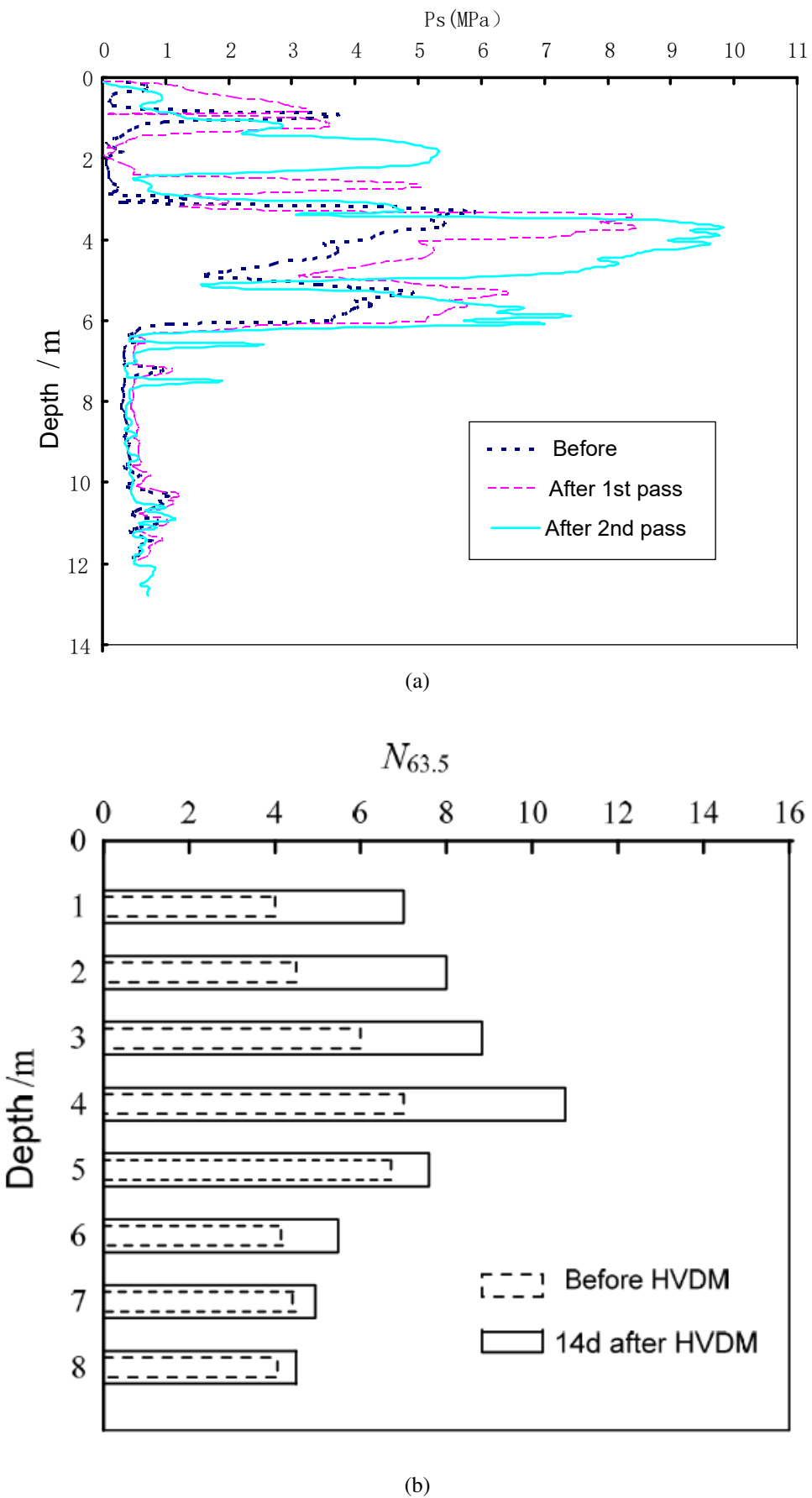


Figure 2.16: CPT and SPT test results between before and after soil improvement by HVDM method- a) CPT test results; b) SPT test results (after Ji-hong, 2014)

Shi and Chai (2017) introduced the high-vacuum densification (HVDM) process in their study. Each time a soft soil foundation treatment was completed and a 5-month period had passed, testing was carried out to examine the proposed method's effectiveness. After the creation of the hydraulic fill sand surface, a plate load test was performed. HVDM significantly improves the foundation soil's strength. More than 406.3 percent of the original sand's cone tip resistance, 360.8 percent of its side friction, and 60.3 percent of its undrained shear strength have been added. At depths of 6 to 7 meters, therapy had the greatest impact. To varied degrees, the physical and mechanical qualities are improved. There was a 6.08 percent rise in dry density. By 8.96 percent, the compression coefficient of the pore had decreased. There was a 10.53 percent drop in the A_{1-2} . A 12.18 percent rise in the compressive modulus of E_{s1-2} was observed. Shear strength in the direct direction grew by 8.91 percent. A 41.01 percent rise in the internal friction angle was observed. Triaxial (UU) test results showed a 33.44% increase in cohesiveness. From less than 50 kPa to above 120 kPa, the foundation-bearing capacity can match the foundation treatment requirements.

2.6 Summary

Recently developed soft clay improvement techniques based on the principles of vacuum dewatering and deep dynamic compaction were discussed in this chapter. This chapter also describes a succession of inventions collectively referred to as the High Vacuum Densification Method. This chapter described the HVDM work principles, as well as its two versions, which are vacuum consolidation and dynamic compaction, respectively. This literature review found many examples of how HVDM successfully improved very soft to soft cohesive soil in different projects worldwide. Also, HVDM's favourable effects on water content and cone resistance were validated by different researchers.

Chapter 3

Field and Laboratory Investigation

3.1 General

This chapter contains investigations conducted in the field and the laboratory. The location of the site chosen for this research, as well as the fundamental geological and depositional history of the site, are provided in the first section. The next section presents in-situ geotechnical investigations, soil samples collection for laboratory testing, and laboratory investigation.

3.2 Site Selection

The site selected for this research is located in Taltoli Upazila of Barguna district, Barishal, Bangladesh. The research site is significant because of the location of a 700-megawatt (MW) coal-fired power station. The power station is sometimes called the Khottar Char power station or Barishal power station.

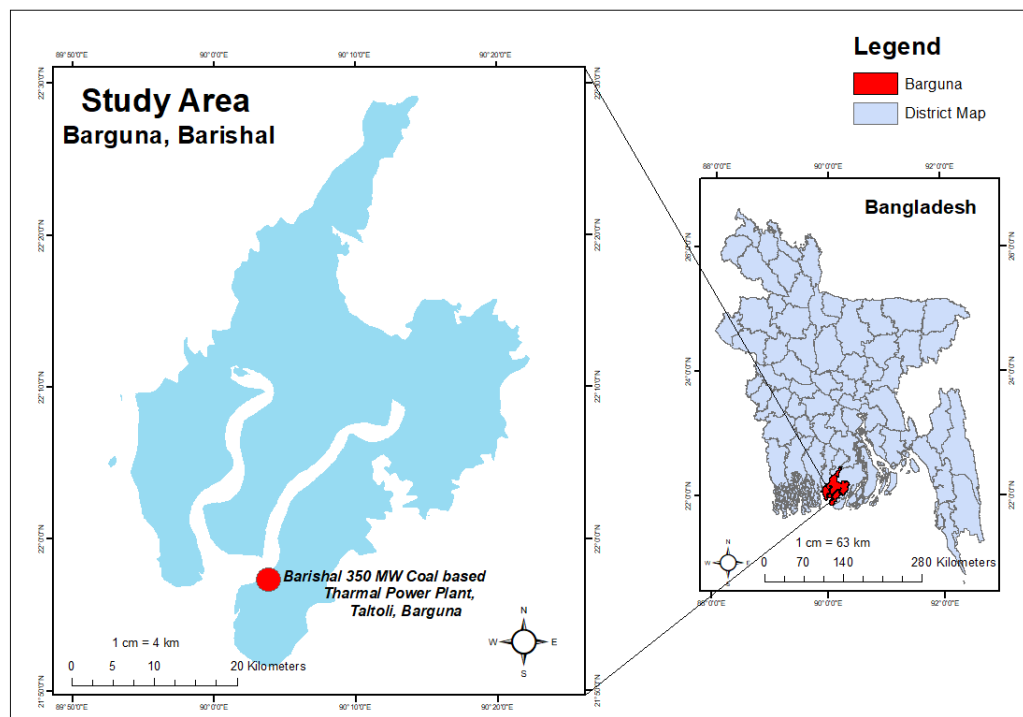


Figure 3.1: Research site location

The 700-megawatt (MW) coal-fired power station is divided into two units per production size. Unit -1, “350 MW coal-fired power plant,” is selected for this research. Figure 3.1 shows the study area location.

3.3 Reclamation Area

The ground elevation of the study site varies from 0.4-3.0 m at mean sea level, and the final levelling elevation was set at 5.4 m on the construction site. The land reclamation area was about 48.57 hectares (The main factory and living area) + 13.09 hectares (middle area) of the channel and yard area (34.17 hectares).

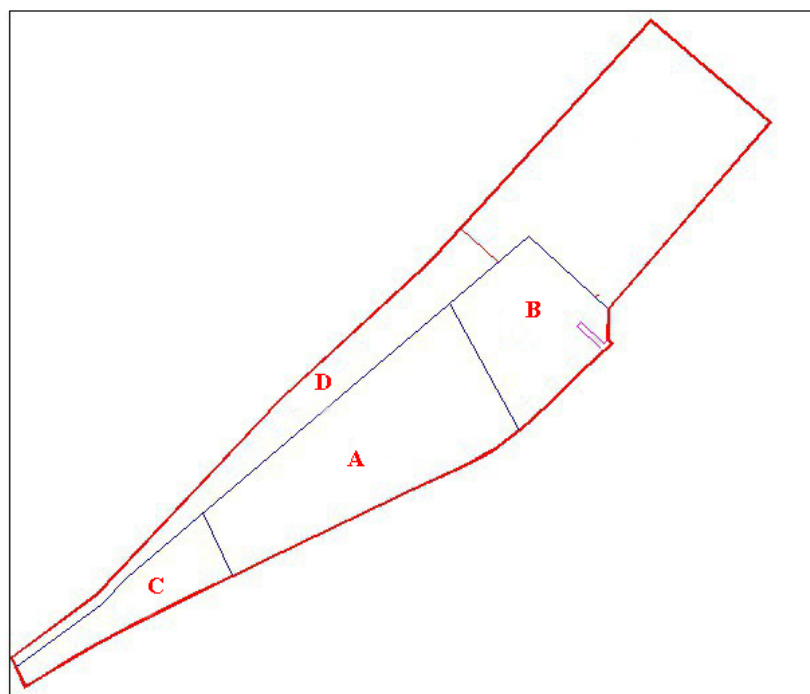


Figure 3.2: Autocad drawing of study area

It was planned to divide the site into five reclamation areas. The main field requiring foundation pre-treatment area was divided into four reclamation areas, and the ash field was treated as a reclamation area (no foundation treatment was required). Figure 3.2 shows the actual illustration of the reclamation area. The subdivision areas of the foundation pre-treatment are presented in Table 3.1.

Table 3.1: Reclamation areas of research site

No	Zone	Area (m^2)
1	A	230429
2	B	130940
3	C	122706
4	D	132580

3.4 In-situ Investigations

3.4.1 Site Characteristics

The undisturbed ground level of the proposed reclamation site increases gradually from northwest to southeast elevation. The elevation of the ground in most areas of the site is 0.5-1.7m, the elevation of parts of the northwest coastal beach was 0.5-0.5m, and the elevation of the boundary area of the southeast site was up to 2.7m. From the sub-soil investigation report conducted by the Barisal Coal Power plant authority, the primary material of this project is silt mixed sand. The main composition is quartz feldspar, which contains mica and a small amount of shell debris mixed with silt.

3.4.2 Soil Profile

A soil profile is a cross-section through the ground that reveals the various soil layers, from the topsoil down to the unaltered parent material. In geotechnical investigations, a study of the soil profile is essential because it provides the foundation for the investigation and serves as a historical record of the various processes that contribute to soil formation. The soil profile is the determining factor for soil categorization and the basis for the practical use of soils. In the research site, 35 borings have been done for the project. Bore-log HA16 was selected for this research for sample collection and investigation. Five distinct layers may be distinguished in the soil profile of the research region. Clay, silt, fine, and medium sand particles predominate in the deposited soil in this area. As a result, mixtures of fines and sand typically exhibit non-plastic behavior, mixtures of fines and clay typically exhibit semi-plastic behavior, and mixtures of pure clay typically exhibit plastic behavior. The bore-log of HA16 is presented in Figure 3.3.

The first layer is 3 m thick grey, very soft silty clay with Standard Penetration Test (SPT-N) results ranging from 0 to 1. Near the ground's surface, there was occasionally very soft soil with an SPT-N value of less than 2. The second layer is made up of soft silty or clay mixed with sand that is also moderately soft. The thickness of the layer can range from roughly 1.5m. The third layer is mostly slit or silty clay that is soft to medium stiff. Most SPT-N values were between 4 and 7 and went up with depth. The thickness is usually between 12.5m. The fourth layer of the bore log is typically stiff silty clay with some sand. This layer could typically be found at depths ranging from 16.5 to 25.5 meters with SPT N values between 7-15 at a layer thickness of 8.5 meters.

Chapter 3. Field and Laboratory Investigation

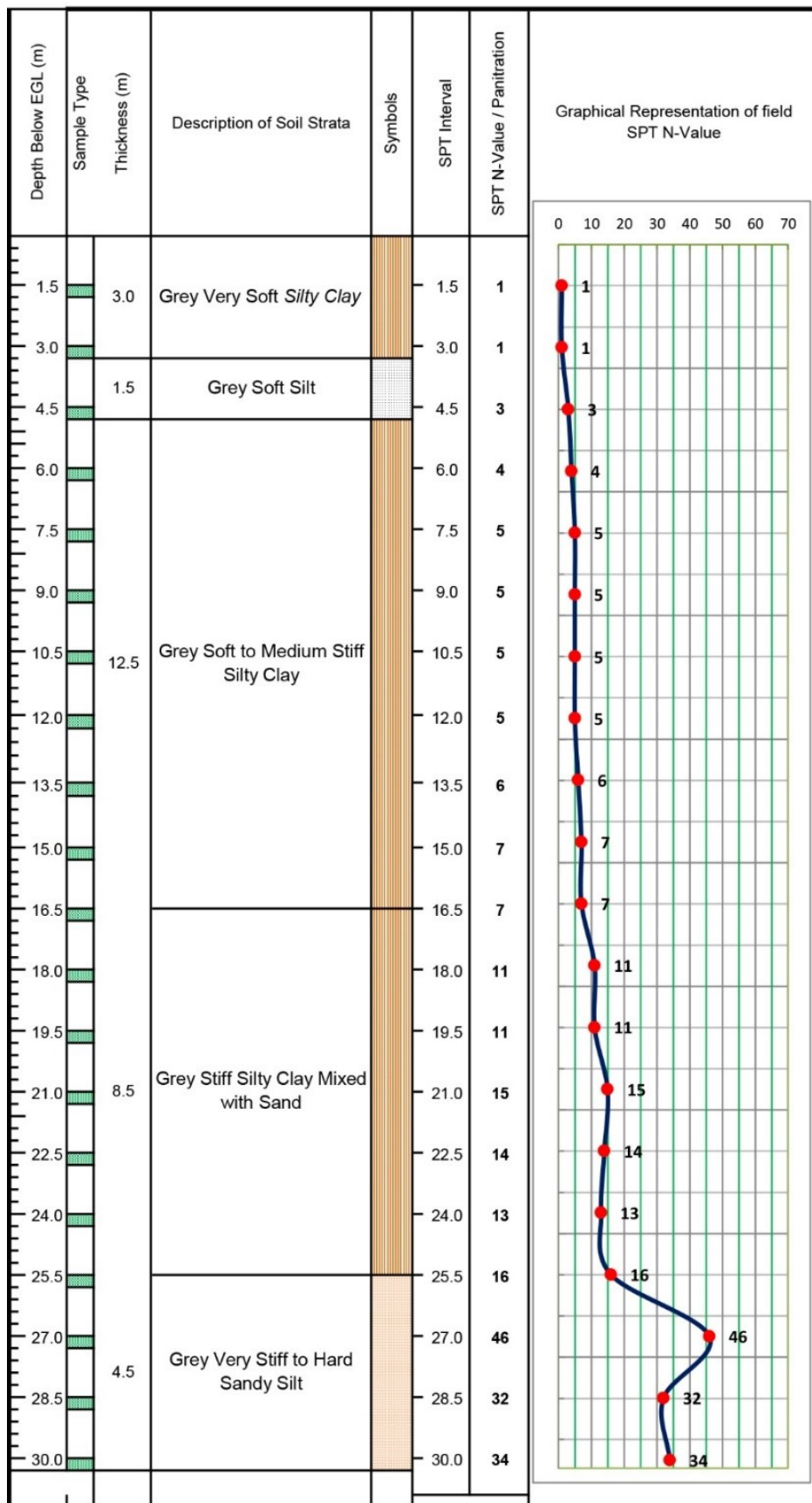


Figure 3.3: Field Borelog of HA16 for the research site

The fifth layer of bore log is very stiff to hard sandy silt with SPT N values between 16-46 at a layer thickness of 4.5 meters. Based on the findings of the site study, it can be said that a layer of soft clayey silt was observed below the existing ground surface, followed by a layer of soft to moderately soft silty soil. After passing through the soft clayey silt layer, one arrives at medium-to-stiff clayey silt interbedded with dense to very dense silt.

3.4.3 Site Visit and sample collection

Site visit event was organized by Geoharbour Bangladesh Engineering & Construction Limited, held on 10th November 2019, at 350 MW coal-fired power plant construction site located at Taltoli Upazila of Barguna district, Barishal, Bangladesh. During the site visit, safety was adequately maintained by wearing safety helmets and shoes. After arrival at the site, the site manager briefly explained the project and started the tour around the site. The site manager showed the step-by-step procedures of HVDM in the field. The following procedure was followed to conduct HVDM on the research site.

3.4.3.1 Filling work

Filling work is the first step to apply the HVDM on the research site. After completing all necessary subsoil investigations, the site was filled with sandy soil up to a depth of 6 m from the existing ground level. The site location was in a coastal area, so it was necessary to fill the construction area to apply the high vacuum densification method.



Figure 3.4: Filling work on the research site

3.4.3.2 PVD installation

Prefabricated vertical drains have a high flow discharge capacity and are frequently used with surcharging to enhance preconstruction soil consolidation. Also, it prevents intrusion and clogging of soil particles. After completing the filling work, the next step was PVD installation for executing HVDM in the research site. For this site, the prefabricated vertical drains (PWD) were installed by a hollow steel mandrel encasing the PVD material. A stitchery joined to an excavator carrier inserted the mandrel into the ground. The PVD was looped through a steel anchor plate at the bottom layer of the mandrel. The anchor plate was installed together into the compressible soft soil at a constant speed to firmly hold and retain the installed PVD at a depth of 15 m. After the design depth was reached, the mandrel was extracted back up into the ground, retrieved from the mandrel the ground, and cut off the PVD. All the steps for the entire installation process were repeated to install the PVD at the whole site. Figure 3.5 represents the installation process of PVD at the research site.



(a)

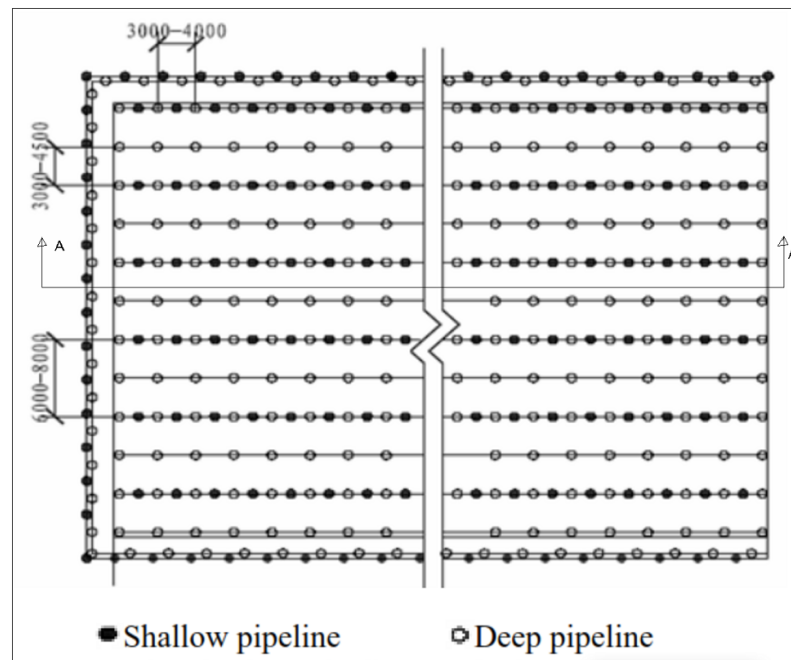


(b)

Figure 3.5: Installation process of PVD at the research site- a) Installing PVD at the site by PVD Rig; b)After Installation of PVD

3.4.3.3 Vacuum Consolidation

After the PVD installation work was completed, the vacuum pipes arrangement was the next step for applying HVDM. The vacuum construction adopted two types of modified vacuum pipe.



(a)

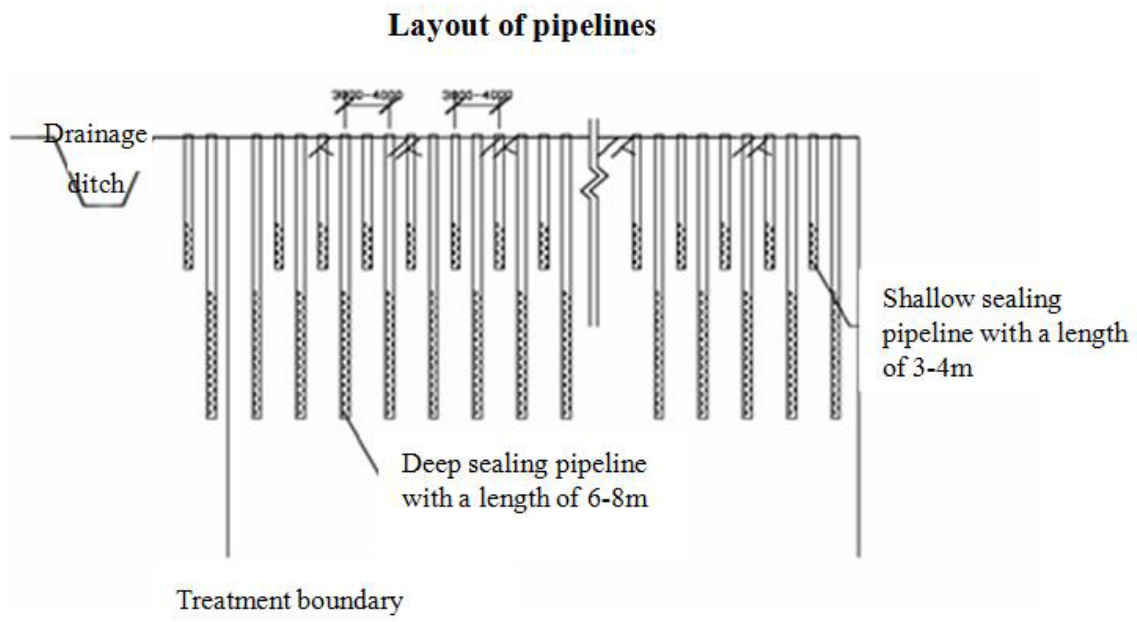


Figure 3.6: Vacuum Pipe Arrangement in the site-(a) Layout of the vacuum pipeline on the research site, (b) Sectional (section A-A) view of the vacuum pipeline on the research site (after Guo, Mei Ling, 2016)

The length of the deep sealing pipeline was 6 m, while that of the shallow one was 3 m. The 3 m pipeline mainly adjusted the water content of the filling sand or shallow-depth soil, and the 6m pipeline mainly adjusted the water content of the deep soil. The spacing between the vacuum pipelines was 1.5 m from center to center. The peripheral high vacuum pipeline closed systems could not be demolished until the foundation treatment within the area had been finished. Figure 3.6 shows the layout of the vacuum pipeline on the site.

During the pipeline plugging, the high-pressure water gun was used to punch the hole to assist in the manual plugging. Meanwhile, mechanical pipeline plugging could also be adopted to improve work efficiency. The vacuum pipeline adopted the dia 1 inch steel pipeline, and two layers of nylon leakage membranes (Figure 3.7.a) wrapped the lower inlet opening. The horizontal pipeline adopted the 2 inch PVC pipeline. The horizontal pipeline was connected with the vacuum pipeline by the flexible rubber hose with the steel wire twined. Meanwhile, the outside of the connection joint was tightly sealed by tape. After the completion of the arrangement and installation of vertical vacuum pipes and horizontal drainage pipeline, the workers started up the vacuum system for vacuum consolidation. During the vacuum consolidation, it was found that the vacuum pressure was maximum of 80 kPa. The vacuum system runs for 24 hr. until the final stage of HVDM.

Chapter 3. Field and Laboratory Investigation



(a)



(b)

Figure 3.7: Vacuum arrangement in the site-(a) Vacuum pipes with nylon membranes at the research site, (b) Vacuum pump in research site

3.4.3.4 Dynamic Compaction

After the water level dropped to a place 3 meters below the compaction level by the application of vacuum consolidation, the densification stage was started. For dynamic compaction purposes, a crawler crane of 50 tons and a pounder with a weight of 10 tons and a diameter of 2 m were used at the research site. The tamping was applied in three cycles. A square grid of 8 m center to center was marked for the first cycle of dynamic compaction. In the first cycle on the tamping location, repeated four drops from a height of 15 m were applied and for the second cycle same height and drops as the first cycle was applied at the middle point of two compaction points on the grid. In the final cycle, all vacuum pipe was pulled out and applied one drop at the height of 10m all over the construction area. Figure 3.8 shows the dynamic compaction process at the research site.

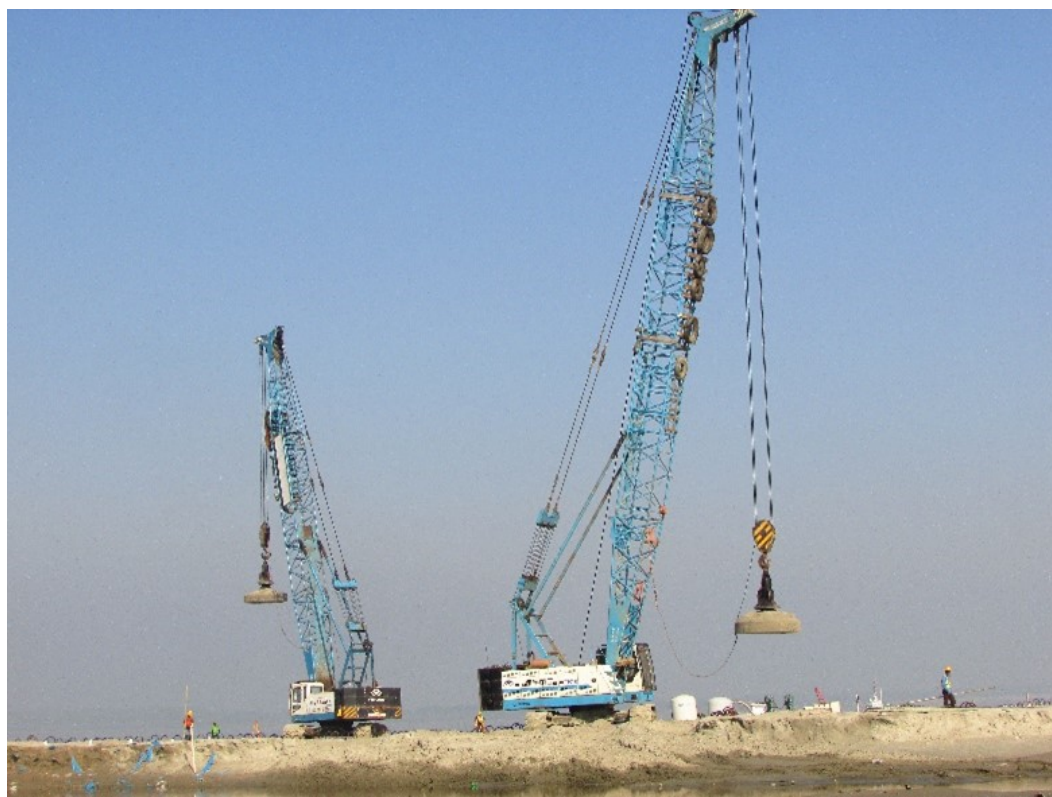


Figure 3.8: Dynamic compaction process at the research site

After the dynamic compaction process was completed, a Vibrating Smooth Wheeled Roller was used to level the surface of the research site to ready the other construction process. Finally, after seven days of HVDM application, the Plate Load Test was conducted to check the bearing capacity of the soil.

3.4.4 Disturbed Sample Collection

Disturb soil sample from the selected location of the research site was collected for the present investigation. Disturbed sample of approximately 1000 kg was collected from the borehole HA16 location through excavation by the excavator. All samples were packed in large polyphone bags covered by gunny bags and were eventually transported to the Geotechnical Engineering Laboratory of Bangladesh University of Engineering and Technology, Dhaka. The initial water content test was carried out from the collected soil sample. After that, the soil sample was dried in air and pulverized for sample preparation of the high vacuum densification method in the physical model.



Figure 3.9: Air drying and pulverization process of collected disturbed sample

3.5 Laboratory Soil Testing Program

3.5.1 Moisture Content test

The water content of fine-grained soils is a vital soil index feature, as their behaviour is greatly affected by water concentration variations. Moisture content affects various characteristics and is frequently used to convert observed bulk density to dry density. It is difficult for water to move through the soil because water and the surfaces of soil particles are attracted to one another, which prevents water from moving freely through soil pores. In this study, the Moisture Content test by the oven-dry method was carried out following ASTM D2216-19 standard. The average moisture content of the collected sample was 42%.

3.5.2 Specific Gravity

Specific Gravity is a crucial soil mechanics characteristic related to mineral content and weathering. Important soil properties, including porosity, dry and saturated density, and saturation level, can all be calculated from these parameters. Specific Gravity is the ratio of a particular volume of soil particles at a specific temperature to an equivalent volume of distilled water at the same temperature. ASTM D854-14 is used to figure out the specific Gravity of the representative sample in this study (standard test methods for specific Gravity of soil solids by water Pycnometer). The Specific Gravity of the representative sample is 2.72.

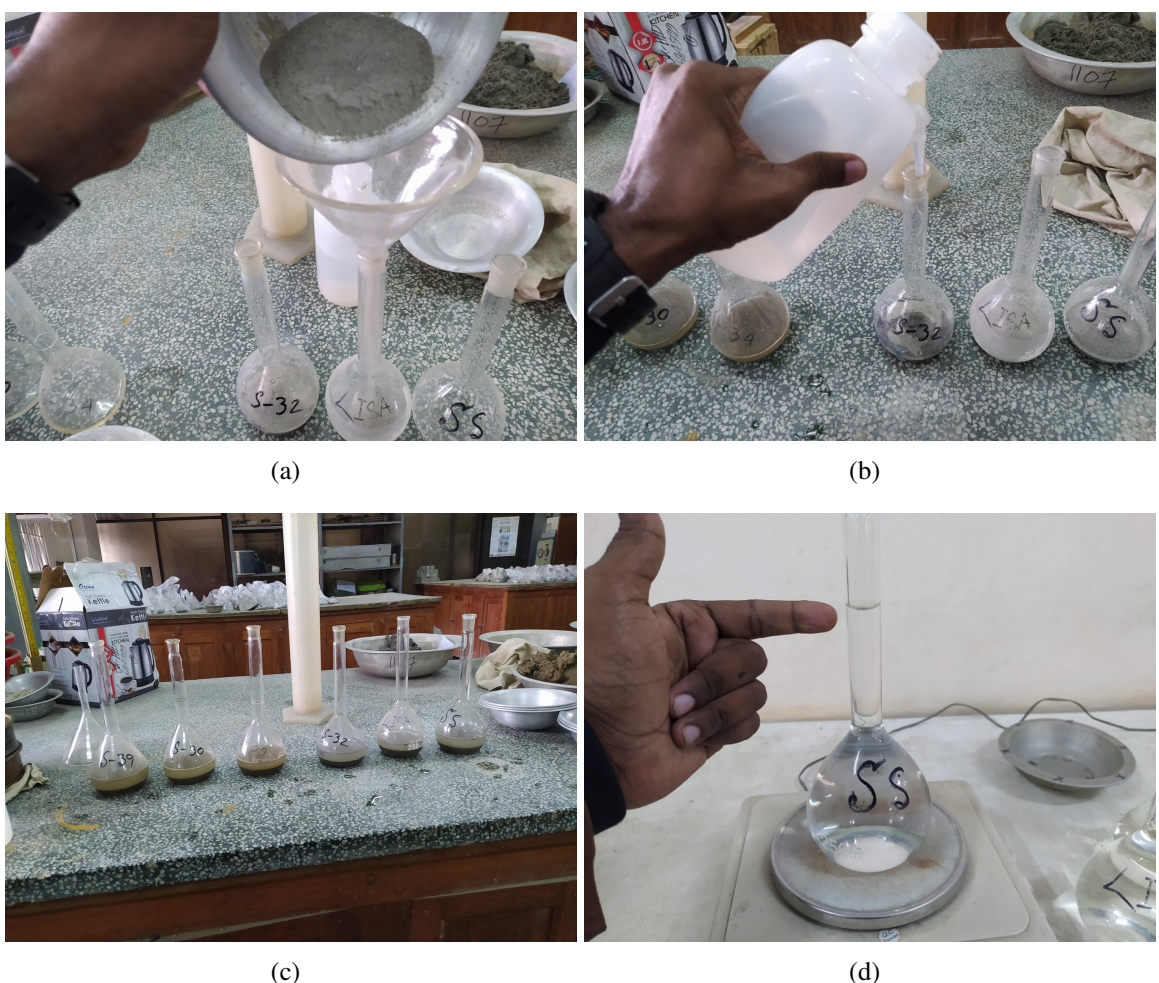


Figure 3.10: Some steps of Specific Gravity Test-(a) Taking the sample in Pycnometer, (b) Mixing water to the sample, (c) After mixing water and sample, (d) Final reading

3.5.3 Index Properties Test

The characteristics of soil known as “index properties” aid in identifying and categorizing soil for general engineering purposes. Typically, these qualities are determined in the laboratory. To determine the index property of the soil, either disturbed samples or remoulded samples can be used. Index properties are also known as the indication of engineering properties such as shear strength, compressibility, and permeability. The geotechnical engineer may often be interested in a quick evaluation of the engineering characteristics without doing extensive experiments, which can only be done if the index properties of the soil are known. Particle size and relative density are the primary index features of coarse-grained soils, whereas the primary index properties of fine-grained soils are consistency and Atterberg’s limit.

3.5.3.1 Sieve Analysis

A sieve analysis test on a representative sample was conducted according to ASTM D422.



After the wash sieve, sieving was carried out on a dry sample for particles retained on a 0.075 mm in wash sieve. Particle size distribution of a soil sample is obtained using sieve analysis, and this approach is only applicable for measuring particle size distribution larger than 0.075 mm. The following steps (Figure 3.11) were taken to conduct a sieve analysis of the representative soil sample. ASTM standard sieve mesh was used for this test. The standard sieves are assembled in ascending order by placing the larger(#4) openings on the top and smaller(#200) on the bottom. Then a lid and a pan were attached to the top and bottom of the series and taken to a mechanical sieve shaker. The mechanical sieve shaker was set for 10 min. After the shaking task, the mass of soil that is retained on each sieve is measured, and the results are represented as a percentage of the sample’s total mass.



Figure 3.11: Some steps of mechanical sieve analysis test-(a) Performing Wash Sieve, (b) Retained Sample after wash, (c) Taking washed dry sample on ASTM Standard Sieve set, (d) Sieve shaking process

3.5.3.2 Hydrometer Analysis

Since mechanical sieve analysis cannot accurately measure the size distribution of soil particles smaller than 0.075 mm, hydrometer analysis was used. Hydrometer analysis can easily obtain particle size distribution from 0.075 mm to 0.001 mm. The hydrometer analysis was conducted following the ASTM D7928-16 standard. The representative sample was sieved through a #200 sieve to get approximately 50 grams of dry soil sample that is finer than 0.075 mm for the purpose of hydrometer analysis. The hydrometer sample is soaked for 12 hours in 125 cc of sodium hexametaphosphate solution and well mixed with a mixture machine. A reading was taken at the point where the hydrometer stem and the reference solution created a meniscus. A reading greater than zero is recorded as a positive (+) correction, whereas a reading less than zero is recorded as a negative (-) correction. This value is known as zero correction. Also, the adjustment for the meniscus is the vertical distance between the upper edge of the meniscus and the liquid level in the reference container. It is also called meniscus correction. During the test, (-) 1 and (+) 5 were recorded as zero correction and meniscus correction, respectively, for the representative sample. Before taking hydrometer readings, The cylinder was appropriately mixed with the help of a mixer and inset a hydrometer immediately. After that, the hydrometer reading was recorded at elapsed times of 0.25, 0.5, 1, 2, 4, 8, 15, 30, 60, 120, 240, 480, and 1440 minutes. Also, the temperature of the sedimentation jar was recorded simultaneously. In order to eliminate any potential sources of ambiguity, the test is carried out with great care. Figure 3.12 illustrates the hydrometer analysis test procedures.



Figure 3.12: Some steps of Hydrometer analysis test-(a) Taking dry sample into the jar, (b) Add chemical and water to the sample, (c) Mixing After 12 hrs soaking, and (d) Start to take reading

3.5.3.3 Permeability Test

In the presence of a potential gradient, water moves through the soil's pores from high to low potential. The soil particles' surface provides resistance to the flow of water. When the voids are more irregular and narrower, the water flow is encountered with more resistance. On the other hand, the more open the voids are, the more easily water can move through the soil. If the soil grains are larger, there will be more space between them, and the pores will be better connected. This means that much water can flow through them easily, and the water flow will be higher, which means the soil is more permeable. Two different types of laboratory tests are typically used to measure the coefficient of permeability. Those are 1. Constant head permeability and 2. Falling head permeability. For this study, the Falling head permeability test was conducted on representative soil following the ASTM D5084-16a standard. A relatively small soil sample is used for the falling head permeability test and

Chapter 3. Field and Laboratory Investigation

water is allowed to flow through it while being attached to a standpipe that serves as both the water head and a gauge for the amount of water passing through the sample. The test's first step involved letting water flow through the sample until the amount of water in the standpipe exceeded a predetermined minimum standard. The time it took for water in the standpipe to flow down from the highest to the lowest point was recorded. Figure 3.13 shows some steps of conducting Falling head permeability test.



(a)



(b)



(c)

Figure 3.13: Conducting Falling head Permeability test-(a) Permeability test arrangement, (b) Falling head apparatus Setup, and (c) Execution of Falling Head test

3.5.3.4 Relative Density

The relative density or density index of soils can be defined as their state of compactness with respect to its loosest and densest possible state.

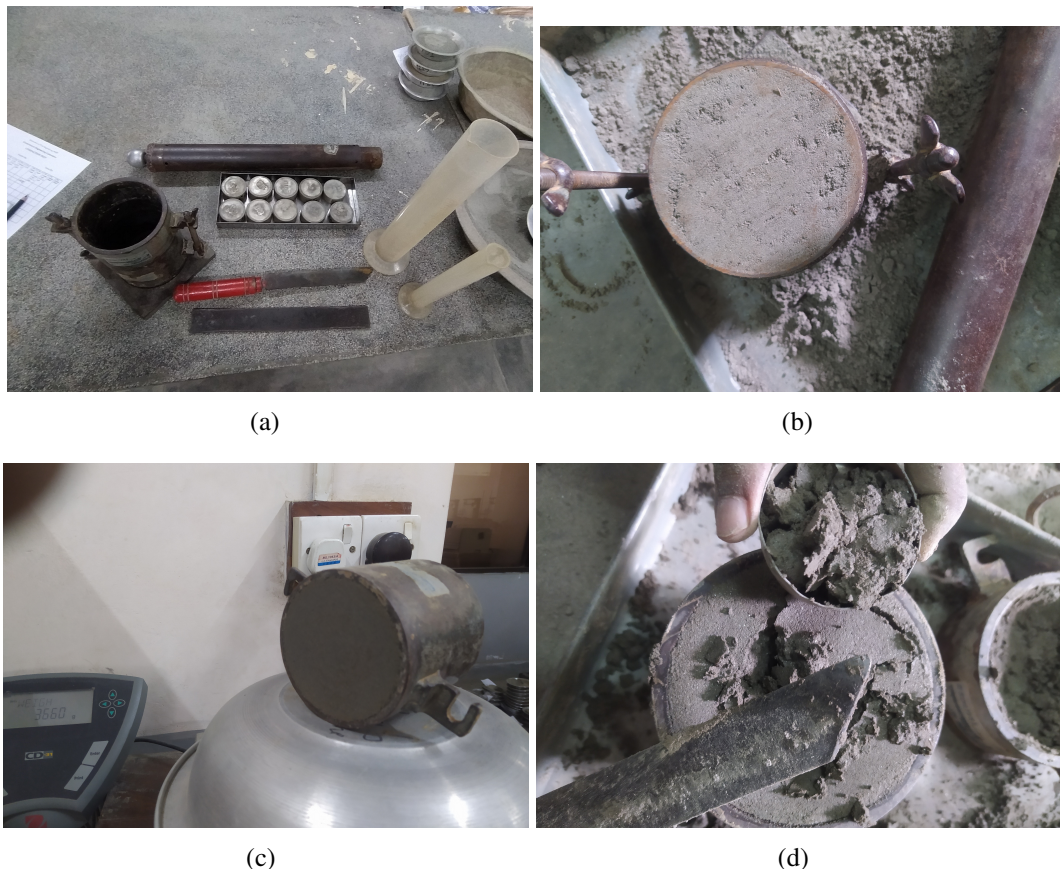


Figure 3.14: Conducting Relative Density test-(a) Measuring the initial height before the test, (b) Setup the mould in the vibrator machine, (c) Measuring the final height after vibration, and (d) Final compacted Soil

Relative density calculates how dense cohesionless soil is compared with its maximum density. Calculating relative density requires determining the maximum and minimum densities of the soil. The relative density test of the representative sample was conducted by following the ASTM D4253-16e1 standard at BUET Geotechnical laboratory. Figure 3.14 shows some steps of conducting Relative Density test of the representative sample.

3.5.4 Standard Proctor Test

The Proctor Compaction Test establishes the maximum dry density that a particular type of soil can be compacted using a controlled compactive force at an optimum moisture content. This is the most common laboratory soil test and the basis for all engineered compacted soil placements for embankments, pavements, and structural fills. In-situ measured densities of the compacted fill are compared to the Proctor test results to determine the degree of soil density(or compaction). For this research, the Standard Proctor test was executed by following ASTM D698-12(2021) standard. Figure 3.15 represents some steps of conducting Standard Proctor test of representative soil.





(e)

Figure 3.15: Executing Standard Proctor test- (a) Standard Proctor test Apparatus, (b) After compaction of the sample, (c) Weighting the compacted sample, (d) Taking Sample for moisture content, and (e) 5 trials samples collection for moisture content

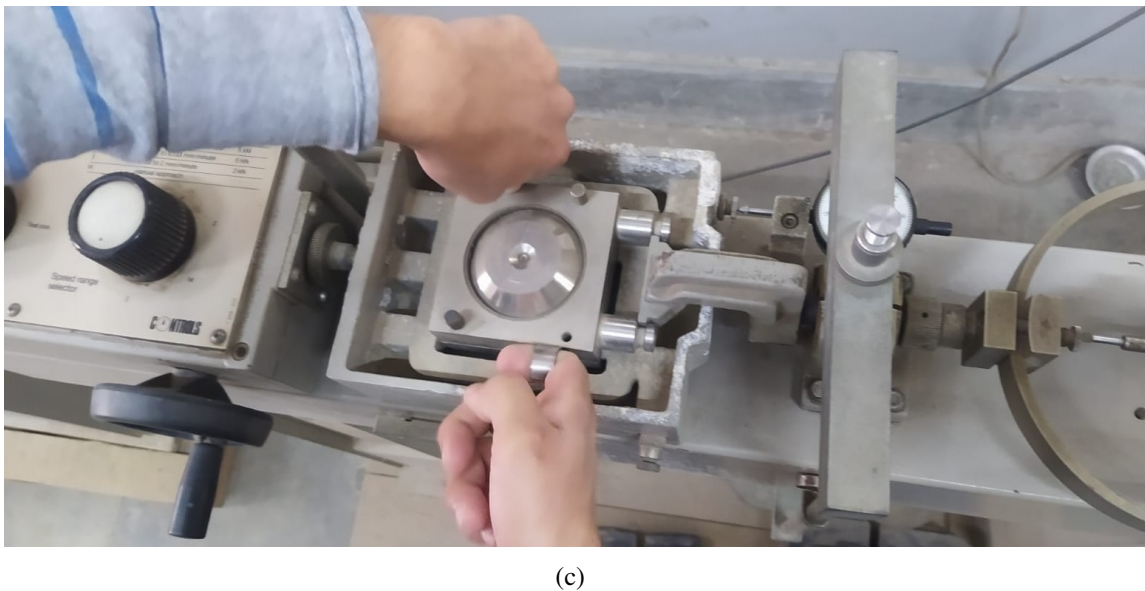
3.5.5 Direct Shear Test

The direct shear test of soil is a relatively simple shear strength test run on cohesive or non cohesive samples of an undisturbed or remoulded soil sample to evaluate the shear strength properties. The test can be carried out with different moisture contents; however, it is common to saturate the sample before running the test.



(a)

(b)



(c)

Figure 3.16: Executing Direct Shear Test-(a) Undisturbed Sample, (b) Placing sample into the shear box, and (c) Direct Shear Test full setup

For this research, the consolidated drain test was carried out on three undisturbed specimens of HVDM treated samples following ASTM D3080-04 guidelines. In order to carry out a direct shear drained test using the shear box, the specimen was first allowed to consolidate completely under the normal load provided. Then the shear displacement was delivered to the soil. Following consolidation stage, the specimen was progressively sheared over two to three hours to maintain drained shearing. In order to determine the shear strength, normal stresses of 31, 62, and 124 kPa were applied to the test. Figure 3.16 shows some basic steps of conducting Direct shear drained test.

3.5.6 Unconfined Compressive Strength Test

The Unconfined Compression Test derives the Unconfirmed Compressive Strength of a soil. The Unconfirmed Compressive Strength (UCS) stands for the maximum axial compressive stress that a specimen can bear under zero confining stress. Since stress is applied along the longitudinal axis, the Unconfined Compression Test is also known as Uniaxial Compression Test. This test is strain-controlled, and when the soil sample is loaded rapidly, the pore pressures undergo changes that do not have enough time to dissipate. Hence it is representative of soils in construction sites where the rate of construction is speedy, and the pore waters do not have time to dissipate. For this research, 7 sets of HVDM treated undisturbed and 4 sets of remoulded samples were tested in BUET geotechnical laboratory following ASTM D2166-06 guidelines. Those test's results are presented in Chapter 5. Following Figure 3.17 presents some procedures of execution of UCS test.

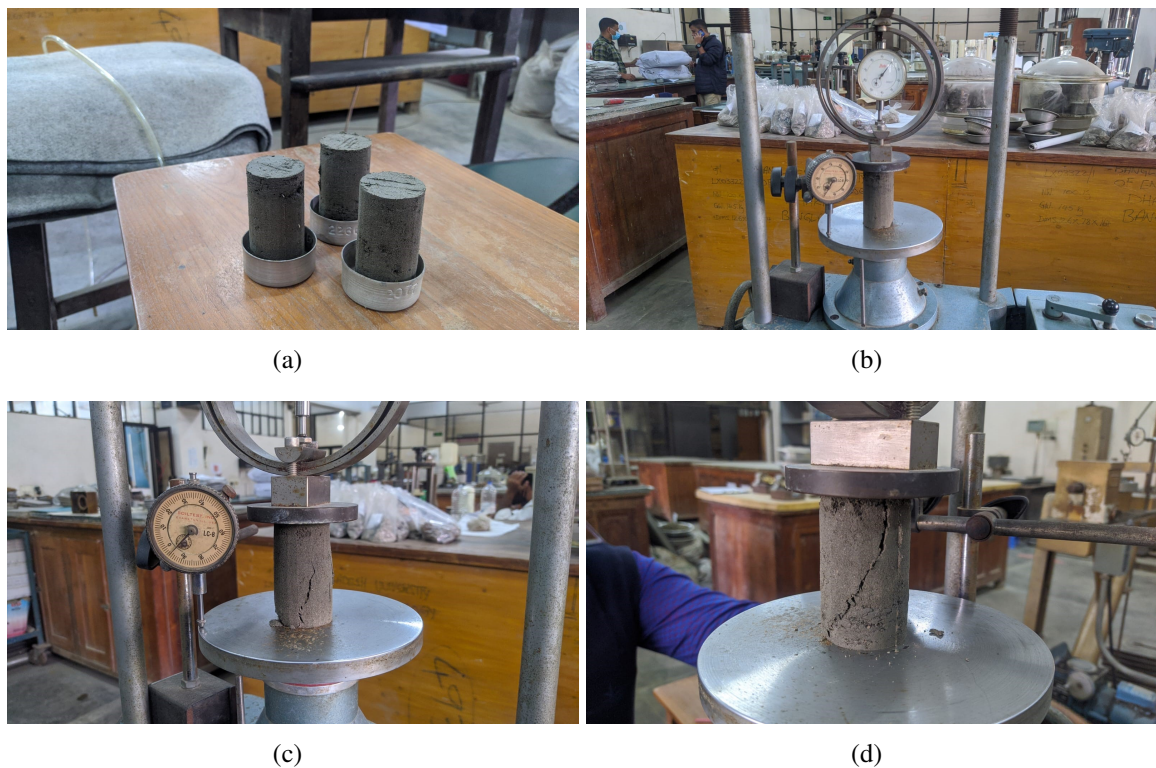


Figure 3.17: Executing Unconfined Compressive Strength test-(a) Undisturbed ready samples, (b) UCS machine setup , (c) Failure of sample-1 at maximum axial compressive stress, (d) Failure of sample-2 at maximum axial compressive stress

3.5.7 1D Consolidation Test

The consolidation test determines the rate and magnitude of soil consolidation when the soil is restrained laterally and loaded axially.

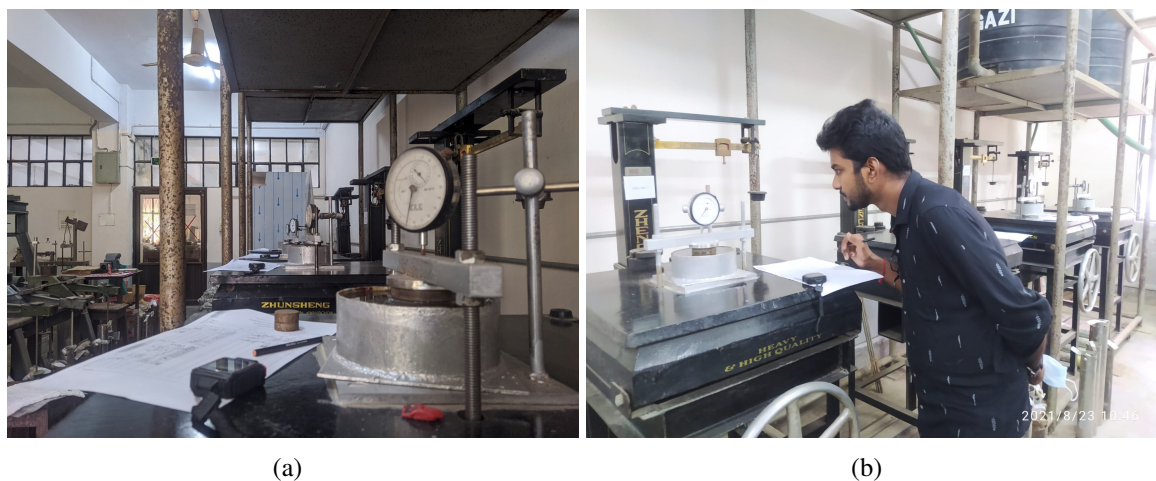


Figure 3.18: Conducting consolidation test-(a) Consolidation test setup and (b) Taking dial reading

The Consolidation test is also referred to as the Standard Oedometer test or One-dimensional compression test. This test is carried out on fully or partially saturated soil specimens, especially in cohesive soils. When a load is applied to a low permeability soil, it is initially carried by the water that exists in the porous saturated soil. This results in a rapid increase in pore water pressure. This excess pore water pressure is dissipated as water drains away from the soil's voids. The pressure is transferred to the soil skeleton, which is gradually compressed, resulting in settlements. The consolidation procedure lasts until the excess pore water pressure is dissipated. The consolidation test was conducted for this research on HVDM-treated undisturbed and remoulded samples following ASTM D2435. The details of the results are presented in chapter 5.

3.5.8 Triaxial Compression Test

The Triaxial Compression test is a mechanical soil test in which a cylindrical specimen of soil or rock encased in an impervious membrane is subjected to a confining pressure and then loaded axially to failure in compression. The confining pressures are generated in a fluid chamber to simulate stresses from surrounding soil materials. It then can give a clearer picture of the behaviour of materials in place.

The shear strength of saturated soil in Triaxial compression test depends on the stresses applied, time of consolidation, strain rate, and the stress history experienced by the soil. In this test, the shear characteristics are measured under drained conditions and are applicable to field conditions where soils have been fully consolidated under the existing normal stresses and the normal stress changes under drained conditions similar to those in the test method. The shear strength determined from the test is commonly used in embankment stability analysis, earth pressure calculations, and foundation design. There are three primary Triaxial tests conducted in the laboratory, each allowing the soil response for differing engineering applications to be observed. These are

- Unconsolidated Undrained test (UU)
- Consolidated Undrained test (CU)
- Consolidated Drained test (CD)

CD tests can be performed on all types of soils. Drainage is allowed in both phases of Triaxial testing; isotropic consolidation and shearing. The soil is consolidated under a chosen confining pressure, and after completion of the consolidation, it is tested for shear by applying deviator stress gradually at a slow strain rate while allowing full drainage. It takes more time to complete a test than the CU test, commonly known as the “slow” test, which is seldom

Chapter 3. Field and Laboratory Investigation

conducted except for research interests. For this research Triaxial Consolidated Drained test (CD) was carried out on HVDM-treated undisturbed and remoulded sample. During the CD test, the specimen is allowed to consolidate completely under the confining pressure prior to the application of axial load. The confining pressure acts as an effective stress throughout the soil specimen. The axial load is applied at a slow rate (0.025 mm/min) to allow drainage of pore water so that there is no buildup of excess pore water pressures, the stresses imposed by the axial load are effective stresses. The shear stresses induced in the specimen by the axial load result in failure. The details of the results are presented in Chapter 5. Figure 3.19 shows some procedures of execution of Triaxial CD test.



(a) Sampling arrangement

(b) Wearing membrane to soil sample

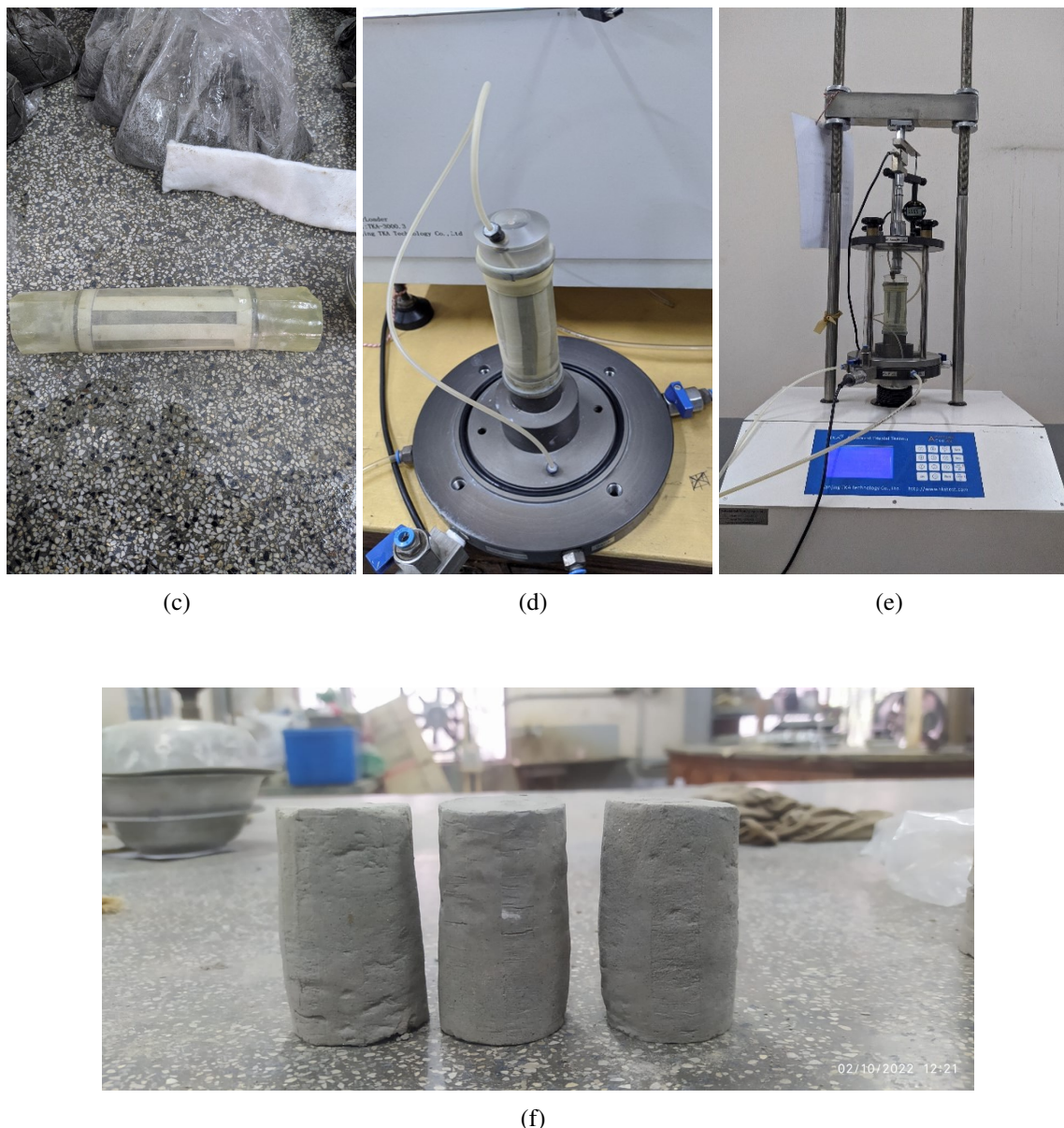


Figure 3.19: Some steps of Triaxial CD test-(a) Sampling arrangement, (b) Wearing membrane to soil sample, (c) Ready sample for triaxial Test, (d) Sample loading on Triaxial Apparatus, (e) After full setup of Triaxial machine, and (f) Three specimens after successful execution of Triaxial CD test

3.6 Summary

This chapter describes research site geology, field HVDM procedures, and laboratory soil testing program. A site visit event was arranged to see the field procedure of HVDM. The site visit described step-by-step HVDM procedures and disturbed sample collection with soil bore log. Different types of soil index properties and mechanical tests conducting procedures were also described. For comparison, some mechanical tests of soil were done on remoulded and HVDM-treated samples.

Chapter 4

Experimental Investigation Program

4.1 General

The primary scientific problems should be addressed in developing the physical model, which in turn is based on the study's objectives. The primary actions involved in the construction of the model include determining the type of physical model, the size of the physical model, the scale factor, the analogue materials, and the instrumentation of the model. An extensive and complicated structure (such as an underground excavation, building, or buried structure) is “Prototyped,” or scaled-down, to replicate the structure’s actual behaviour under relevant loading conditions using physical modelling. Analytical expressions between their pertinent geometrical and physical properties to determine the connection between the prototype and the model (similarity, similitude laws or scale factors). There are many reasons why engineers might opt to use a small-scale physical model to analyse an engineering problem. However, the main ones are the model’s low complexity, and cost, it’s ability to shed light on the behaviour of complex structures or processes, and it’s ability to provide experimental data for validating numerical models, and parametric studies. This chapter briefly describes the experimental setup and methodological steps to simulate the High Vacuum Densification Method in a prototype 1g physical model.

4.2 Physical Model

Using laboratory small-scale physical modelling to replicate wide range of geotechnical phenomena is a powerful technique. The ISSMGE Technical Committee (TC104) defines physical modelling as “a reduced physical representation of a finite boundary problem for which similarity is sought in the framework of scaling laws” (Al Heib et al., 2020). Physical modelling has been widely used for many years in civil and environmental engineering (Green, 2014). Since it helps with visualizing the problem, validating, and qualifying the numerical modelling (Shiau et al., 2016). The Complex physical problems can also be solved by physical modelling and experimentation; the advantages of practical instruction and utilising experimental efforts have been widely documented (Shiau et al., 2016). Size reduction, simplicity, convenience, and the examination of complicated systems are some of the advantages of physical modelling. It helps to verify theoretical and analytical approaches

by providing experimental data and observations. The kind of physical model is determined by how similar the prototype is on a large-to-small scale and from 1g to ng scales (Aklik et al., 2010; Allersma, 1996).

4.2.1 Model Type

Physical modelling in the geotechnical field has been focused on small-scale laboratory models due to the constraints of full-scale simulation. Experiments are carried out primarily using two distinct methodologies: geotechnical centrifuge, and unit gravity, sometimes known as the 1 g and n-g model. The centrifuge method requires the test to be carried out within a predetermined container while the container is rotated around a vertical axis. Depending on how quickly the rotation occurs, this will produce an artificial form of gravity.



Figure 4.1: Beam geotechnical centrifuge in University of California (after Zhou et al., 2018).

The goal is to achieve consistent soil behaviour between the prototype and the scale model by applying analogous stresses in the real world. This notion not only overcomes a significant obstacle in geotechnical modelling but also makes it possible to improve the accuracy of the findings acquired. On the other hand, centrifuge modelling has several inherent constraints, the most notable of which is that the small container size creates challenges for the loading and monitoring systems. The second method, known as “unit gravity laboratory modeling”,

Chapter 4. Experimental Investigation Program

comprises conducting studies in a controlled setting under “normal gravity” conditions. This approach is often utilized in the discipline of geotechnical engineering. In the field of Geotechnical Engineering, this method is frequently used. This facilitates actualization of more comprehensive models, sophisticated loading and monitoring systems, and more extensive experimentation. The low degree of stress, however, causes practical challenges. First, it is essential to use correct scaling rules to compensate for this stress level discrepancy to achieve significant results. Second, experimental variability (how the system is mounted and moves) becomes more critical and affects the ability to repeat the experiment.



Figure 4.2: 1g physical model of shaking table (after Hore et al., 2020)

4.2.2 Scale Factor

In order to develop a scale model that is representational of a given phenomenon, it is necessary to take into consideration all of the factors that are involved in that phenomenon. “Scaling laws” refers to the process that was utilized in order to scale the prototype. Centrifuge simulation has light scaling laws because it conserves genuine stress and soil dynamics. These laws consider, in addition to the dimensions, several other criteria depending on the problem being addressed (time, viscosity, permeability, etc.). The 1g scaling method is utilized for the purposes of this investigation. In order to account for the difference in stress levels between the prototype and the scale model, this technique incorporates supplementary laws. The objective of building this 1g prototype physical model is to investigate the vacuum

Chapter 4. Experimental Investigation Program

consolidation and dynamic compaction process of soft soil treated by the High Vacuum Densification Method. When all of the rules of similitude (Scaling laws) are followed, a model can be said to represent the actual accurately. (Wood, 2004) and (Garnier et al., 2007) used this approach to determine three scale factors—geometric scale factor, influential stress scale factor, and effective stress-gradient ratio—to be considered in developing physical models. When doing small-scale physical modelling, the length is typically used as the reference, and the geometric scale factor may be calculated using the formula $L^* = L(m)/L(p)$, where $L(m)$ is the length of the model, and $L(p)$ is the length of the prototype. This is known as the length scale factor. Since $L^* = 1/n$ and L^* is less than 1. Both the geometric scale factor and the scale factor on gravity and unit weights contribute to the formation of the scale factors that govern the effective stress and the gradient of that stress with depth. The scaling factors for this investigation are presented in Table 4.1.

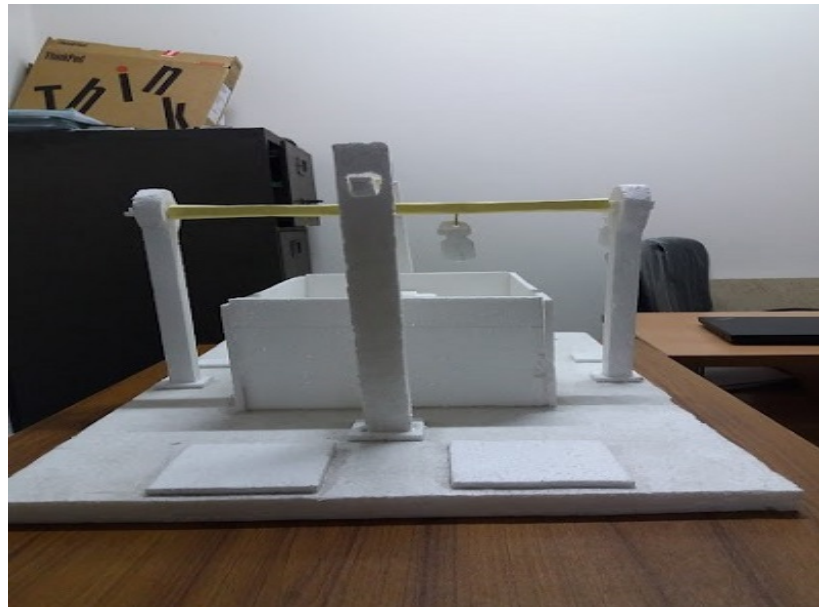
Table 4.1: Scaling factors in physical model testing

	Parameter	Unit	Prototype(P)	Field Section(F)	Scale factor(P/F)
Prototype size					
Length	m	0.9144	4.5	0.2	
Width	m	0.6096	3	0.2	
Area	m^2	1.8288	13.5	0.14	
Compaction Parameter					
Hammer Diameter	m	0.02	2	0.01	
Hammer Weight	m	5	100000	0.0005	
Drops Height	m	2.1336	15	0.14224	
Vacuum consolidation Parameter					
Vacuum Pipe Diameter	m	0.016	0.0254	0.63	
Vacuum Pipe Length	m	1.89	3	0.63	
Vacuum Pressure	kPa	80	80	1	
Dynamic & Kinematic	Acceleration	m/s^2	1	1	1
	Gravity	N	1	1	1
	Time	Sec	1	1	1

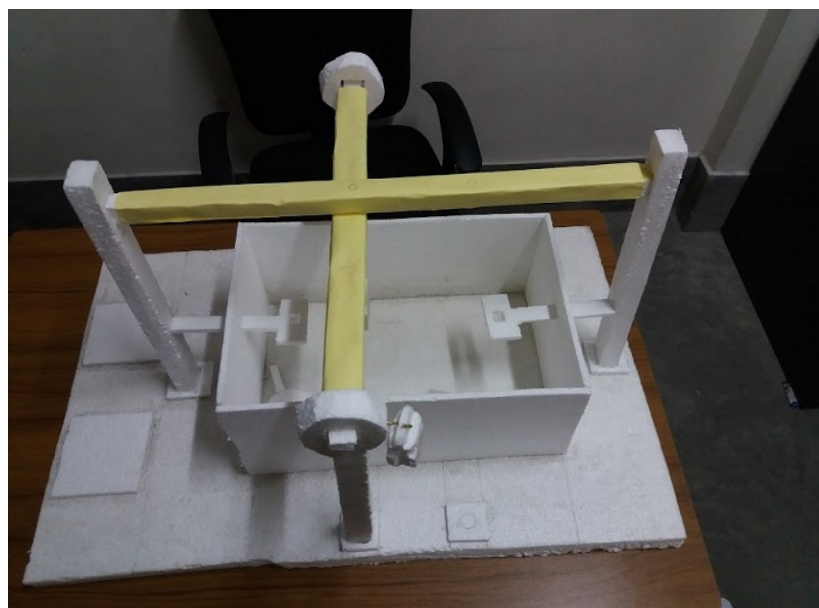
4.3 Physical Model Design and Implementation

4.3.1 Planning Of 1g Physical Model

During the field visit, the methodology of the High Vacuum Densification Method was captured. From this field idea and literature, it was decided to make a physical model to simulate the HVDM at the laboratory. After deep research on the HVDM, a prototype cork sheet model was built (Figure 4.3). Then it has been decided to make this 1g physical prototype model in the workshop.



(a)



(b)

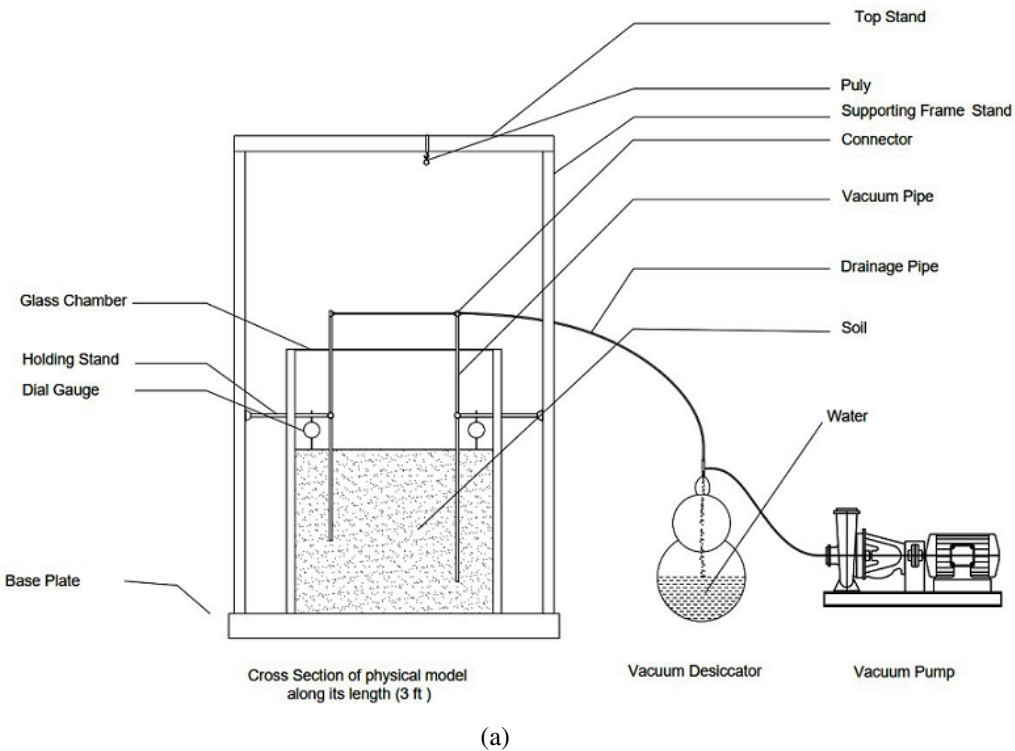
Figure 4.3: Cork sheet dummy model idea-a) Side view of Cork sheet dummy model, (b) Top view of Cork sheet dummy model

4.3.2 Test Facility

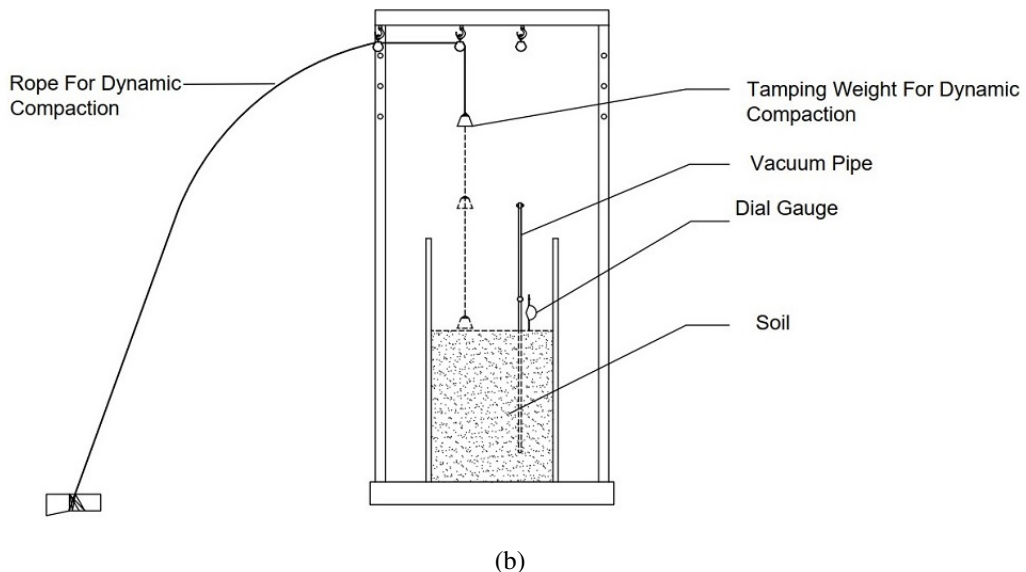
The prototype's primary purpose was to simulate the high vacuum densification method similar to the field. All the arrangement of the prototype physical model considered the necessary to simulate the HVDM in the laboratory. The test facility developed in this study consists of a steel test box, dynamic loading frame, vacuum pump, drainage system, water level monitoring system, vertical and horizontal drain, pore pressure measuring sensor,

Chapter 4. Experimental Investigation Program

vertical displacement sensor, dial gauges, and vacuum sealing system.



(a)



(b)

Figure 4.4: Schematic view of the experimental setup of 1g physical model-(a) Vacuum Consolidation Stage of Physical Model, (b) Dynamic Compaction Stage of Physical Model

The schematic view of the experimental setup is given in Figure 4.4. The details of the above facilities are presented in the following sections.

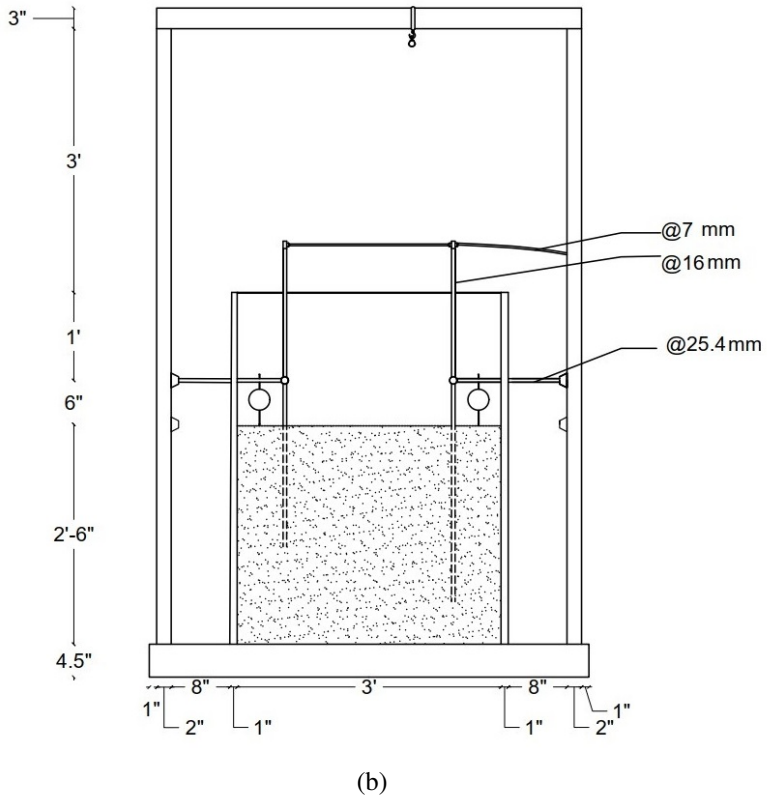
4.3.3 Equipment and Materials

4.3.3.1 Test Box

A rectangular rigid steel test box of inner dimensions 2 ft \times 3 ft \times 4 ft with 10mm wall thickness was fabricated and used for conducting the experiments in the laboratory. An MS plate thickness of 4.5 inch and dimensions of 4 ft \times 5 ft are used for the model's base. The box has four vertical stands with a height of 7 ft; among them, two are fixed along the box length(Figure 4.5(a) notation B), and two are movable for changing the location of the dynamic compaction point along the length of the box(Figure 4.5(a) notation D). On two sides of the box along its length, a transparent glass of 10mm thickness is used to see the soil conditions from the outside of the box (Figure 4.7(a) notation A). An anchoring system is arranged inside the box to hold the soil sample in a stable position(Figure 4.7(a) notation B). A drainage system is created for washing the box after the experiment in the base of the box (Figure 4.7(a) notation C).



Chapter 4. Experimental Investigation Program



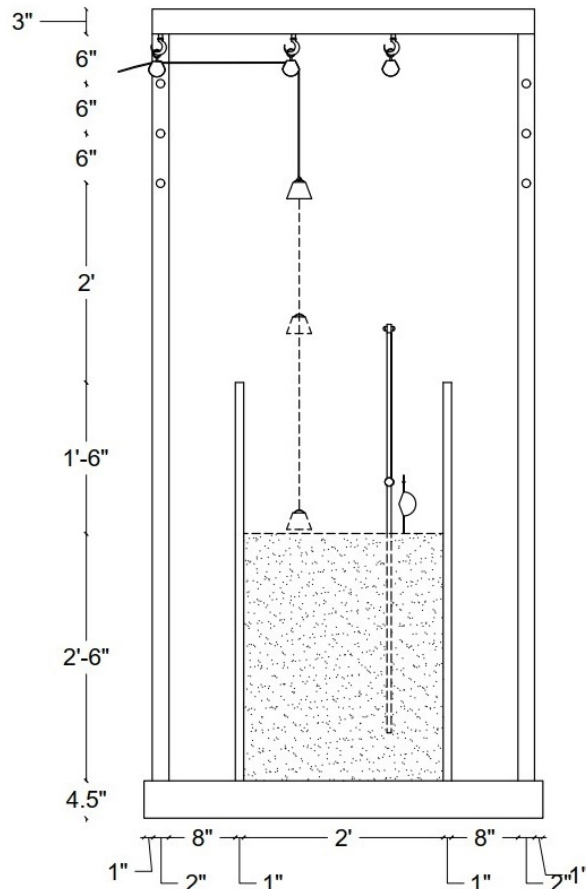
(b)

Figure 4.5: Side view of Physical model - (a) Actual Physical Model Side View, (b) Cross section of the Model with dimension (side view along its length)



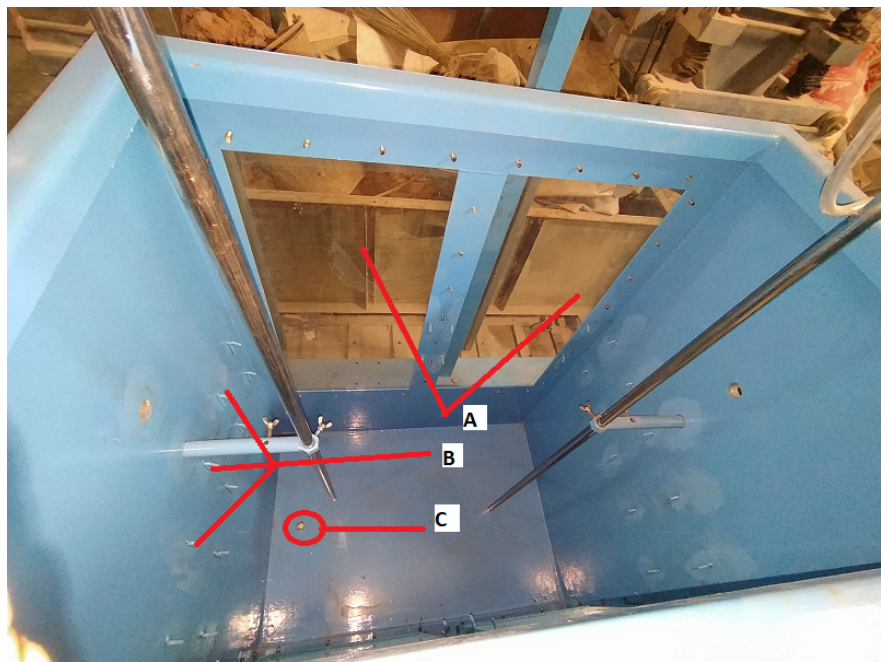
(a)

Chapter 4. Experimental Investigation Program

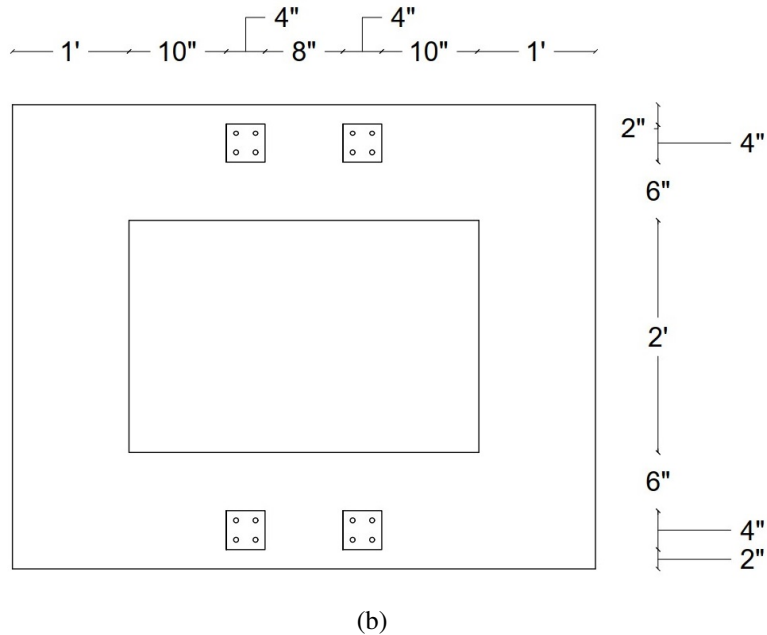


(b)

Figure 4.6: Side view of Physical model-(a) Actual Physical Model Side View,(b) Cross section of the Model with dimension (side view along its width)



(a)



(b)

Figure 4.7: Top View of Physical Model-(a) Actual Physical Model Top View, (b) Top view with dimension

4.3.3.2 Dynamic Compaction Arrangement

A framework is attached to the test box for dynamic compaction purposes. It contains four vertical steel stands holding two horizontal stands (Figure 4.5(a) notation B & D notation). The vertical stands support the top horizontal stand that holds the rope with pulley for the tamping weight (Figure 4.8b). Based on the design requirements at improvement depth, a 5 kg and diameter of 20 mm iron metal tamper was employed for tamping purposes (Figure 4.8a).



(a)



(b)

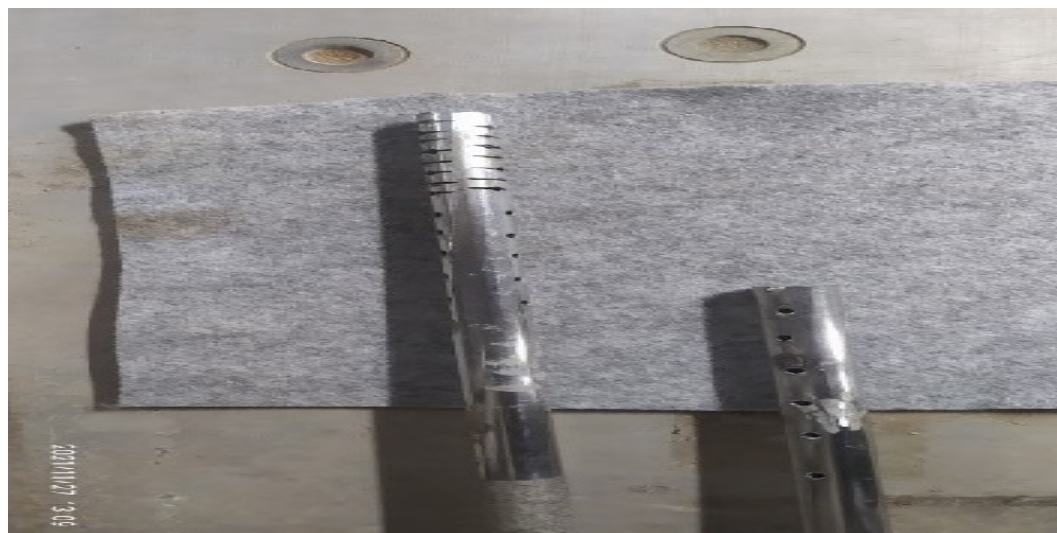
Figure 4.8: Dynamic compaction arrangement- (a)5 kg iron metal tamper, (b) Tamping rope with pulley holding the tamper

4.3.3.3 Vacuum Arrangement

The vacuum consolidation arrangements consist of vacuum pipes, a vacuum pump, and a vacuum sealing system. A brief description is given for the all-vacuum arrangements system in this section.

Vacuum Pipe

Two vacuum pipes were used for this experiment as the vacuum pipes used in the field. Both of them are modified according to the field used vacuum pipes. The inner diameter of the pipe is 16 mm, with 2 m and 2.5 m lengths. In the bottom, the vacuum pipe was perforated similar to the perforated vacuum pipe used in the site. Figure 4.9(a) shows the vacuum pipe used in this experiment. Also, a nylon membrane (Figure 4.9c) was used in the vacuum pipe's perforated area to prevent the pipes' blockage during the experiment.



(a)

Chapter 4. Experimental Investigation Program



(b)



(c)

Figure 4.9: Vacuum pipe arrangement-(a) Perforated vacuum pipe, (b) Nylon membrane, and (c) Nylon membrane attached vacuum pipe

Vacuum Pump

Rocker 300 vacuum pump was used for this experiment to apply vacuum in the soil. The vacuum pump has a regulator and a maximum vacuum capacity of 100 kPa. The dimension of the pump was 26.8 x 13.5 x 20.4 cm, and the weight was 4.1 kg.



Figure 4.10: Vacuum pump

Vacuum Sealing System

A vacuum sealing system is attached to the top of the test box, and build arrangement for air proofing. The vacuum sealing system is made of rubber glass, and for sealing purposes, silicon gum was applied with the help of a silicon gun.



Figure 4.11: Vacuum sealing system

4.3.3.4 Drainage Arrangement

The drainage arrangement consists of a vertical and horizontal drainage system and an outlet for collecting drainage water. The vertical vacuum pipe is connected with a small diameter pipe horizontally to drain the water from the soil sample and store it in a desiccator. For horizontal drainage purposes, the prototype model has four horizontal drainage systems at different depths of the machine. For the application of HVDM, this horizontal drainage is not required. If another ground improvement method is applied to the model, the horizontal drainage system will be used for horizontal drainage purposes. For this HVDM experiment, horizontal drainage system was used for holding the dial gauges with holding stands.

4.3.3.5 Water Level Monitoring System

A water level monitoring system was attached to the test box. Also, a 100 cm scale was attached to the test box, and a 5 mm diameter transparent glass pipe was set from the base level of the model. This water table monitoring device is built to check the capillary action rise of the soil.

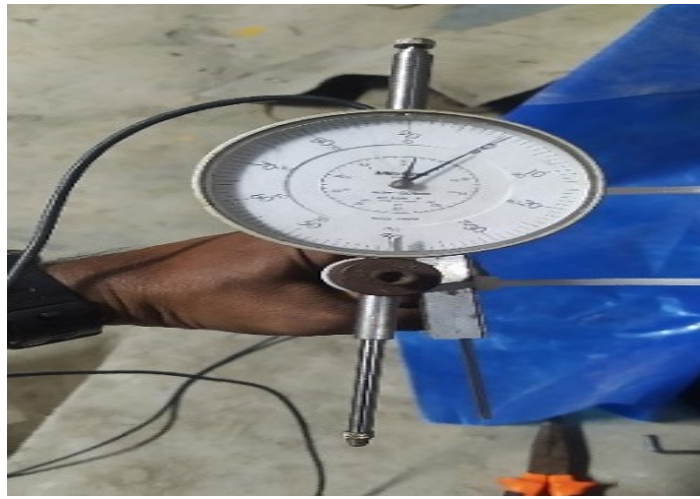


Figure 4.12: Water Level Monitoring System

4.3.3.6 Vertical displacement measuring arrangement

In this physical model, four vertical displacement devices were used to measure soil samples' vertical displacement or settlement. Among them, two were 50 mm dial gauges for measuring the manual settlement, and another 2 LVDT sensors with data loggers were used for continuous settlement monitoring purposes.

Chapter 4. Experimental Investigation Program



(a)



(b)



(c)

Figure 4.13: Vertical Displacement Measuring setup-(a) 50mm manual dial gauge, (b) 50 mm digital dial gauge, and (c) Dial gauge with LVDT sensors setup

4.3.3.7 Pore Pressure Measuring Arrangement

This physical model test used a pore pressure sensor for pore pressure measuring purposes. The sensor has a measuring range of 70 kPa.

4.3.3.8 Data Acquisition System

Data collection software DCS 100A was installed on personal computer. This Windows based software provides a means of remote configuration of instruments, data collection, and trend plot display. KYOWA datalogger with three channels each was used to record data.



Figure 4.14: Data Acquisition System

4.4 Methodology of Experimental Investigation

4.4.1 Trial on Physical Model

After completing the setup and placement of the physical model, it was decided to execute some trials to measure the workability and accuracy of the model before the actual experiment. All trials of the model are briefly described below.

4.4.1.1 Trial 1

This trial used 700 kg medium fine sand as a dummy sample. The dummy sample was loaded in the text box and added water to the sample. After the addition of water to the dummy sample, the vacuum was run through the vacuum pipe, and it was found that the vacuum

Chapter 4. Experimental Investigation Program

pressure was unable to control by the regulator because of air leakage from the sample. It was recommended to use a glass chamber on the top surface of the box.

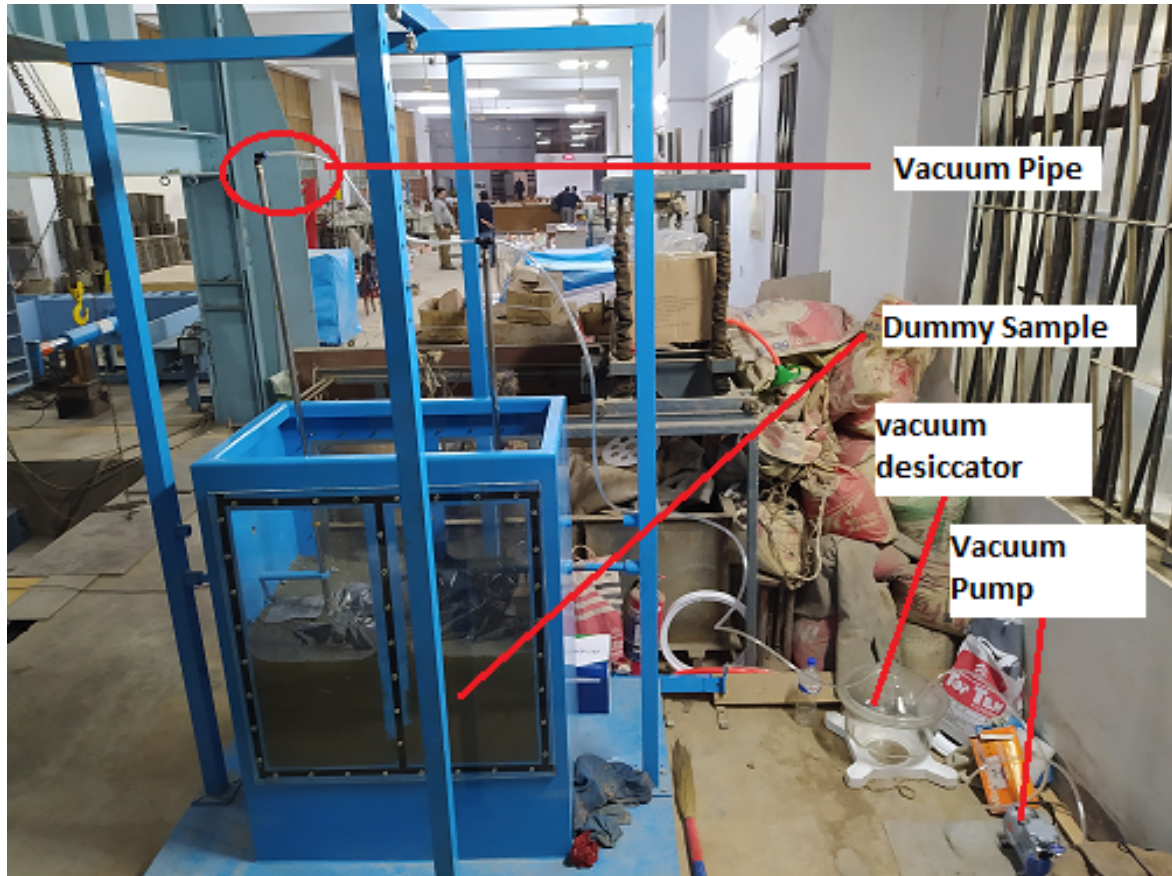


Figure 4.15: Trial-1 experiment with dummy sample

4.4.1.2 Trial 2

After trial 1, a glass chamber was built to airproof the box for applying the vacuum. The attachment of the glass chamber was unable to fix air leakage. In this trial, grease was used to stop the air leakage. However, grease could not prevent air leakage and chamber glass was found bent due to the vacuum pressure. Strong support under the chamber glass and silicon glue was recommended as a solution.

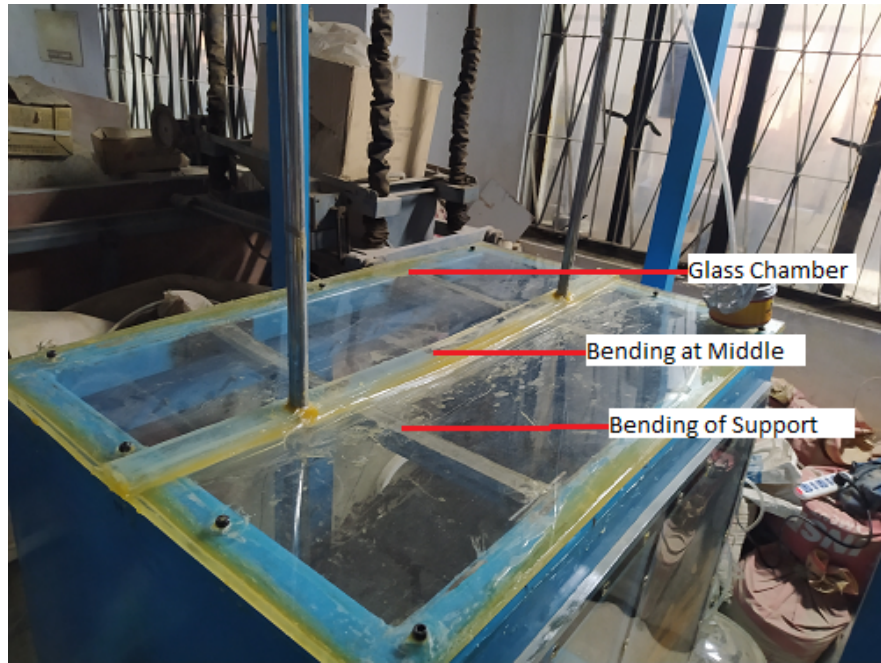


Figure 4.16: Trial-2 experiment with dummy sample

4.4.1.3 Trial 3

After building a perfect supporting system under the chamber glass and using silicon glue, the air leakage problem was solved in trial 3. A water table monitoring system was recommended to measure the water level in the soil sample of the model.



(a)



(b)

Figure 4.17: Checking process in Trial-3- (a) Stronger support, and (b) Using silicon gum for air proofing

4.4.1.4 Trial 4

After adding the water level system to the model, 40 % fine sand and 60 % silty clay were mixed and prepared for the final trial. In this trial, everything was working perfectly, and the glass chamber was not required to prevent air leakage from the sample for impervious behaviour of clay mixed sample. After this final trial, all necessary steps were taken for the final HVDM experiment.

4.4.2 Procedure of The Experiment

The whole experiment was divided into five sections for conducting HVDM in the physical model. All the steps are described briefly in the following sections.

4.4.2.1 Sample Preparation

The representative sample was air-dried and well-pulverized. The experiment requires around 600 kg of sample and considers adding 30 % water by sample weight. Firstly, 5 kg sample was taken in the sample mixing machine (Figure 4.18) and about 30 % of water by weight was added to the 5kg sample and mixed using the mixer machine. After mixing the sample, it was transferred to the physical model. This process was continued until the sample reached the desired depth (2.5 ft from the base of the physical model).



(a)



(b)

Figure 4.18: Sample preparation arrangement- (a) Soil Mixer Machine, and (b) Soil Mixing Procedures

4.4.2.2 Model Setup

Before the soil sample loaded on the model box, two vacuum pipes at two variant depths, 1 ft and 2 ft, were fixed with the help of a modified handle on two ends of the box. Then the prepared sample was loaded into the box. During the sample loading process, a pore

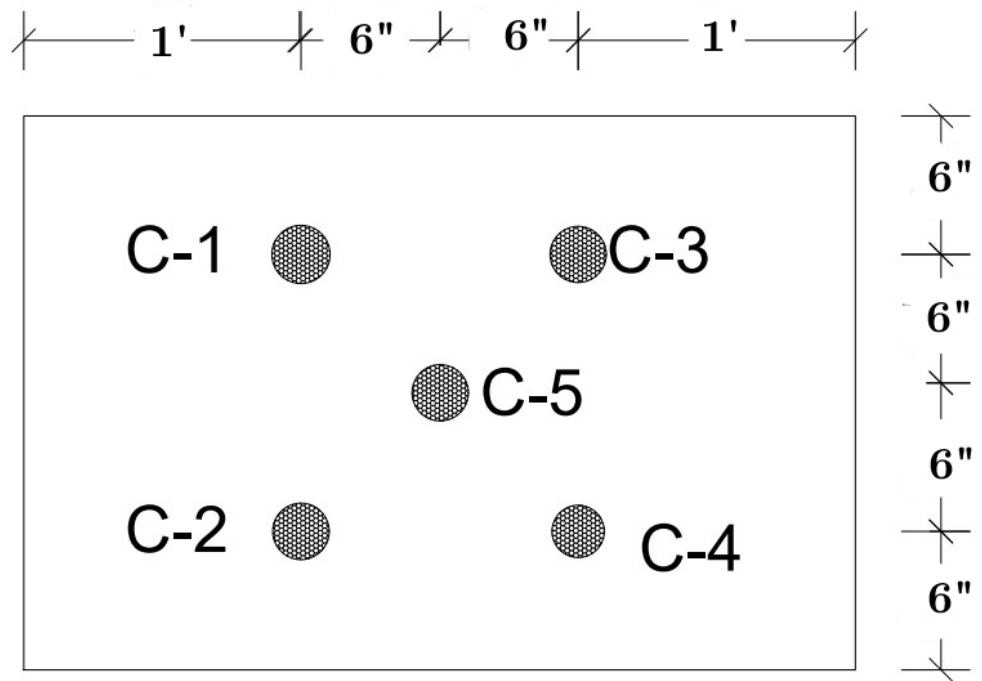
pressure sensor was inserted into the sample at a depth of 2 ft below the top surface of the sample for pore pressure measuring purposes. The 1st step was levelling the surface of the sample. After the levelling, two 50 mm dial gauges and two 50 mm, LVDT sensors were placed on the sample to measure the vertical displacement. Also, the glass chamber with a supporting platform on the top surface of the model was sealed with silicon glue for air proofing. After 24 hr. of loading the sample, the vacuum pipe was connected to a modified vacuum desiccator with the help of a 7mm inner diameter horizontal pipe. Another end of the vacuum desiccator was connected to the vacuum pump with the help of an 8 mm inner diameter plastic transparent pipe for applying vacuum.

4.4.2.3 Experiment Procedure

1st step: After finishing all the model setup, the pore pressure sensor and LVDT sensors were connected to the data logger. The DCS 100A software was used in a windows laptop for data collection and calibrated before starting the test. Then the experiment started by applying the first cycle vacuum into the soil. The first cycle of applied vacuum helps to reduce the water content and initial degree of saturation. After starting the vacuum pump, the DCS 100A software was run to collect automatic data as soon as possible. Simultaneously, the manual vertical dial gauge reading and water table reading were recorded and this cycle was continued for about four days. After four days, it was noticed that there was no water in the water level indicator. After that it was decided to apply the dynamic compaction by following the literature.

2nd step: Before the dynamic compaction, the vacuum glass chamber was removed, and all required equipment was prepared to apply the first drop of dynamic compaction. Dynamic compaction increases the soil's effective stress and generates excess pore pressure. The direct impact of heavy tamping creates a crater, resulting in the displacement of soil and a reduction of void ratio resulting in positive pore pressure in the influence zone. A 20mm diameter tamper with 5 kg weight was used to drop from 7 ft height. The tamping was desired at 4 points (in Figure 4.19.a C-1, C-2, C-3, C-4 points) , and each point was considered four repeated drops by comparing field investigation. The vacuum was run simultaneously with the dynamic compaction. The combined effect of vacuum-generated negative pore pressure and dynamic compaction-generated positive pore pressure creates a very high pore pressure gradient that helps quick dissipation of pore water pressure. Generally, the time required for this phase depends on the area of the treatment site. As the experiment area was smaller, it required one hour. to complete the dynamic compaction process in the model.

Chapter 4. Experimental Investigation Program



(a)



(b)



(c)

Figure 4.19: Dynamic compaction arrangement-(a) Compaction Location, (b) Execution of Dynamic Compaction, and (c) After 1st cycle of Dynamic Compaction

Step 3: After the first cycle of dynamic compaction, it was noticed that the water was only coming through the 2 ft depth vacuum drainage pipe. The 1 ft depth vacuum pipe was pulled out in this stage. Then the second vacuum cycle was run for several days through the 2 ft depth vacuum pipe. The second dynamic compaction was executed after seeing no water coming through the drainage pipe. In this stage, the tamping was desired at 1 point (in Figure 4.19(a) C-5 Location) middle of the previous points, and it was considered four repeated drops at the same height as the previous compaction.



2021/12/27 10:55

Figure 4.20: After 2nd cycle of dynamic compaction

Step 4 : After the second vacuum cycle and dynamic compaction, the third cycle vacuum was run for 24 hours. From 24 hours of observation of the vacuum, it was noticed that there was no water coming through the drainage pipe. So, it was decided to pull out the vacuum pipe and run the third dynamic compaction over the test area. The tamping was desired all over the model's test area, and each point was considered one drop per point at the height of 6 ft to compare the field HVDM procedure. Then the final levelling was done by a small steel roller. The field density test by sand replacement method was executed after the final levelling. Finally, all data were collected from the PC for further data analysis.



(a)



(b)

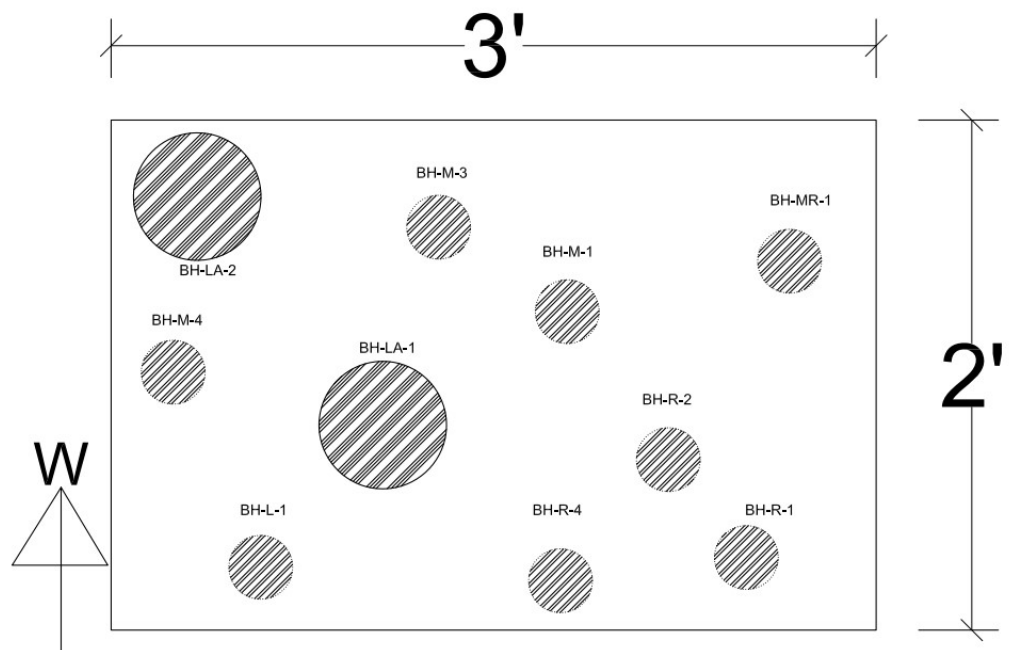


(c)

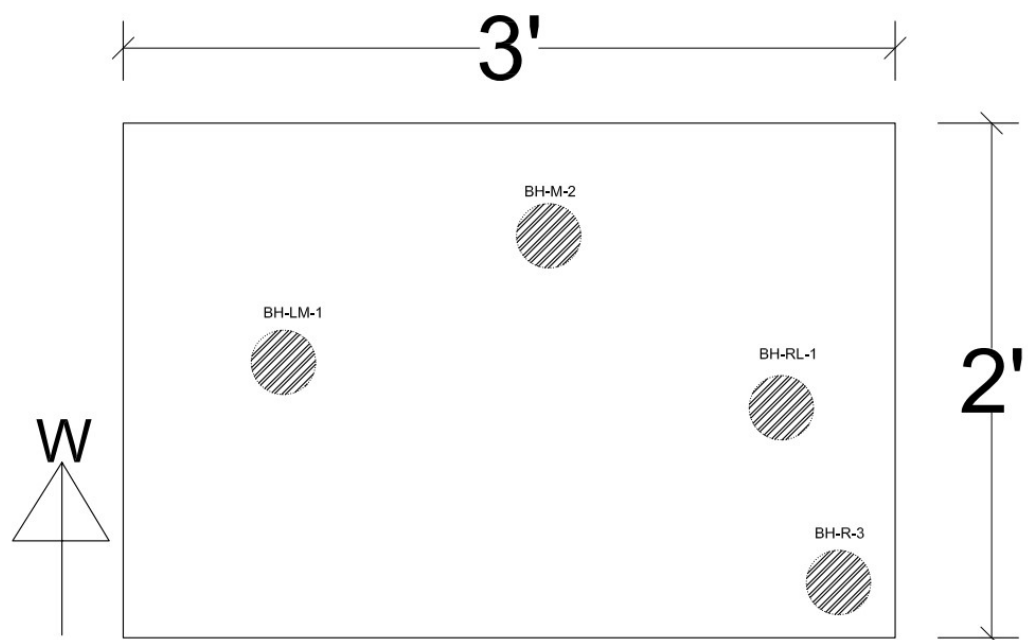
Figure 4.21: Execution of Field Density Test after levelling of the treated sample in the physical model- (a) After Levelling of HVDM treated sample, (b) Execution of Field Density Test, and (c) Execution of Field Density Test

4.4.2.4 Undisturbed Sample Collection

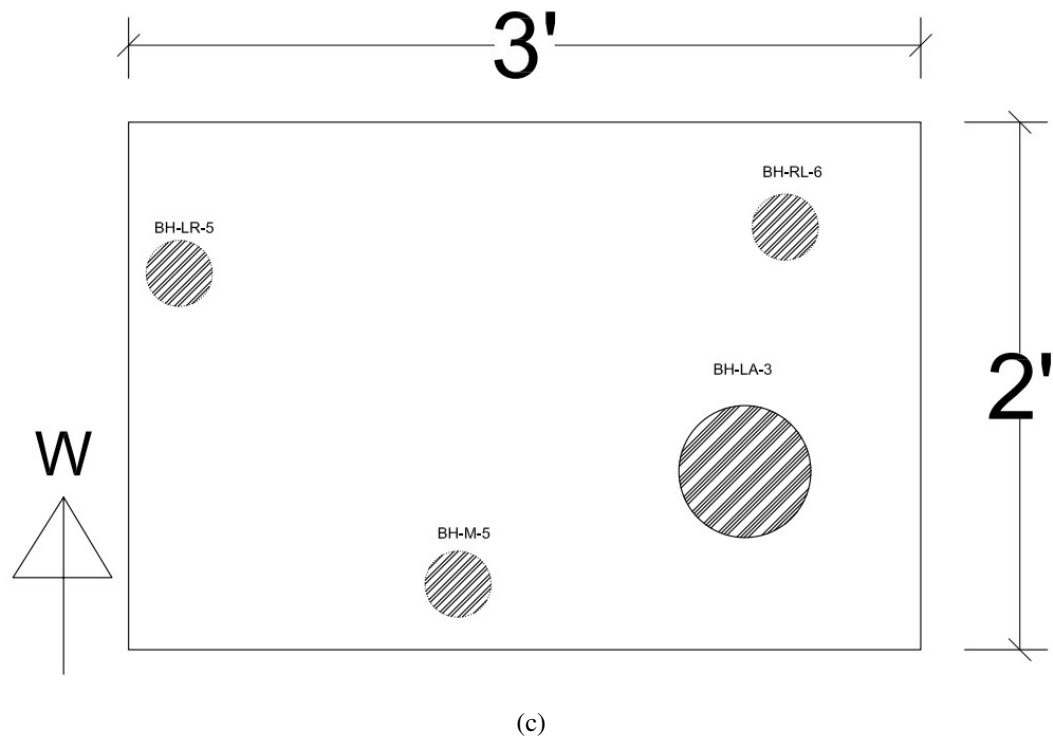
After successfully executing the High Vacuum Densification Method in the physical model, some undisturbed samples were collected by pushing samplers (Core Cutter Method) into the treated soil .



(a)



(b)



(c)

Figure 4.22: Undisturbed sample collection locations from the physical model- (a) UD sample collection locations from 6 in depth, (b) UD sample collection locations from 12 in-depth, and (c) UD sample collection locations from 18 in depth

The undisturbed samples were collected at three different depths (6", 12", and 18") from the physical model(Figure 4.22). The collected samples were used to conduct Oedometer or 1D Consolidation Test, Triaxial Consolidated Drained Test, Direct Shear Test, and Unconfined Compressive Strength Test. Figure 4.23 shows some procedures of collection of UD samples from the physical model at the selected location.



(a)



Figure 4.23: HVDM Treated UD samples Collection-(a) Collecting UD sample by the sampler, (b) Collected UD sample, and (c) HVDM treated UD samples

4.5 Data Processing with Python

The collected data was generated as CSV files. However, the CSV files size was huge. These CSV files could not be read via excel because excel cannot read more than 1 million rows. One day's data from the sensors had more than 1 million rows. So, it was needed to slice data by programming. For this research, the python programming language was used to slice and process the data. Step by step procedures of data processing by Python is described below.

Step 1 : Firstly, it needs to split the big file into parts. To do this, the Panda library was used to chunk the big file. The following code (Listing 4.1) was executed to split the big file.

Chapter 4. Experimental Investigation Program

```
1 import pandas as pd
2 batch_no=1
3 for chunk in pd.read_csv("Source folder",chunksize=100000,
4 delimiter=';', skiprows=0, low_memory=False):
5     chunk.to_csv("day1d" + str(batch_no) + '.csv' ,index=False)
6     batch_no+=1
```

Listing 4.1: Code for chunking the big file

This code was used to chunk the single big file into several files up to 100000 rows.

Step 2 : After splitting the big file, the generated CSV files could be read in excel after using python.

```
1 #Install Library
2 import pandas as pd
3 import os
4 #Fixing input and output location
5 input_loc="C:/Users/USER/Desktop/testpythondata/marge excel/input/"
6 output_loc="C:/Users/USER/Desktop/testpythondata/marge excel/output/"
7 #To show the list in input folder
8 filelist=os.listdir(input_loc)
9 filelist
10 #Code to marge file
11 finalDf = pd.DataFrame()
12 for files in filelist:
13     if files.endswith(".csv"):
14         df = pd.read_csv(input_loc+files)
15         finalDf = finalDf.append(df)
16
17 finalDf.to_csv(output_loc+"HVDMday1.csv", index=False)
```

Listing 4.2: Code to Merge all CSV files

The files were opened in excel and customized the header so that it could be programmed further in python. Data contained four heading 1. Time 2. Pore pressure 3. Right LVDT reading 4. Left LVDT reading. After fixing all headers, it needs to merge all split CSV files into one using the following code (Listing 4.2) in the Pandas framework.

step 3 : After merging the files into one file with the proper header name, it was needed to slice the data by targeting the time header. The actual data frequency was huge, like 1000 data per second. As the experiment was run for a long time, it was decided to keep the data to 1 sec per 1 data. A program was created to eliminate the floating data targeting time header,

which meant the program kept only integer data. In this way, it gets 1 data per second. The following code (Listing 4.3) was created for this action,

```
1 import pandas as pd
2 df=pd.read_csv('D:/thesis/hvdm test data/consolidated
3 data for displacement/min/day1.csv')
4 df.head(5)
5 df = pd.DataFrame(df)
6 s = df['time']
7 df['time'] = df['time'].astype(int)
8 df = df[df['time'] == s]
9 print (df)
10 output_loc='D:/thesis/hvdm test data/consolidated data
11 for displacement/min/'
12 df.to_csv(output_loc+"day1m.csv", index=False)
```

Listing 4.3: Code to eliminate floating data

After the executing the program, the large data was successfully reduced 10 GB CSV file to 650 kB.

Step 4 : After getting the final data for all the days, it was again merged all sliced data into a single file by following step 2. Then the data visualization part was partially done using Python 3 and Microsoft Excel 2019.

4.6 Summary

This chapter describes the detailed methodology of the experimental setup starting from the Physical modelling idea, scaling, model implementation, trial experiment, successful HVDM experiment procedure, data collection, Undisturbed sample collection, and a detailed procedure of data slicing using python programming.

Chapter 5

Results and Discussion

5.1 General

The main objective of this research is to simulate an innovative ground improvement technique named High Vacuum Densification Method (HVDM) in the laboratory to investigate the working principle and effectiveness of soft soil improvement by this method. In this chapter, the research results are presented and discussed concerning the aim of the research. The laboratory test program was briefly explained in Chapter 3 and Chapter 4. This chapter presents the results of soil index properties, Unconfined Compression Strength (UCS) test, Consolidation test, Triaxial Consolidated Drained (CD) test, Physical model test, and their brief discussion have been presented. Also, a detailed comparison has been made on test results of HVDM treated sample with remoulded samples.

5.2 Soil Index Properties

The classification of soils for use in a wide variety of engineering applications depends on their index properties, which are the most fundamental physical characteristics of the soil. They represent the qualitative behavior of soil under various forms of load. As the collected soil sample from the physical test was silty clay, it needed to conduct both a sieve analysis and a hydrometer test. A combination of sieve and hydrometer analysis results is shown in Figure 5.1.

Table 5.1 presents the summarized results of the respective sample from the combined particle size distribution curve of sieve and hydrometer analysis.

Table 5.1: Summary of grain size analysis result

Parameters	Value
Medium Sand Content (%)	0.23
Fine Sand Content (%)	10.57
Silt Content (%)	76.78
Clay Content (%)	12.42
Total Sand Content (%)	10.8
Total Fine Content (%)	89.2

Chapter 5. Results and Discussion

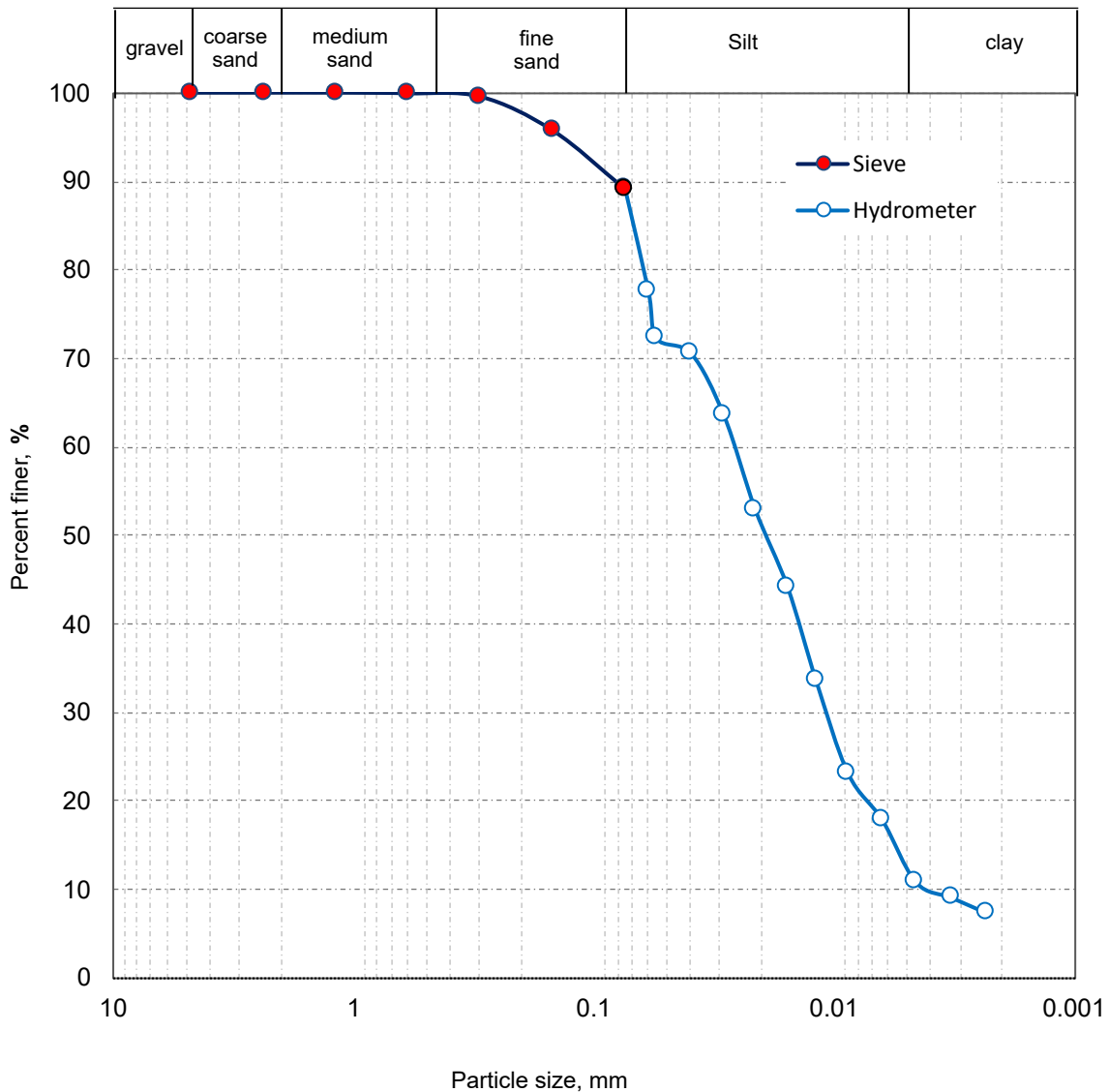


Figure 5.1: Particle size distribution curve of representative sample

The specific gravity test of the representative soil sample was found to be 2.72. Also, the relative density test found that the maximum density of the densest state was 1.57 g/cc, and the minimum density of the loosest state was 1.11 g/cc. The permeability test result is presented in the Table 5.2

Table 5.2: Summary of permeability test result

Compaction Conditions	Void Ratio	Coefficient of Permeability (k) cm/s
Loose Condition	1.34	2.46×10^{-4}
Medium Compaction	1.06	1.82×10^{-4}
Heavy Compaction	0.94	1.41×10^{-4}

Chapter 5. Results and Discussion

Soil classification is the process of placing soil into classes or groups that have similar characteristics and could act in the same way. A variety of methodologies and approaches are used to classify soils. The most widely used of these systems are the American Association of State Highway and Transportation Officials (AASHTO) soil classification system, the Unified Soil Classification System (USCS), and the United States Department of Agriculture (USDA) soil classification system. The common feature of these systems is the use of particle size distribution and plasticity to classify the coarse and fine-grained soil. The USCS classification system was used for this investigation to identify the soil type. Based on the above grain size result, the representative soil sample has fine content of 89.20 % with low plasticity. The representative soil sample is classified as Sandy Clayed Silt with USCS symbol ML.

5.3 HVDM Investigation Result

After the successful experiment of HVDM in the physical model, the Settlement and Pore Pressure data were collected for further analysis. The following sections will present the results of the HVDM investigation of the physical model.

5.3.1 Visual Witness of HVDM Treated Soil Improvement

A visual test of soil improvement on this physical model was executed to visually see the before and after soil conditions. For this test, a laboratory assistant was used as a part of this test. After the soil preparation and loading process of soil into the physical model, the assistant was requested to get into the physical model. After standing on the unimproved soil sample in the physical model, The assistant's legs sink into the sample instantly (Figure 5.2). It indicates that the soil sample was very soft.



(a)

Chapter 5. Results and Discussion



(b)



(c)

Figure 5.2: Visual proof of soft soil before execution of HVDM- (a) Assistant gets into the unimproved soil in the physical model, (b) Assistant leg sank into the soft soil, and (c) Visual indication of soft soil

After a continuous run of the vacuum for several days, the improvement was seen visually (Figure 5.3.a). Also, after the second cycle of dynamic compaction, the assistant was requested to get into the physical model again. This time, the assistant could stand on the sample without any disturbance (Figure 5.3.b), which indicates that the soil sample improved from soft to stiff.



(a)



(b)

Figure 5.3: Visual improvement of soft to stiff soil-(a) Improvement after several days of vacuum and (b) Improvement after Dynamic compaction

5.3.2 Evaluation of Settlement and Comparison with Field Data

This research used two dial gauges and 2 LVDT sensors to measure the vertical displacement. The settlement measuring devices were positioned along the physical model's left and right sides along with its length. Figure 5.4 shows the recorded settlement of the experiment.

Chapter 5. Results and Discussion

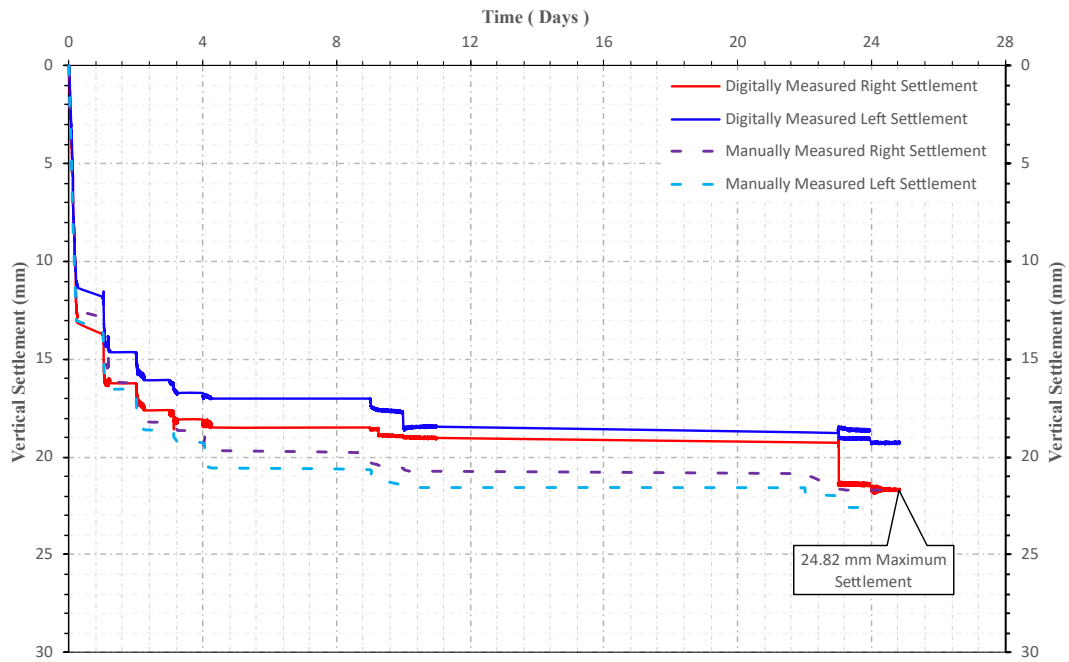


Figure 5.4: Time vs recorded settlement of the experiment

From Figure 5.4, it can be seen that the maximum settlement of the experiment was found to be 24.82 mm. Figure 5.5 presents the field measured settlement during the HVDM execution in the field.

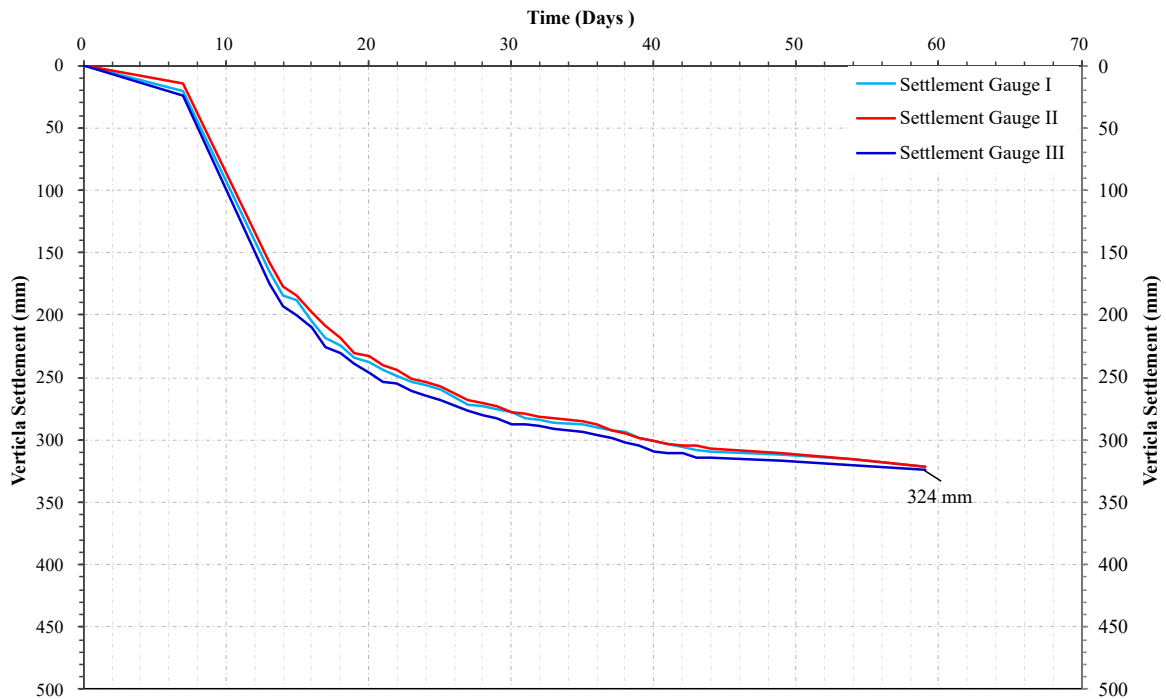


Figure 5.5: Time vs settlement of the research site

Chapter 5. Results and Discussion

If its make a comparison between two graphs, it can be said that the experimental settlement increment is similar to the field.

5.3.3 Evaluation of Excess Pore Pressure and Comparison with Field Result

Pore water pressure is an important design factor for HVDM since its value, rate of growth and dissipation can indicate how well soft soil has improved and the range of its influence. HVDM can rapidly dissipate pore water pressure and accelerate soil consolidation following the “Pressure Gradient” principle. Observations of the pore water pressure are taken at regular intervals throughout the HVDM process so that a profile of the soil’s development can be obtained. This research measured pore pressure with a Vibro wire pore pressure sensor. Figure 5.6 shows the pore pressure growth rate and excess pore water pressure dissipation due to vacuum consolidation and dynamic compaction. It was noticed that some spikes occurred due to each ramming because of the pressure gradient created from positive and negative pressure. In this case, the pressure gradient helps to accelerate the consolidation process.

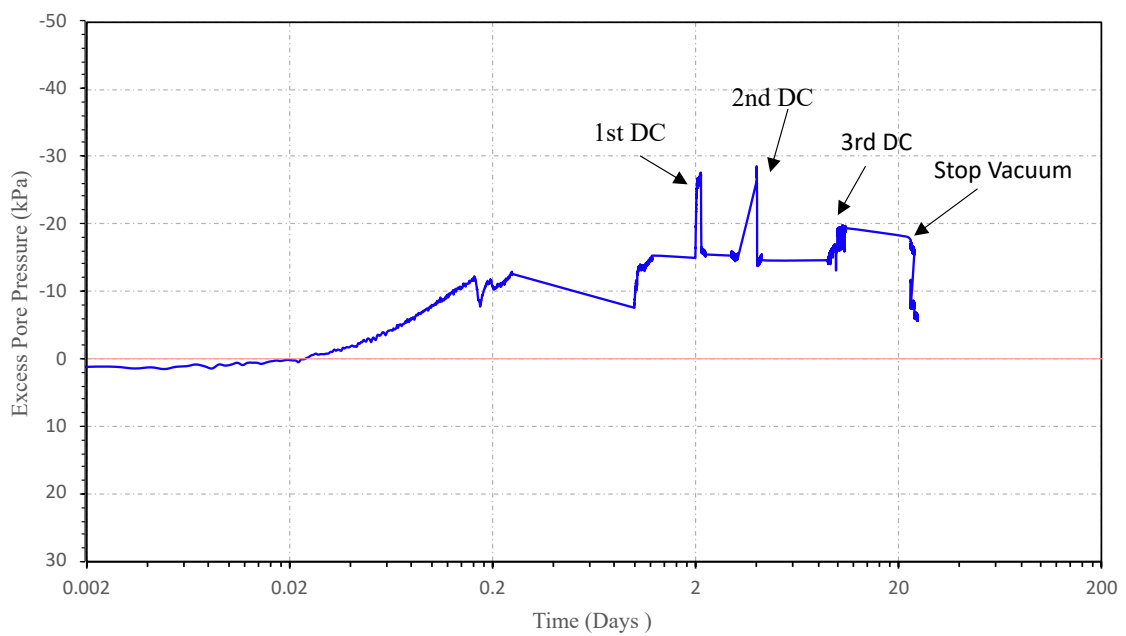


Figure 5.6: Time vs excess pore pressure of the experiment

Figure 5.7 presents the field monitoring result of excess pore water pressure. It was noticed that both graphs’ excess pore pressure dissipation pattern is almost the same, which is a sign of rapid consolidation.

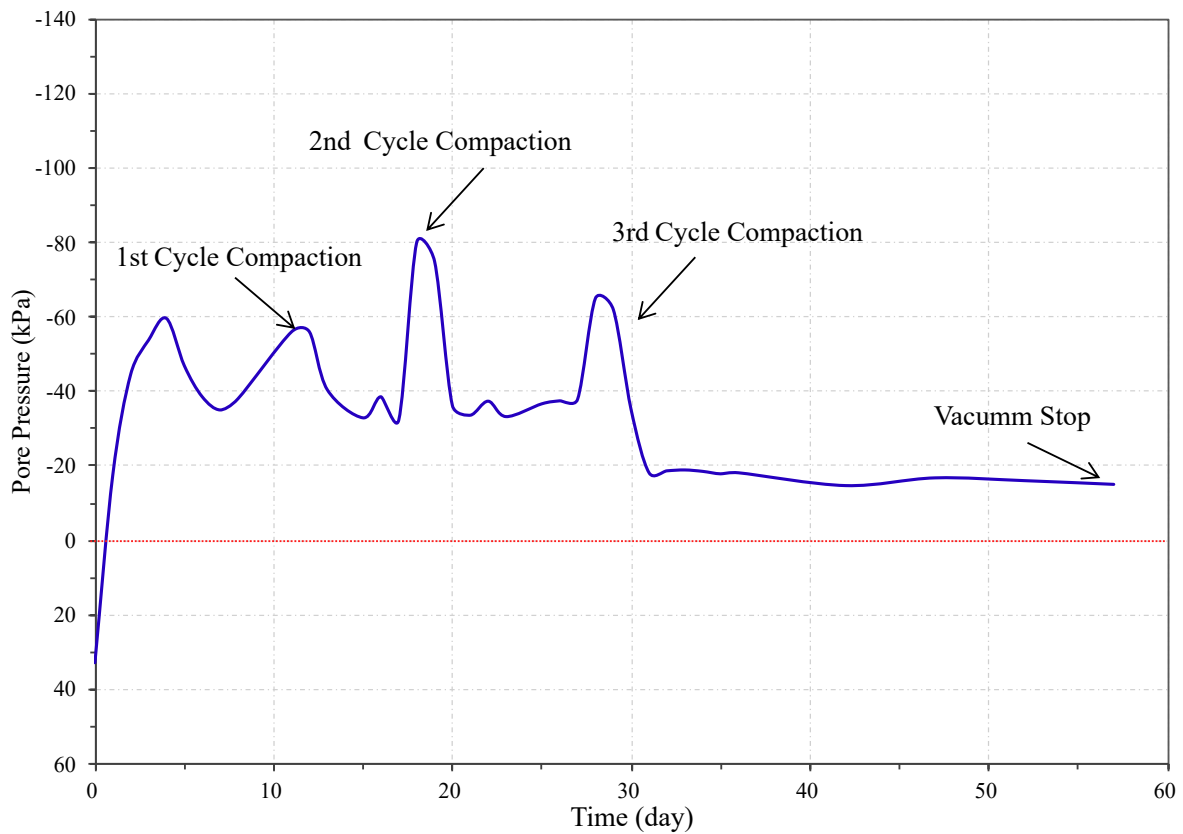


Figure 5.7: Time vs excess pore pressure of the research site

5.4 Compaction Percentage Evaluation

A standard proctor test was conducted to find the maximum dry density and optimum moisture content of the representative soil. This test procedure is briefly described in chapter 3. Figure 5.8 represents the relationship between dry density and moisture content of representative soil. From the dry density and moisture content relationship, it is found that the representative sample has a maximum dry density of 1.66 g/cc at optimum moisture content of 17 %.

After the treatment, a density test by sand replacement method and core cutter method was conducted to find the dry density of the treated sample. Both field density tests found that the treated sample has a dry density of 1.56 g/cc at a moisture content of 21%. The laboratory and field compaction test found that the compaction percentage in the physical model after the experiment was 94 %.

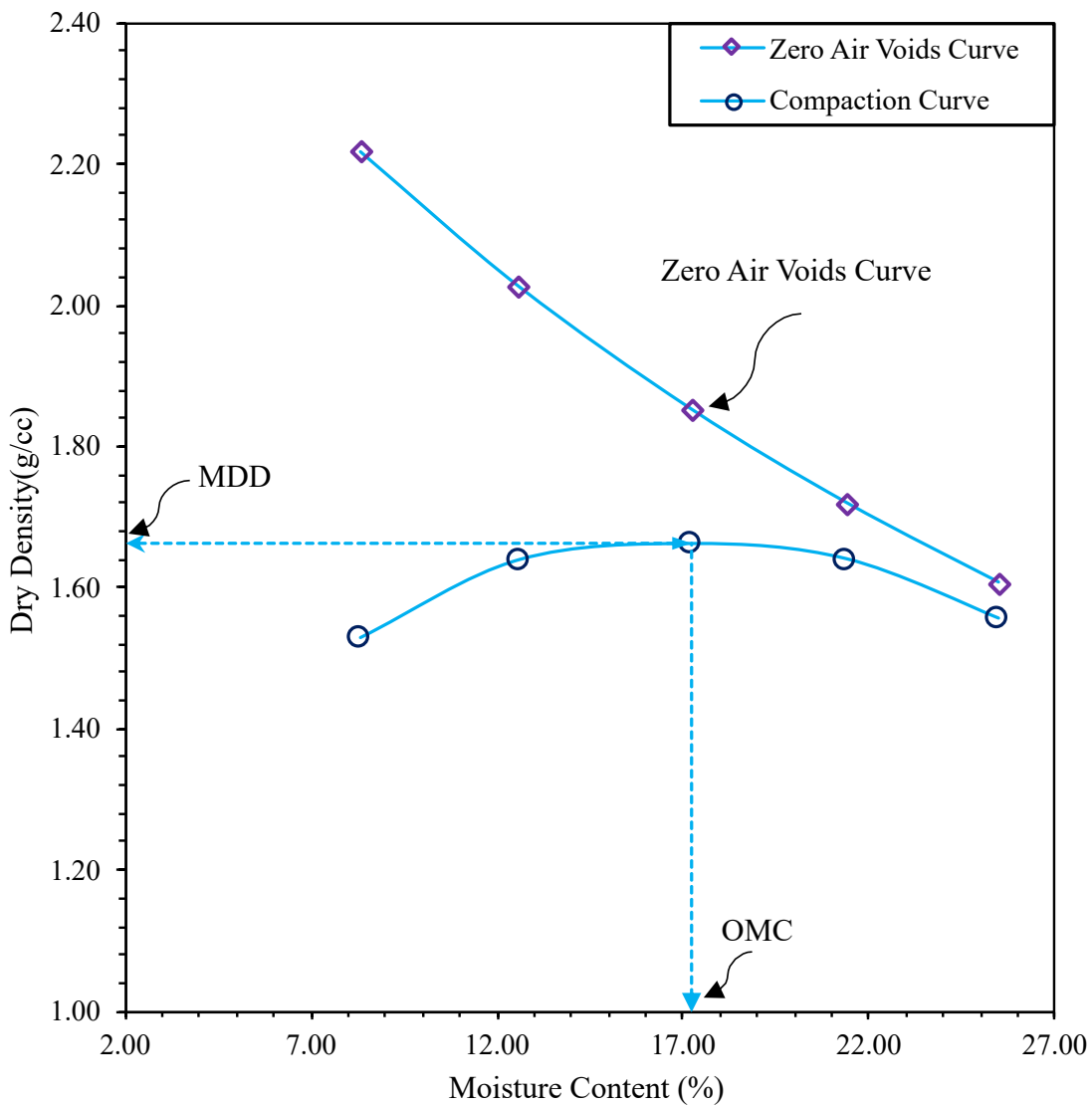


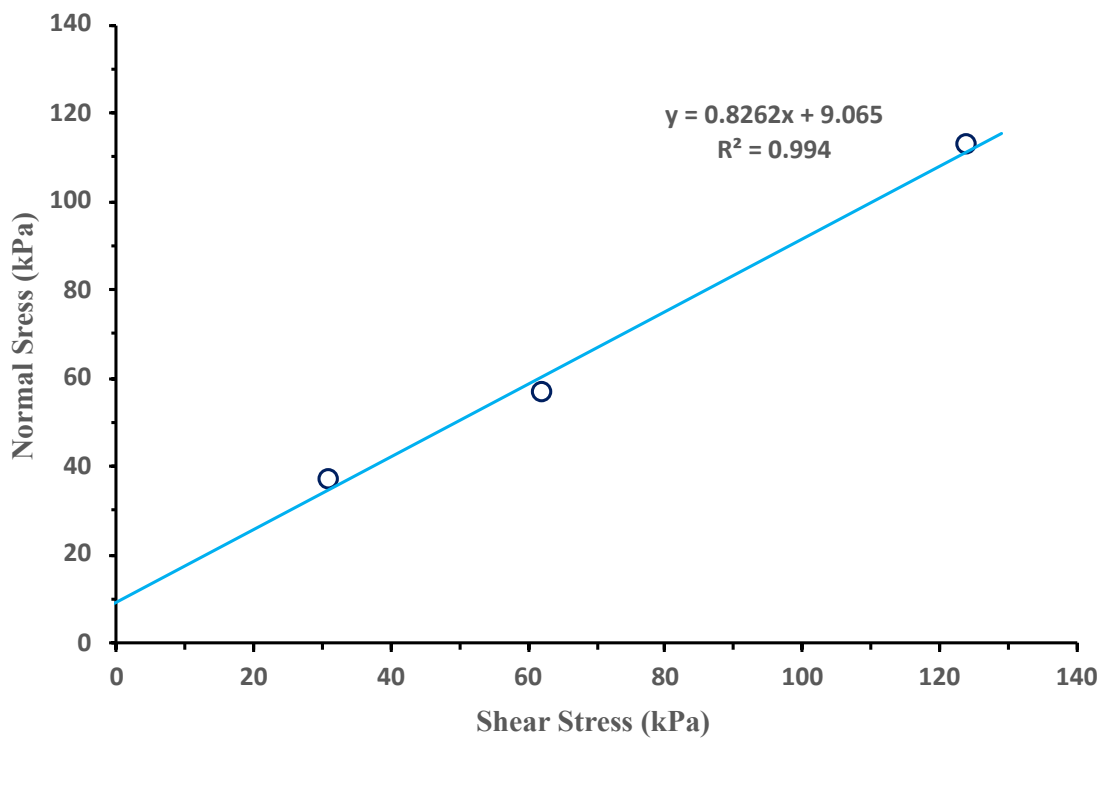
Figure 5.8: Relationship between dry density and moisture content of representative soil

5.5 Evaluation and Comparison of Shear Strength Properties

The shear strength of soil is affected by several factors, including the effective stress, how well it drains, how dense the particles are, the strain rate, and which way the soil is being strained. The shear strength can be measured in the laboratory using various methods or tests. Among them, 1. Direct shear, 2. Unconfined Compression Test (UCS), 3. Triaxial Compressive Test are widely used. For this research, the Unconfined Compression Test (UCS), Direct shear, and Triaxial Compressive Test were conducted on remoulded and treated soil samples. A brief description of those test procedures are presented in Chapter 3. The following sections will present those shear strength test results and compare them based on their results on remoulded and treated samples.

5.5.1 Evaluation of Shear Strength Properties from Direct Shear Test on HVDM Treated Sample

The direct shear test is a simple and widely used test done in a shear box to evaluate soil shear strength characteristics. This test aims to evaluate the shear stress at failure by applying a particular normal stress to a soil specimen in a shear box and shearing it along a predetermined horizontal plane. For this research, the Direct Shear consolidated drain test was carried out on three undisturbed specimens of HVDM treated samples. In order to determine the shear strength, normal stresses of 31, 62, and 124 kPa were applied to the tests. Figure 5.9(a) shows the relationship between shear stress vs normal stress. This relationship found that the treated sample has a cohesion of 9 kPa and the angle of internal friction is 39° . Figure 5.9(b) represents the Shear displacement vs shear stress relationship of the HVDM treated sample from the direct shear test.



(a)

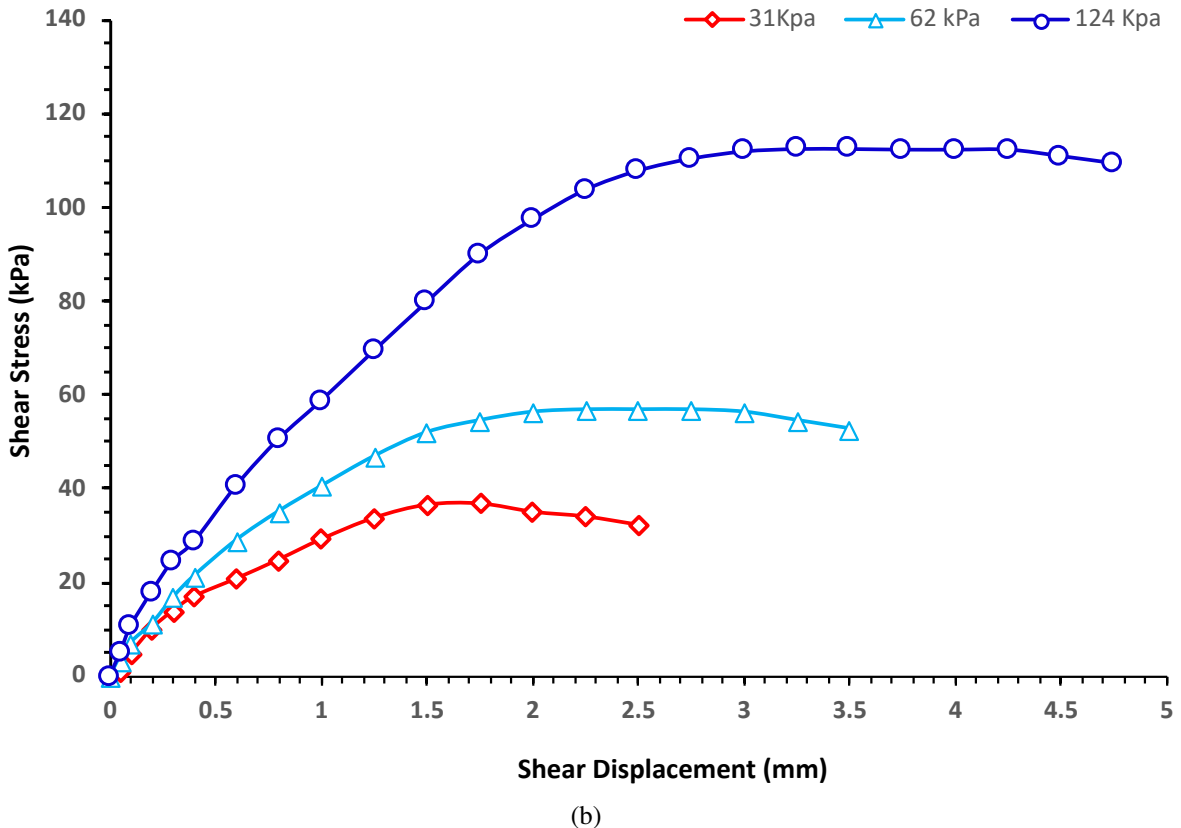


Figure 5.9: Direct shear Consolidated Drained Test result-(a) Shear Stress vs Normal stress curve for treated sample and (b) Shear Stress vs Shear Displacement curve for treated sample

5.5.2 Evaluation and Comparison of Shear Strength Properties from Unconfined Compression Test (UCS) Test on Remoulded and HVDM Treated Sample

The unconfined compression test, also known as the UCC test, is a variant of the triaxial compression test in which, there is no confining pressure during the compression phase. For this research, seven sets of undisturbed soil samples collected from the physical model at different depths (Figure 4.22) and four sets of remoulded samples with the same density and moisture content were tested in BUET geotechnical laboratory by following ASTM D2166-06 standard. The test procedures of these tests are described in Chapter 3 . Table 5.3 presents the summary of those test results.

According to Table 5.3, it is seen that all the UCS test on HVDM treated sample has an average water content and dry density of 21 % and 1.56 g/cc, respectively. Also, the average Unconfined compressive strength is 125 kPa; that range of Unconfined compressive strength indicates the consistency of the HVDM treated sample is stiff (from Table 5.4).

Chapter 5. Results and Discussion

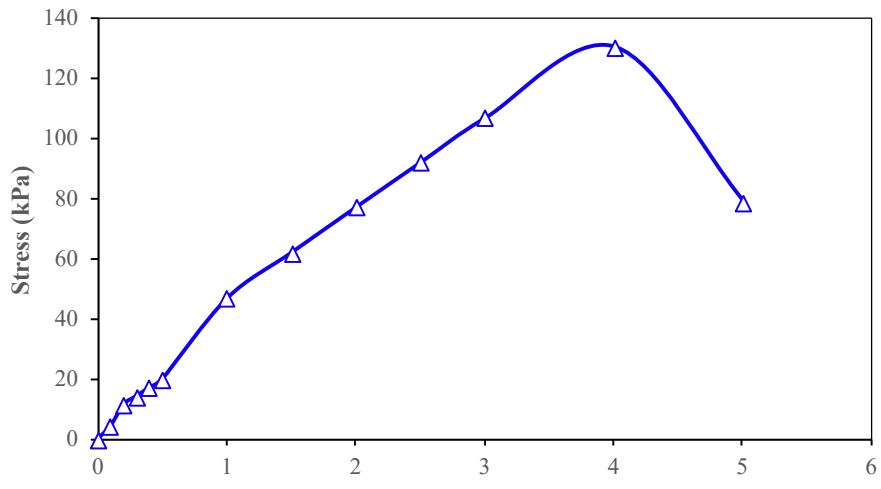
Table 5.3: Summary of UCS test result

Sample No	Sample ID	Depth (inch)	Sample Type	Water Content (%)	Dry Desnity (g/cc)	Unconfined Compression Strength(q_u) kPa	Undrained Shear Strength (S_u) kPa	Axial Strain at Failure (%)	Sensitivity (S_s)
1	BH-R-2	6	Undisturbed	21	1.58	130	65	4	2
2	BH-R-2(Re)	-	Remoulded	20.25	1.57	70	35	2.5	
3	BH-M-1	6	Undisturbed	21.82	1.57	126	63	5.01	1
4	BH-M-1 (Re)	-	Remoulded	20.31	1.56	87	43.5	5	
5	BH-L-1	6	Undisturbed	22.3	1.58	165	82.5	7	2
6	BH-L-1 (Re)	-	Remoulded	22	1.56	91	45.5	5	
7	BH-M-5	18	Undisturbed	21.25	1.55	106	53	6	1
8	BH-M-5 (Re)	-	Remoulded	20.5	1.55	77	38.5	4	
9	BH-M-2	12	Undisturbed	22	1.57	92	46	5.69	-
10	BH-M-4	6	Undisturbed	20.6	1.55	143	71.5	5	-
11	BH-LM-1	12	Undisturbed	21	1.57	115	57.5	5	-

Table 5.4: General relationship of consistency and unconfined compression strength of cohesive soil (after Das, 2010)

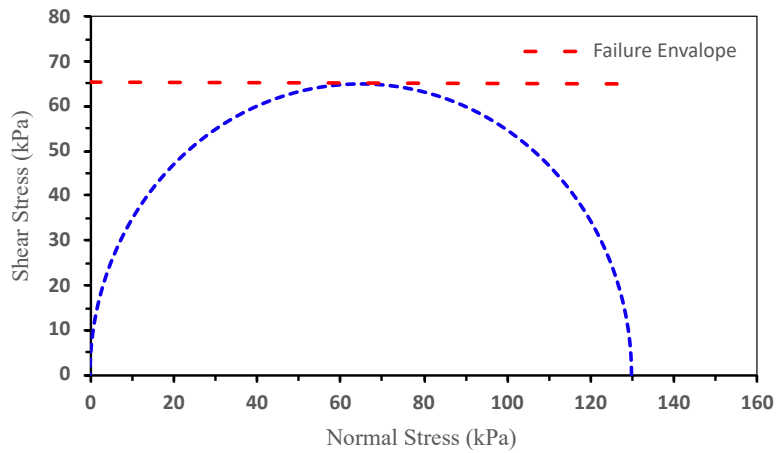
Unconfined Compressive Strength (kPa)	Consistency of Soil
0-25	Very Soft
25-50	Soft
50-100	Firm
100-200	Stiff
200-400	Very Stiff
> 400	Hard

Figure 5.10 shows the strain vs stress curves and Mohr circles obtained from some HVDM treated samples.

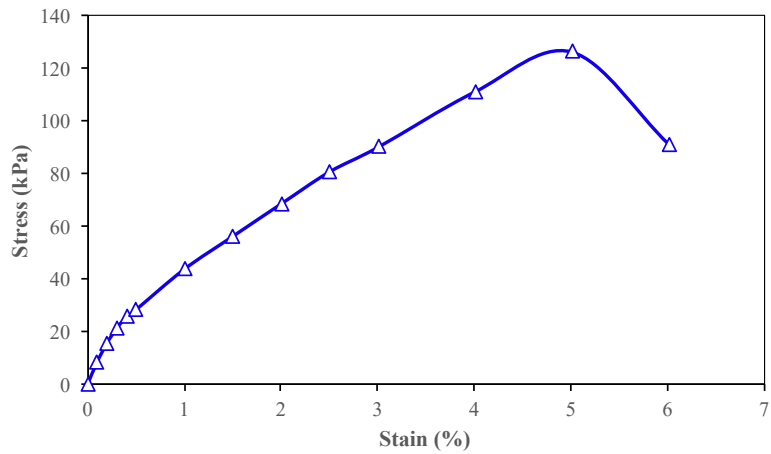


(a)

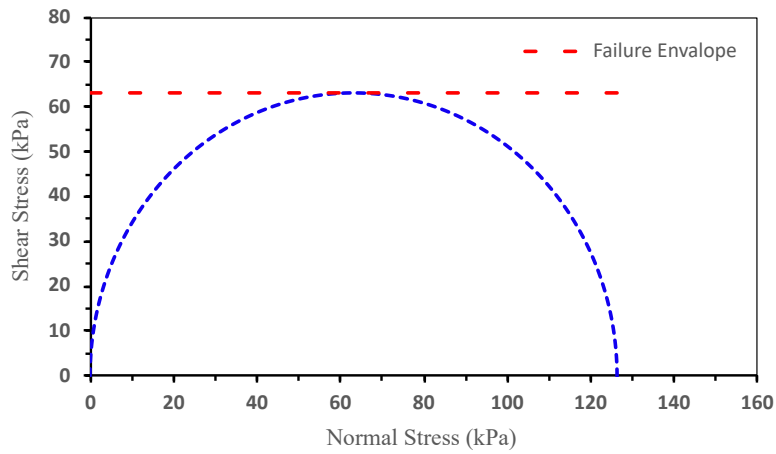
Chapter 5. Results and Discussion



(b)

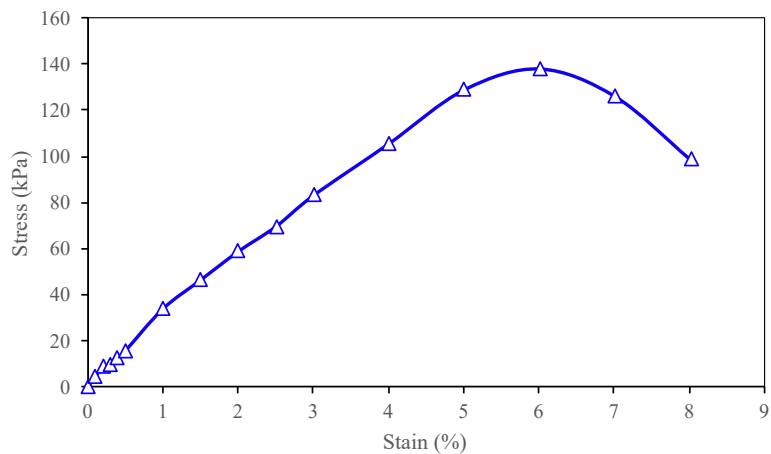


(c)

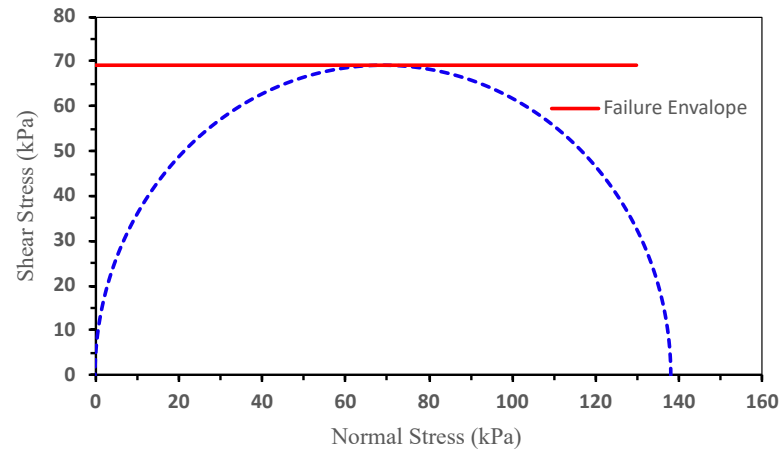


(d)

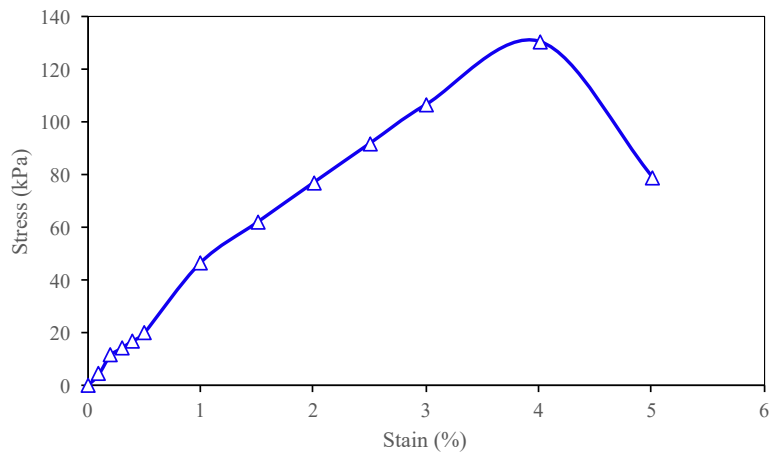
Chapter 5. Results and Discussion



(e)



(f)



(g)

Chapter 5. Results and Discussion

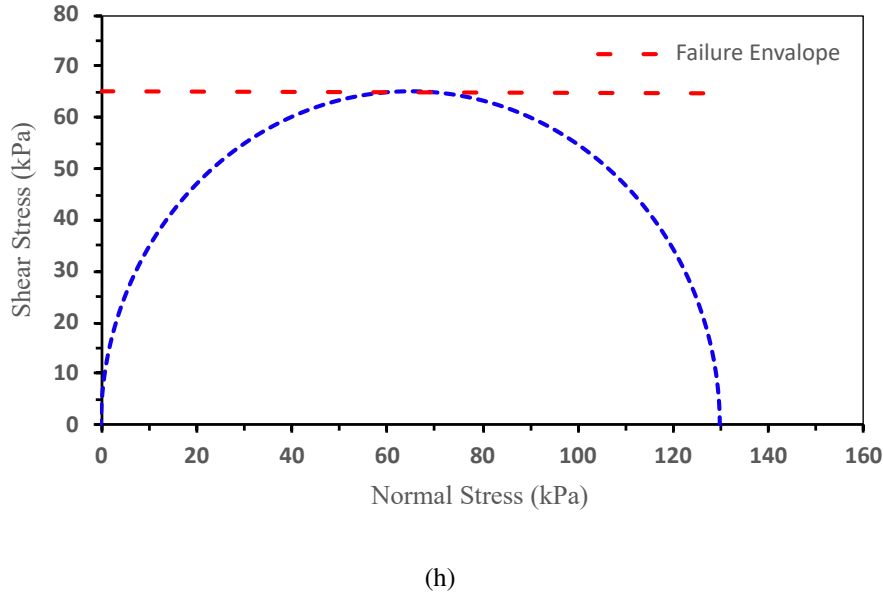


Figure 5.10: Some Strain vs Stress curve and Mohr circle of HVDM treated sample-(a) Strain vs Stress curve for sample ID BH-R-2 , (b) Mohrs circle for sample ID BH-R-2 , (c) Strain vs Stress curve for sample ID BH-M-1 ,(d) Mohrs circle for sample ID BH-M-1 ,(e) Strain vs Stress curve for sample ID BH-L-1 , (f) Mohrs circle for sample ID BH-L-1 , (g) Strain vs Stress curve for sample ID BH-M-5 and (h) Mohrs circle for sample ID BH-M-5

Figure 5.11 shows the combined Mohr circles from the seven sets of UCS tests on HVDM treated undisturbed samples. From the figure 5.11, it can be seen that the average undrained shear strength of the HVDM treated soil is 63 kPa.

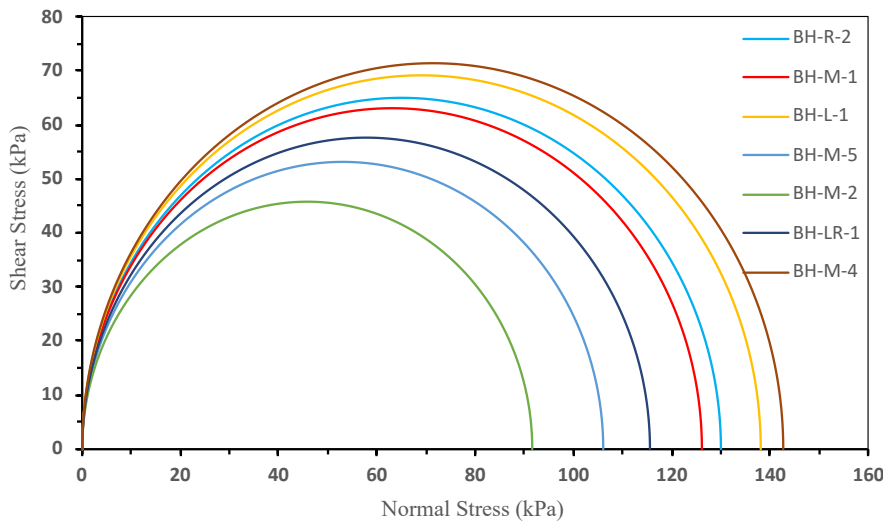


Figure 5.11: Combined Mohr circles of HVDM treated samples

Figure 5.12 shows the combined stress vs. strain relationship from the seven UCS tests on HVDM treated undisturbed samples. From Figure 5.12, it can be seen that the stress

Chapter 5. Results and Discussion

increment of the HVDM treated sample starts from the same pattern, and failure of all samples occurred at 5-6 % of axial strain.

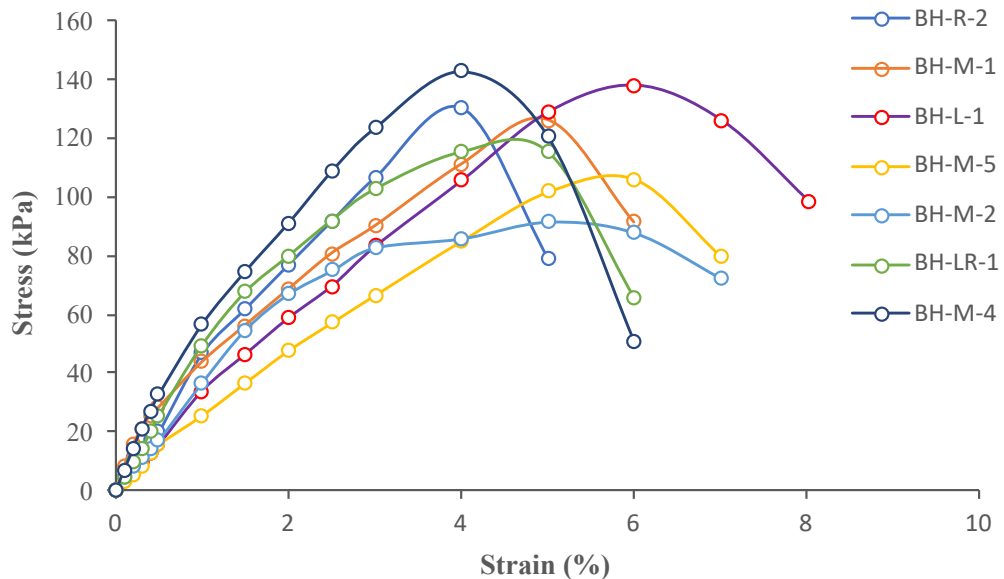
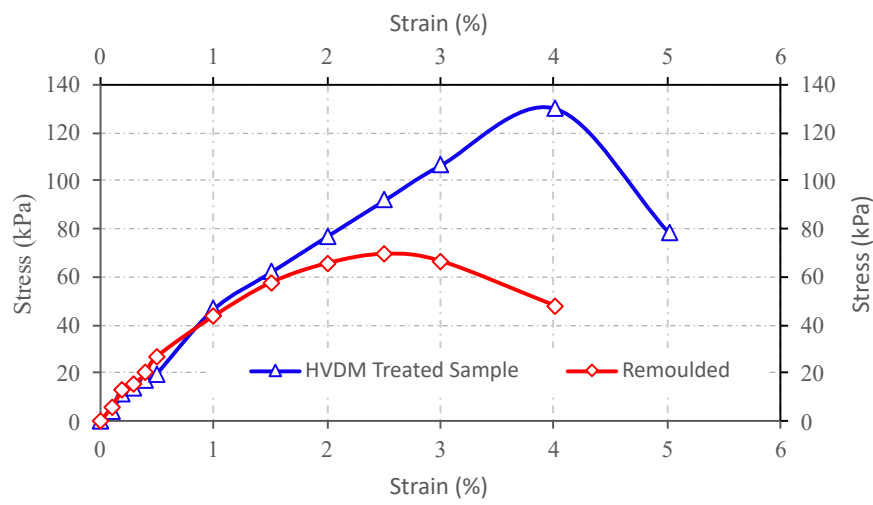


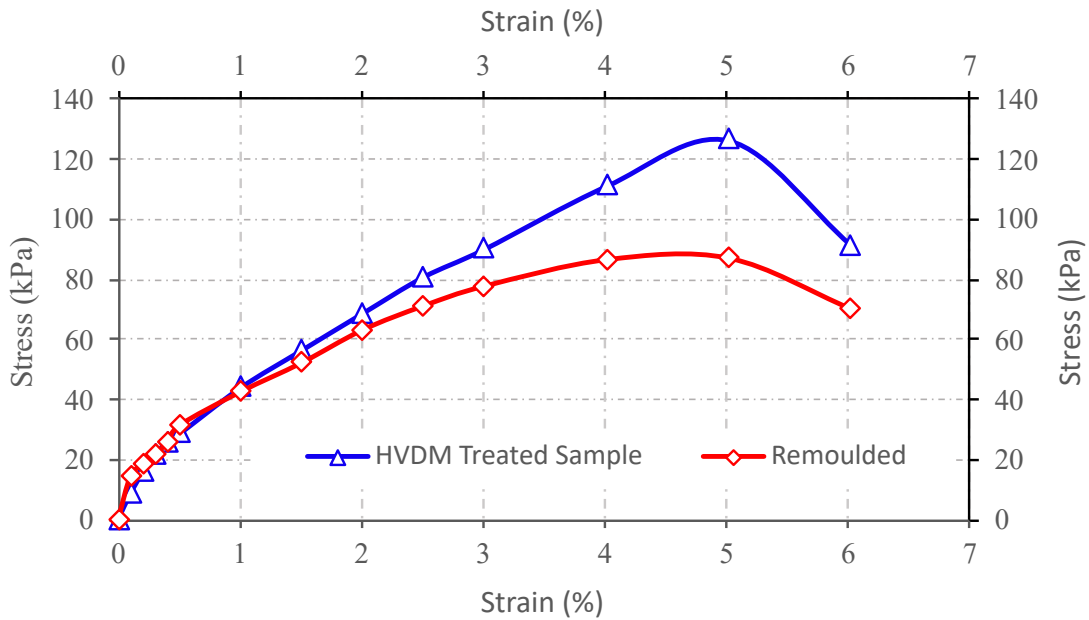
Figure 5.12: Combined Stress vs Strain Relationship of HVDM treated samples

In this research, four sets of remoulded samples were tested at the same dry density and moisture content of HVDM-treated samples to compare the unconfined compressive strength and failure criteria from axial stain. Figure 5.13 shows the compared results of remoulded and HVDM treated samples.

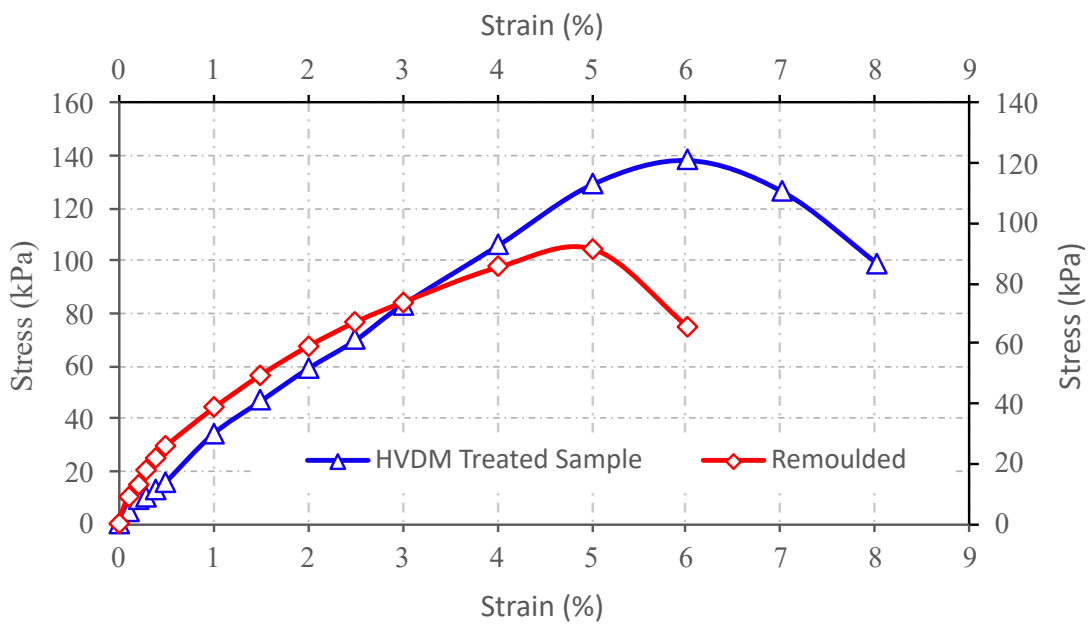
Figure 5.13 shows that all remoulded samples have lower unconfined compressive strength than HVDM-treated samples.



(a)



(b)



(c)

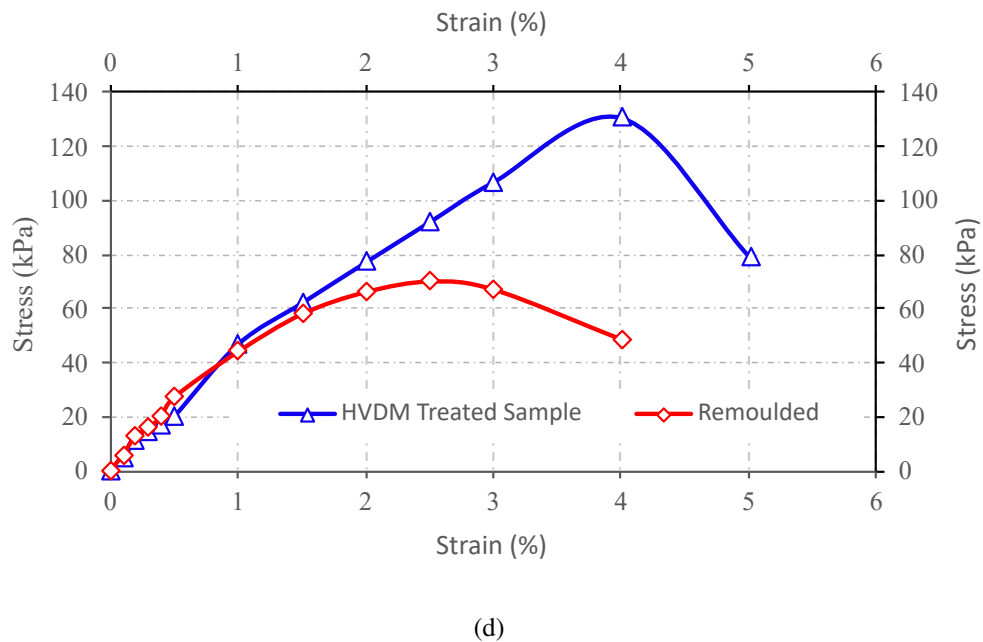


Figure 5.13: Comparative strain vs stress curve of HVDM treated and remoulded samples-(a) Sample ID: BH-R-2, (b) Sample ID: BH-M-10 , (c) Sample ID: BH-L-1, and (d) Sample ID: BH-M-5

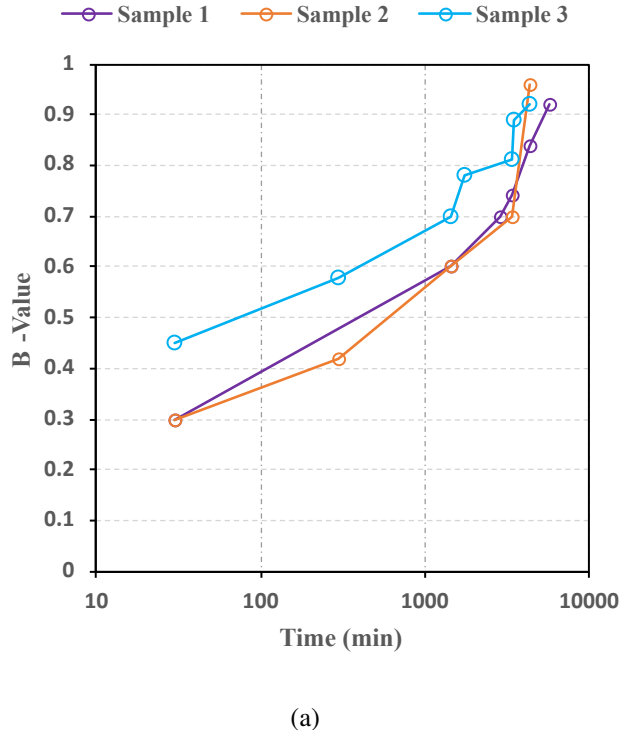
The remould samples have an average of 62% less strength than the HVDM-treated sample. The failures occurred due to axial strain being earlier than HVDM treated sample. So, From the UCS test, it can be summarized that the HVDM treated samples achieve more strength than remould sample.

5.5.3 Evaluation and Comparison of Shear Strength Properties from Triaxial CD Test on Remoulded and HVDM Treated Sample

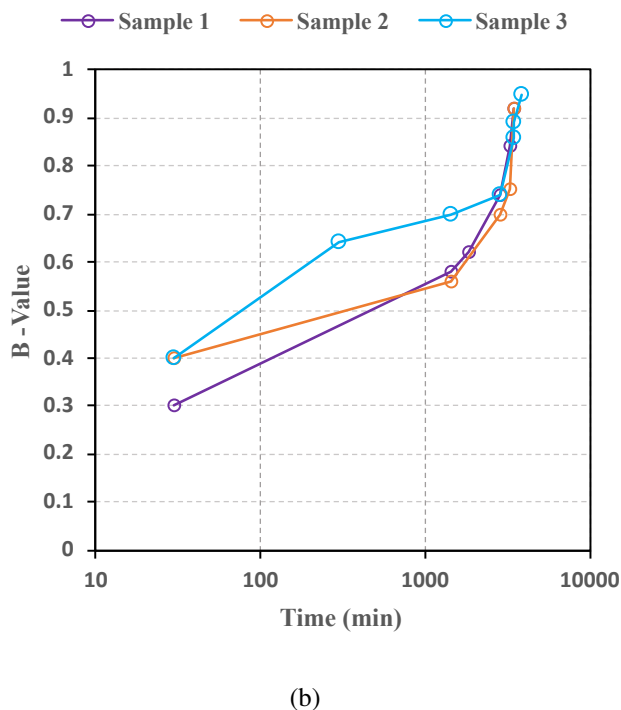
In this research, Triaxial Consolidated Drained (CD) test was conducted to evaluate the shear strength properties at drained conditions. It may take several days to finish a consolidated drained triaxial test on clayey soil. Applying deviator stress too quickly might prevent the soil specimen from draining correctly. So, the deviator stress must be applied very slowly to ensure complete drainage from the soil sample. The test was conducted on remoulded and HVDM treated samples. For each CD test, three specimens were made to test at 50, 100, and 200 kPa confining stress. The details of the experimental procedure of CD tests are described in Chapter 3. The results of those tests and some comparisons between remoulded and HVDM-treated samples are presented in this section.

Saturation Stage : Figure 5.14 shows the time versus B-Value relationship in saturation stage of Triaxial consolidated drained test of remolded and HVDM treated sample.

Chapter 5. Results and Discussion



(a)



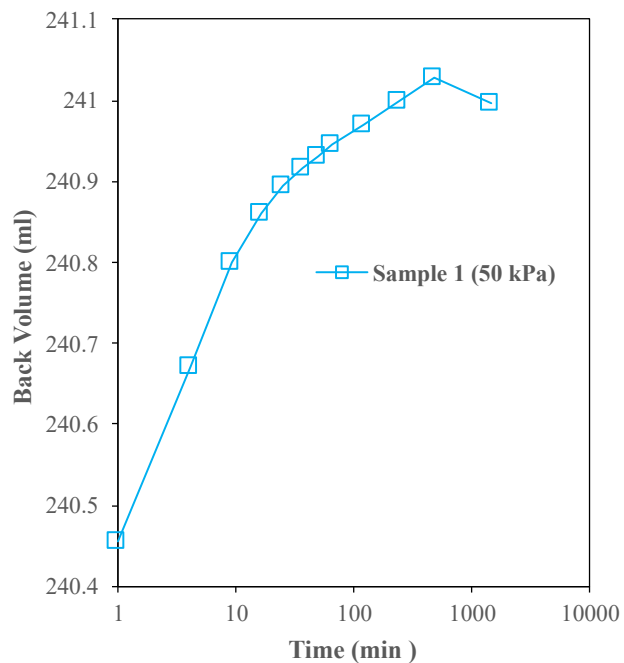
(b)

Figure 5.14: Time Vs. B-Value relationship in saturation stage- (a) HVDM treated sample and (b) Remoulded sample

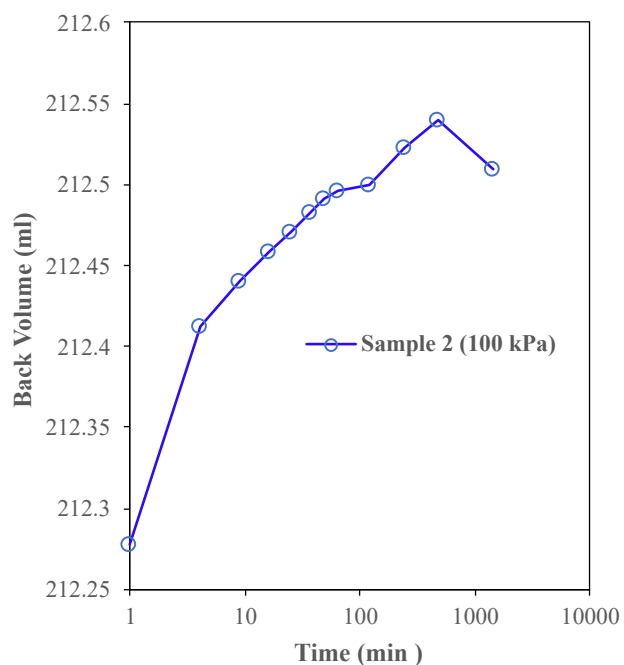
The figure shows that the increment of the B-value was parallel with the increment of time. All the specimens were carried out at $B\text{-value} > 0.90$, which indicates that all the samples were tested at saturation conditions.

Chapter 5. Results and Discussion

Consolidation Stage: Figure 5.15 shows the change of cell and back volume with time for both tests in the consolidation phase of the Triaxial CD test. It is seen from Figure 5.15 that the back volume is increasing with time because of the dissipation of excess pore water both for remolded and HVDM-treated samples.

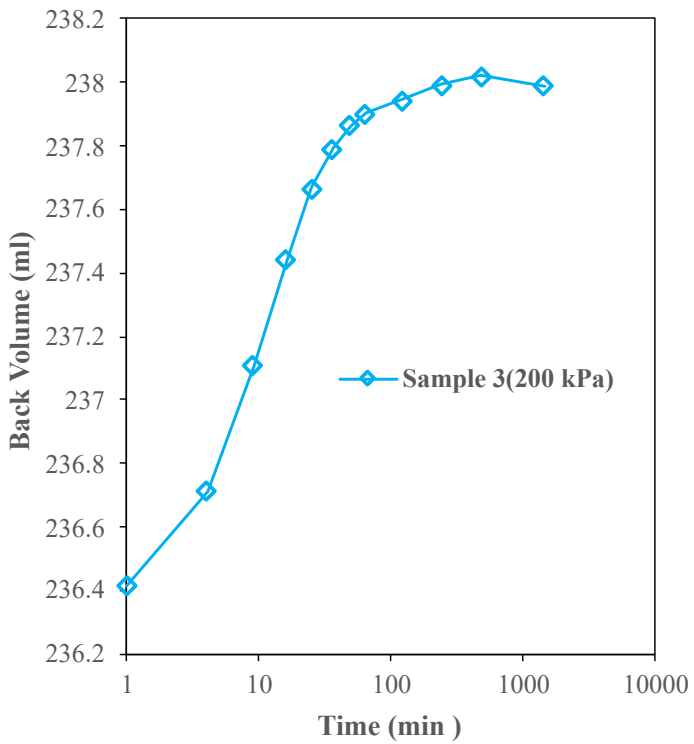


(a)

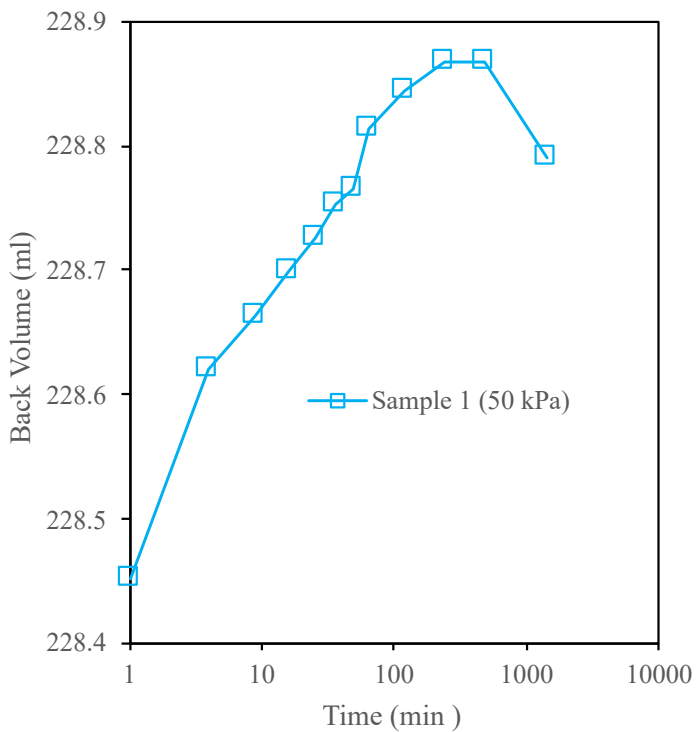


(b)

Chapter 5. Results and Discussion

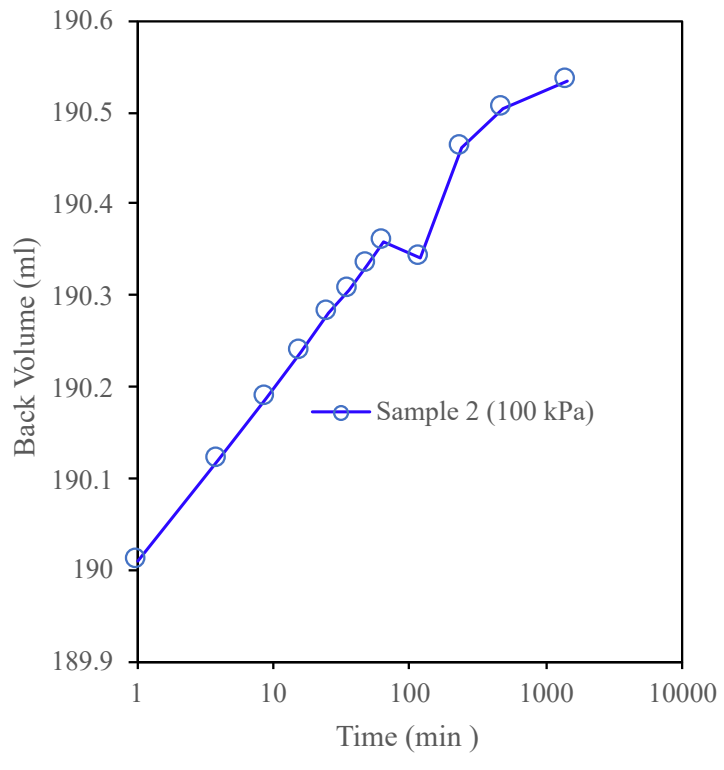


(c)

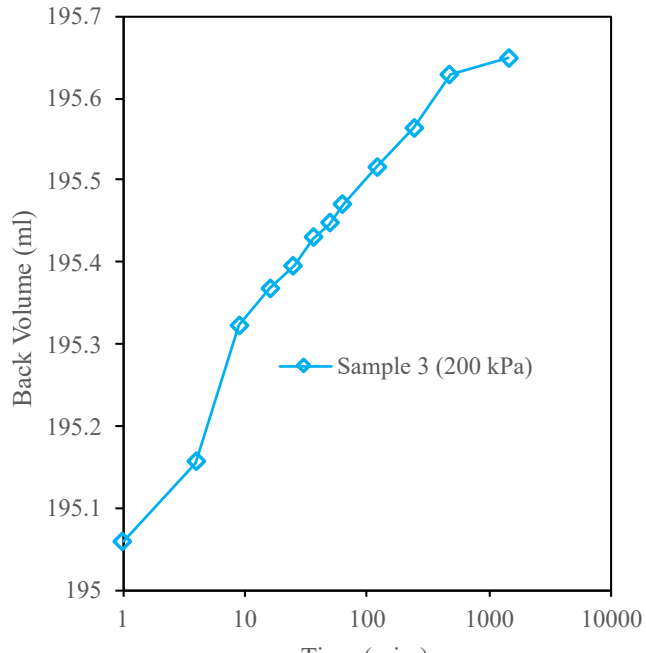


(d)

Chapter 5. Results and Discussion



(e)

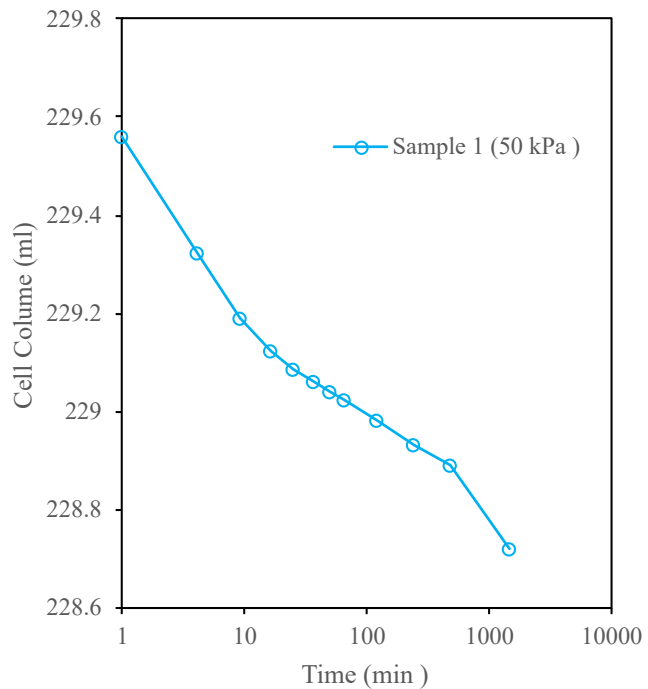


(f)

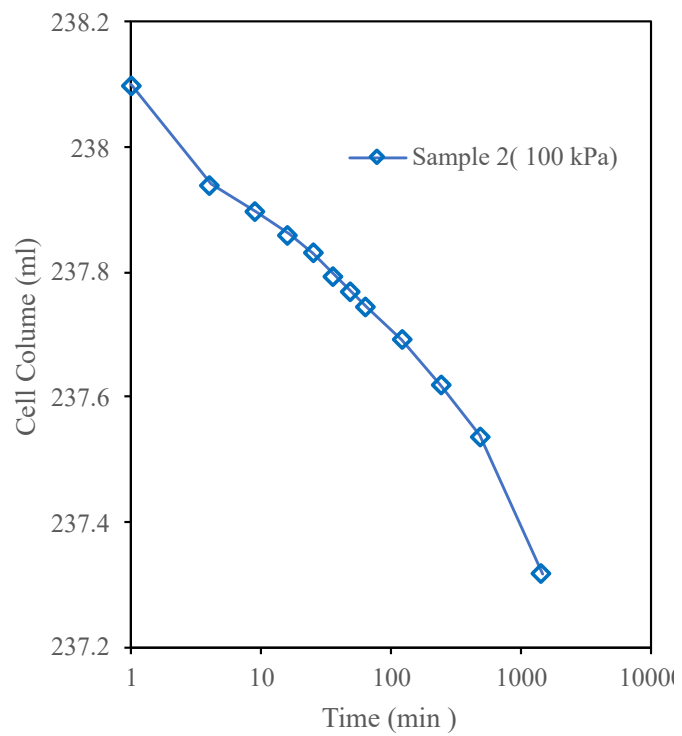
Figure 5.15: Time vs back volume relationship in Consolidation stage for HVDM treated and remoulded sample- (a) HVDM 50 kPa, (b) HVDM 100 kPa, and (c) HVDM 200 kPa, (d) remolded 50 kPa, (e) remolded 100 kPa, and (f) remolded 200 kPa

Chapter 5. Results and Discussion

On the other hand, in Figure 5.16, the cell volume decreases with time in the consolidation stage.

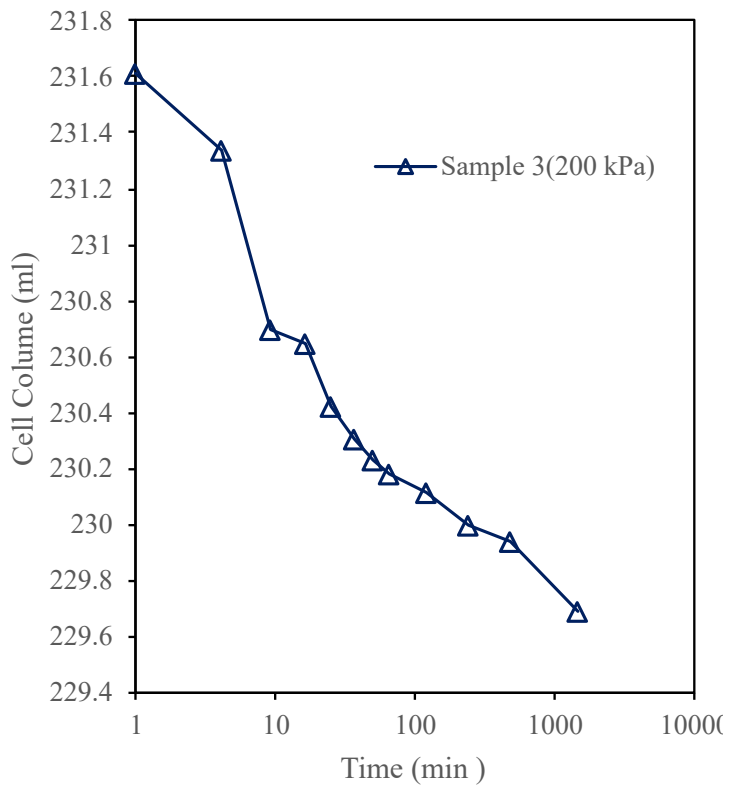


(a)

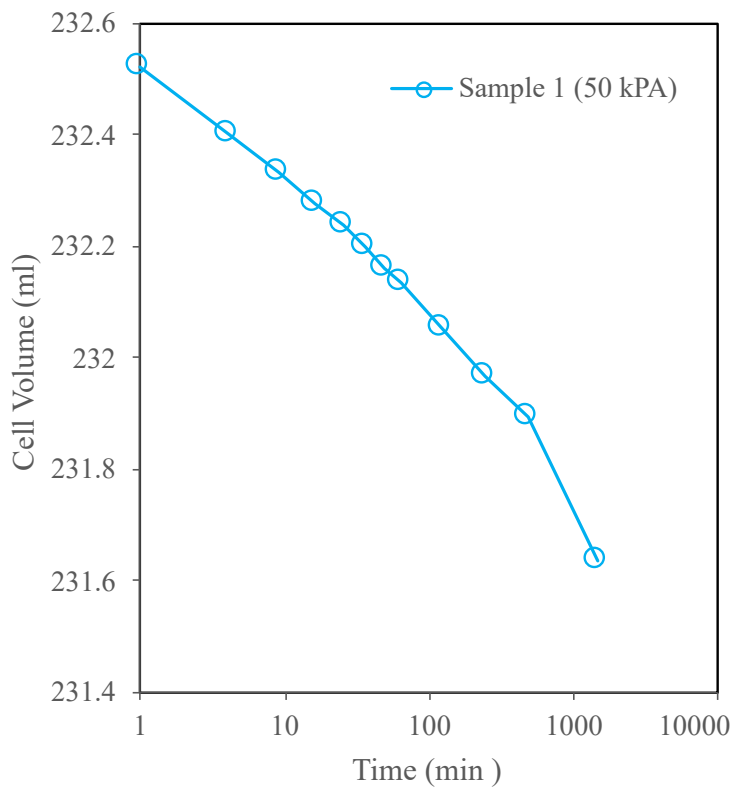


(b)

Chapter 5. Results and Discussion

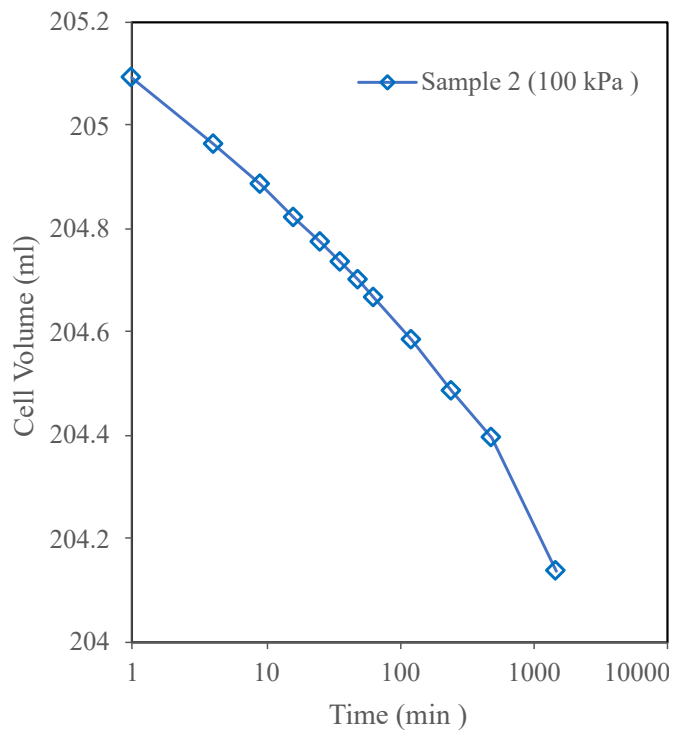


(c)

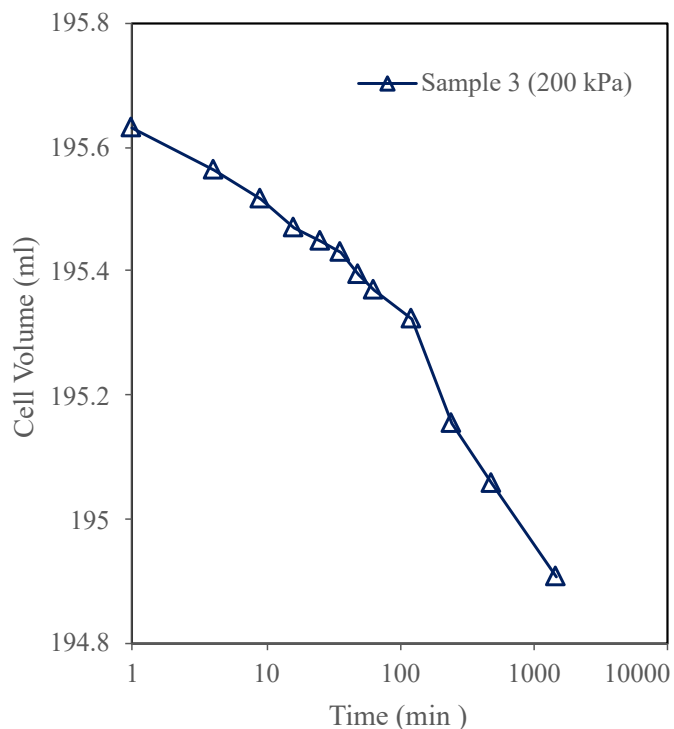


(d)

Chapter 5. Results and Discussion



(e)

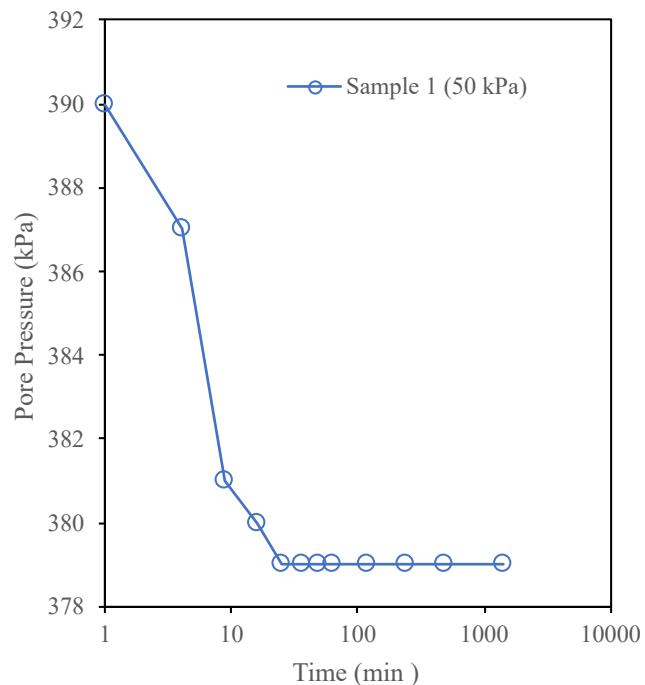


(f)

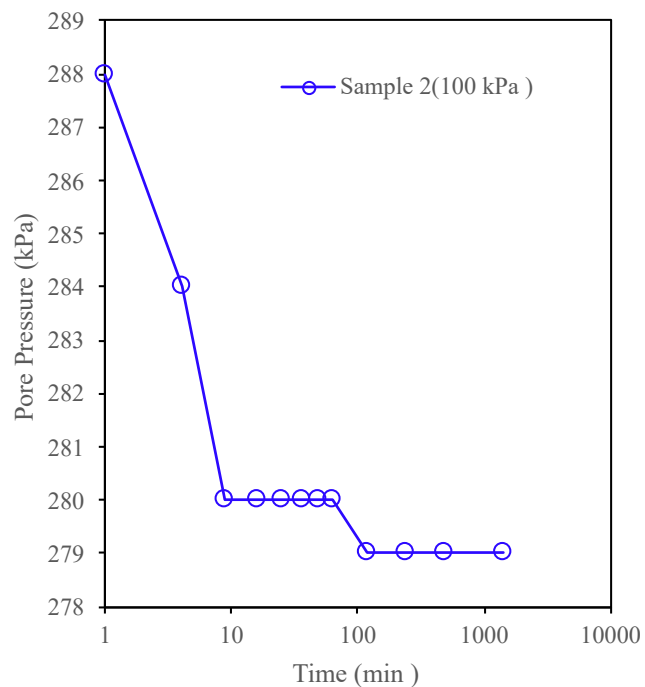
Figure 5.16: Time vs. cell volume relationship in consolidation stage for HVDM treated and remolded sample- (a) HVDM 50 kPa, (b) HVDM 100 kPa, and (c) HVDM 200 kPa, (d) remolded 50 kPa, (e) remolded 100 kPa, and (f) remolded 200 kPa

Chapter 5. Results and Discussion

Figure 5.17 shows that at the beginning of the consolidation stage, the pore pressure is decreasing, but after a while, it remains constant due to the dissipation of excess pore water for all the tests.

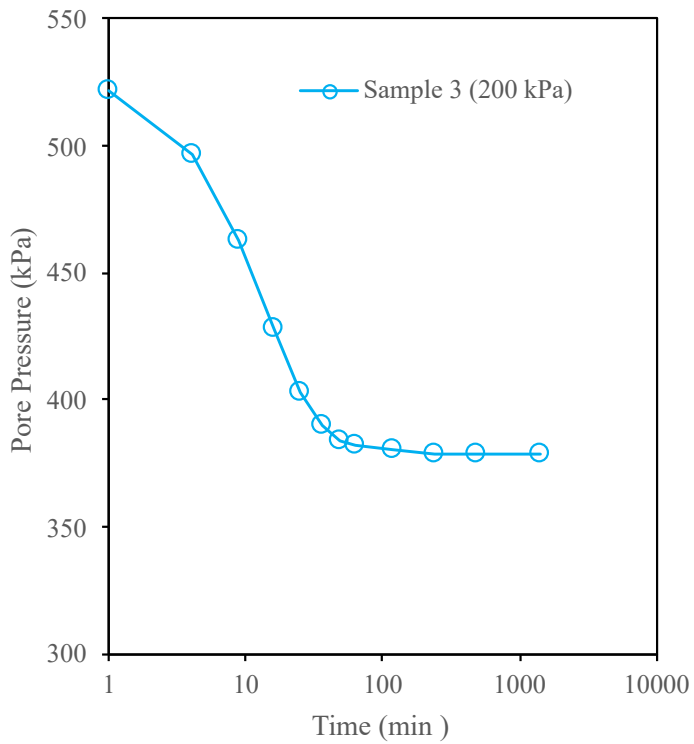


(a)

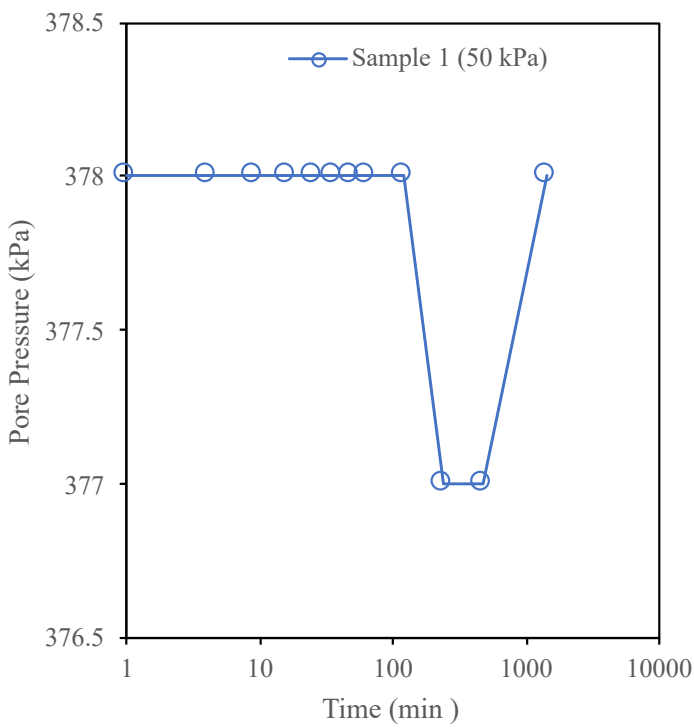


(b)

Chapter 5. Results and Discussion

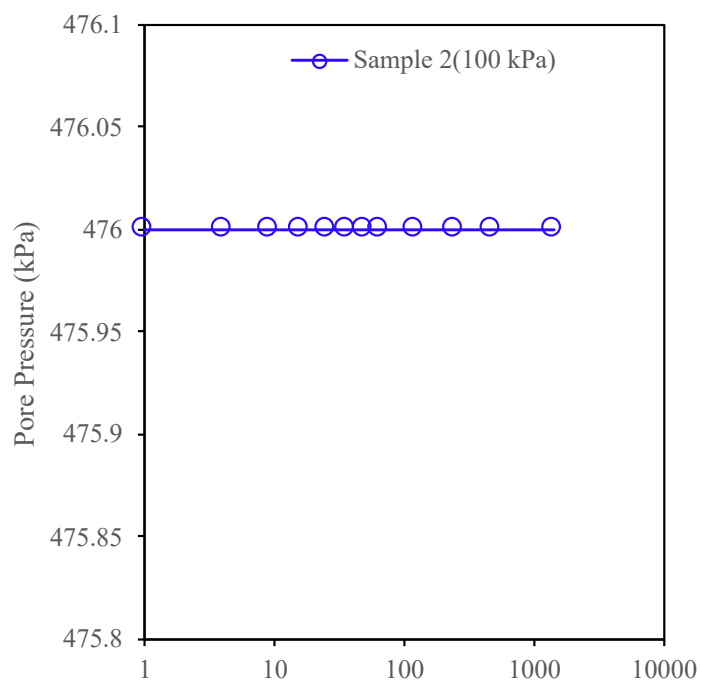


(c)

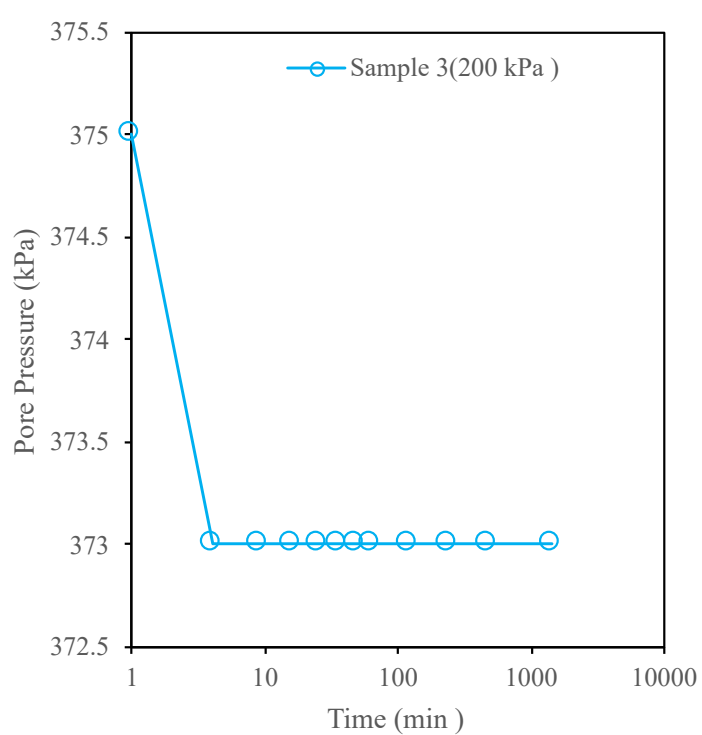


(d)

Chapter 5. Results and Discussion



(e)



(f)

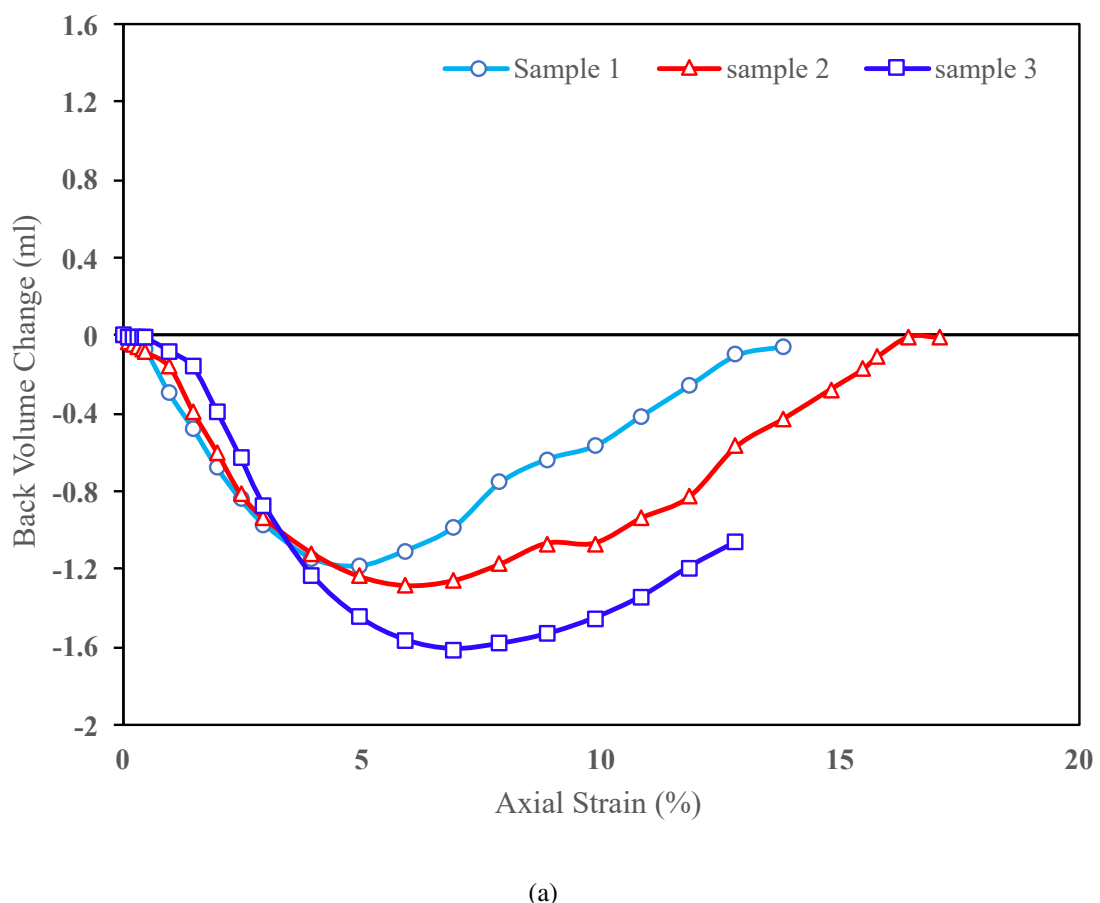
Figure 5.17: Time vs. pore pressure relationship in consolidation stage for HVDM treated and remolded sample- (a) HVDM 50 kPa, (b) HVDM 100 kPa, and (c) HVDM 200 kPa, (d) remolded 50 kPa, (e) remolded 100 kPa, and (f) remolded 200 kPa

Chapter 5. Results and Discussion

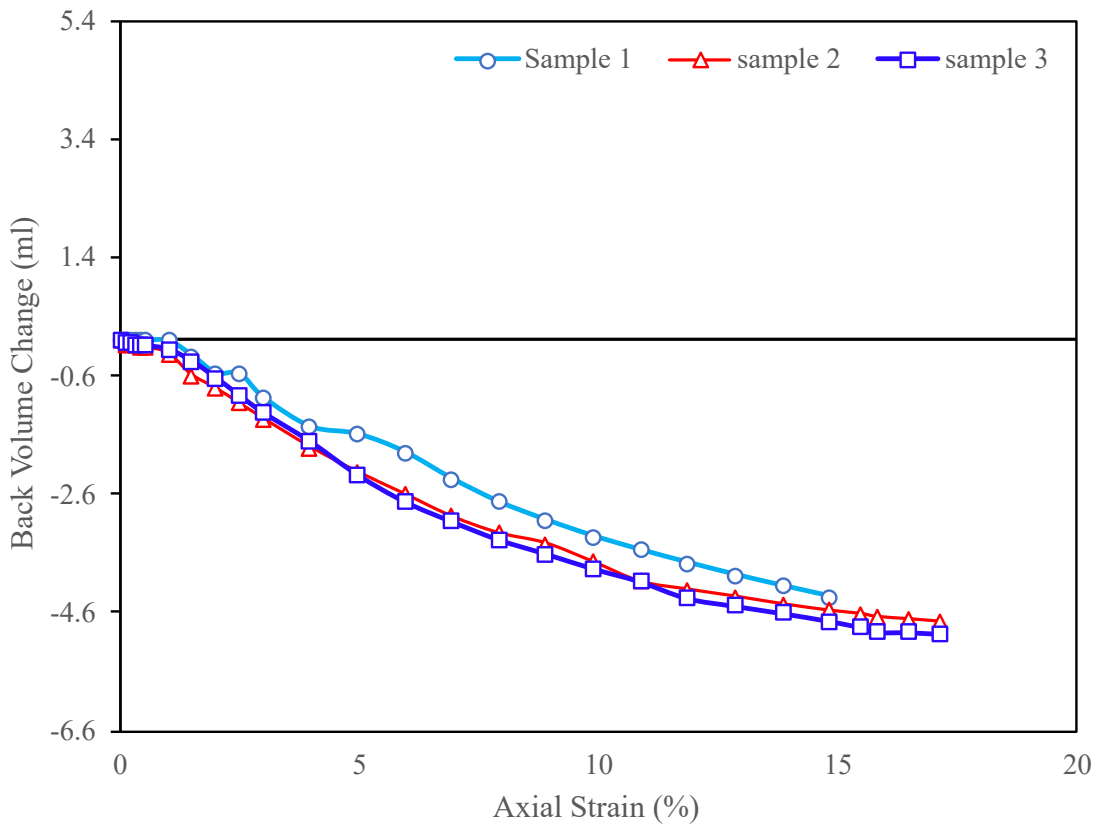
These three scenarios (Figure 5.15, 5.16, and 5.17) are the proof of the proper consolidation of those samples during the consolidation stage of Triaxial test.

Shear Stage

Figure 5.18 shows the axial strain vs. back volume change relationship of the Triaxial test in the shear stage of remolded and HVDM-treated samples. Figure 5.18(a) shows the sign of overconsolidated soil (volume increase after short volume decrease) during the application of deviator stress, which was HVDM-treated samples. On the other hand, Figure 5.18(b) shows the sign of the normally consolidated soils (continuous volume decrease) behavior during the application of deviator stress, which was remolded sample.



Chapter 5. Results and Discussion



(b)

Figure 5.18: Axial strain vs. back volume change relationship of the shear stage of remolded and HVDM-treated samples- (a) HVDM treated sample and (b) Remoulded sample

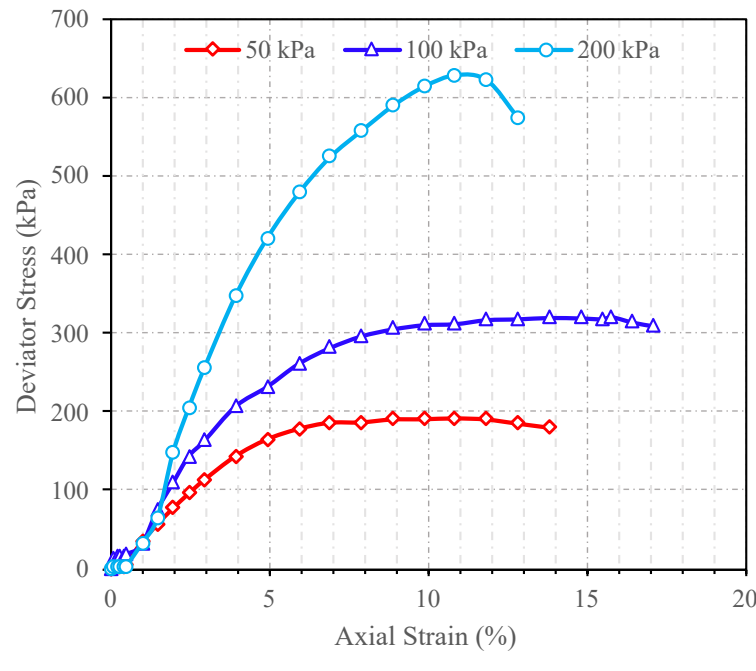
Figure 5.19 shows the relationship between deviator stress vs axial strain at the shear stage of the Triaxial CD test for both remoulded and HVDM-treated samples. Figure 5.19(a) shows that the plot of deviator stress against strain shows the behaviours of dense sand or overconsolidated soil (Das, 2010); on the other hand, plot 5.19(b) shows the behaviours of loose sand or normally consolidated soil (Das, 2010). Table 5.5 summarizes and compares the peak deviator stress at maximum axial strain for both remoulded and HVDM-treated samples.

Table 5.5: Summary of peak deviator stress at maximum axial strain for both remoulded and HVDM-treated samples.

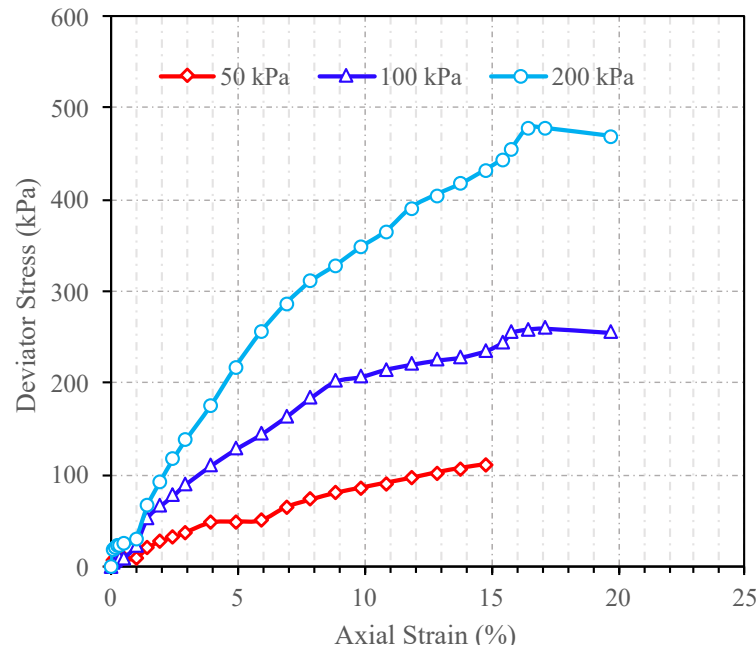
	HVDM Treated Sample			Remoulded Sample		
Confining Pressure (kPa)	50	100	200	50	100	200
Maximum Deviator Stress (kPa)	190.22	320.03	627.25	91.18	255.48	365.5
Axial Strain (%) at Max. Deviator Stress	10.85	15.79	10.85	10.85	15.79	10.85

Chapter 5. Results and Discussion

From Table 5.5, it can be seen that the HVDM-treated samples achieve more strength than remolded samples at desired strain.



(a)



(b)

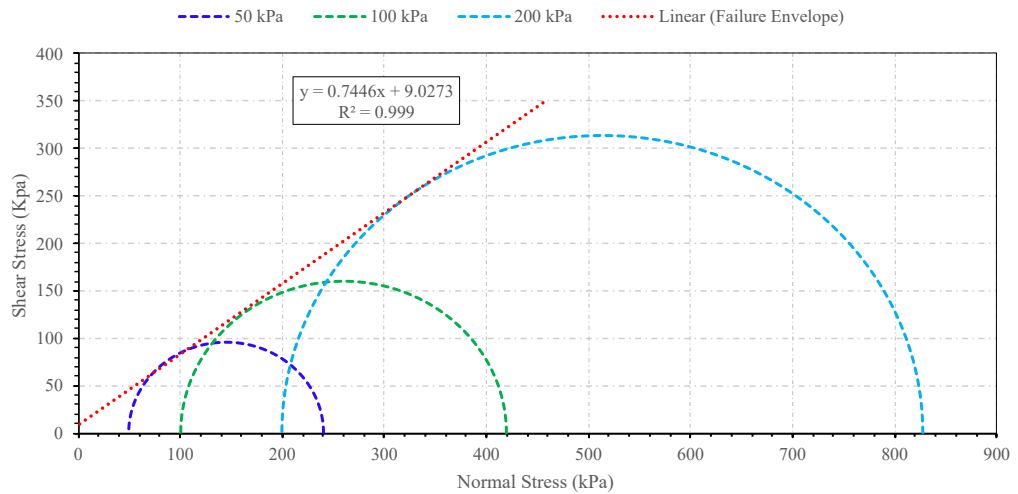
Figure 5.19: Axial strain vs. deviator stress relationship in the shear stage of HVDM treated and remolded samples-(a) HVDM Treated Sample and (b) Remoulded Sample

Chapter 5. Results and Discussion

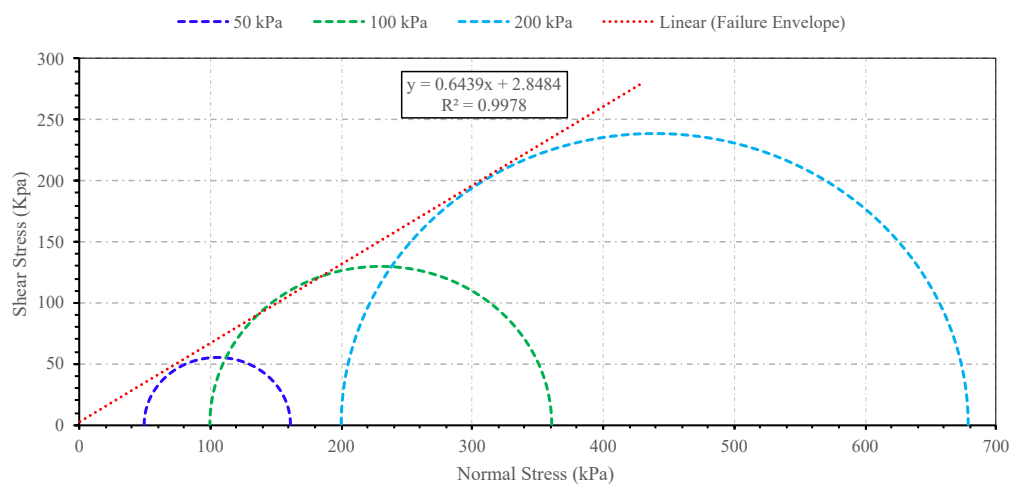
The Mohr's circles are drawn, and the failure envelopes are obtained from major and minor principal stresses at failure for each test (Figure 5.20). Table 5.6 summarizes and represents the comparative c and ϕ value for both HVDM treated and remolded samples. From Mohr's circle and table, it has been seen that the HVDM-treated sample achieved more cohesion and angle of internal friction value than the remolded sample, which indicates the HVDM-treated sample gained more shear strength than the remolded sample.

Table 5.6: Triaxial test result summary

	HVDM Treated Sample	Remoulded Sample
Cohesion c (kPa)	9	3
Angle of Internal Friction ϕ°	23	34



(a)



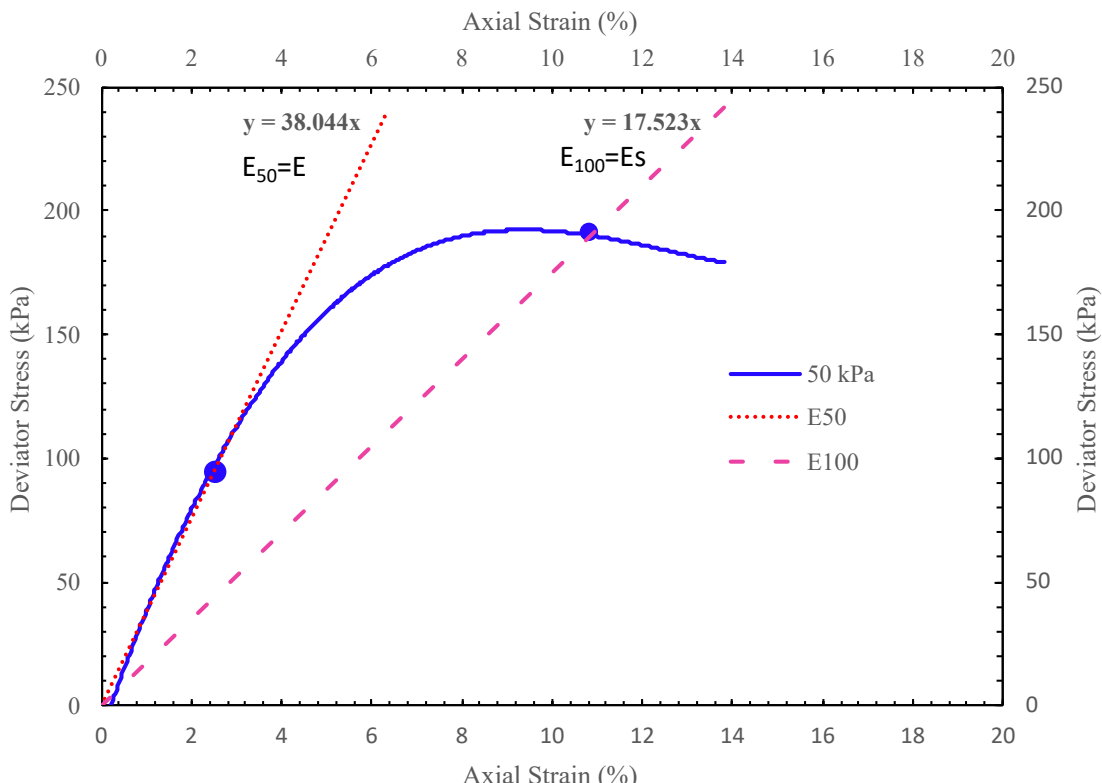
(b)

Figure 5.20: Mohr circle obtained from the drained triaxial test results of HVDM treated and remoulded sample-(a) HVDM treated sample and (b) Remoulded sample

5.5.3.1 Evaluation and Comparison of Young's Modulus from Triaxial CD Test of HVDM Treated and Remoulded Sample

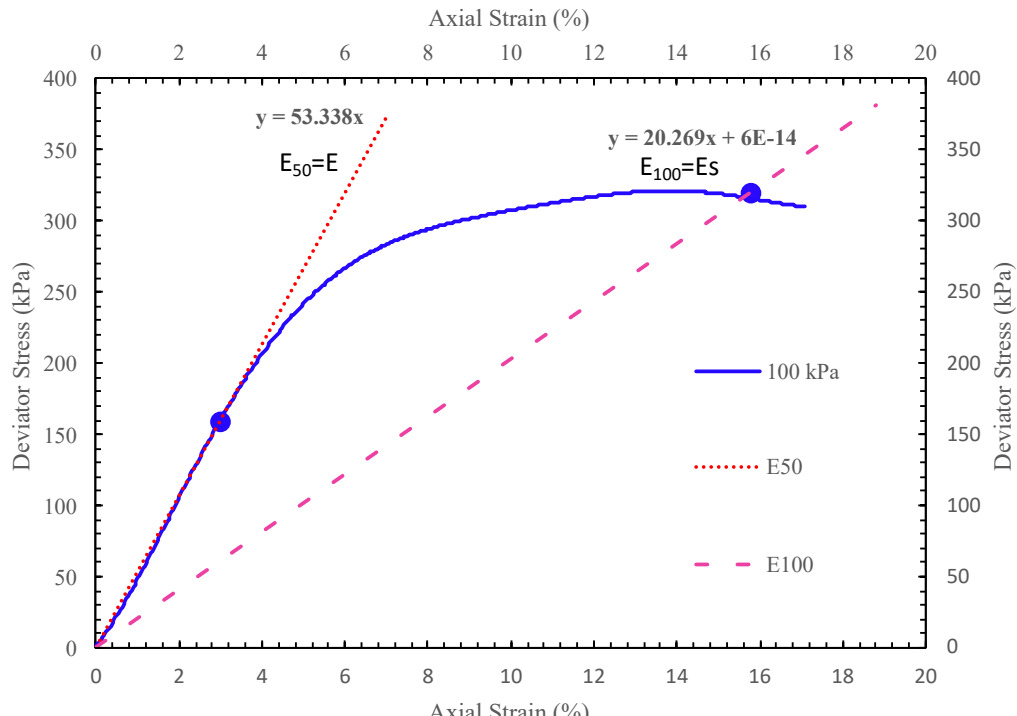
The Young's modulus of soil (E), also known as the soil elastic modulus, is a parameter used to characterize the elasticity of soil and quantify its stiffness. Within the realm of elastic soil behavior, it is defined as the ratio of stress along an axis to strain along that axis. Soil elastic modulus can be estimated from the stress-strain curve obtained from the Triaxial test. In order to calculate Young's Modulus (E), 50% strength of the secant modulus E_{100} is denoted as E_{50} which is considered as Young's modulus of the soil. In this research, the following procedures are followed to estimate Young's modulus E_{50} ,

1st step was to find the maximum deviator stress from the stress vs. strain curve of the shear stage result of the triaxial test. 2nd step needs to divide the peak value of stress by two to get E_{50} . In the 3rd step, A line was drawn between the origin and the E_{50} point. Then regression is used to find the slope of this line, which was used to find E . Figure 5.21 and 5.22 show the criteria for measuring the value of E for both HVDM-treated and Remoulded samples, respectively.

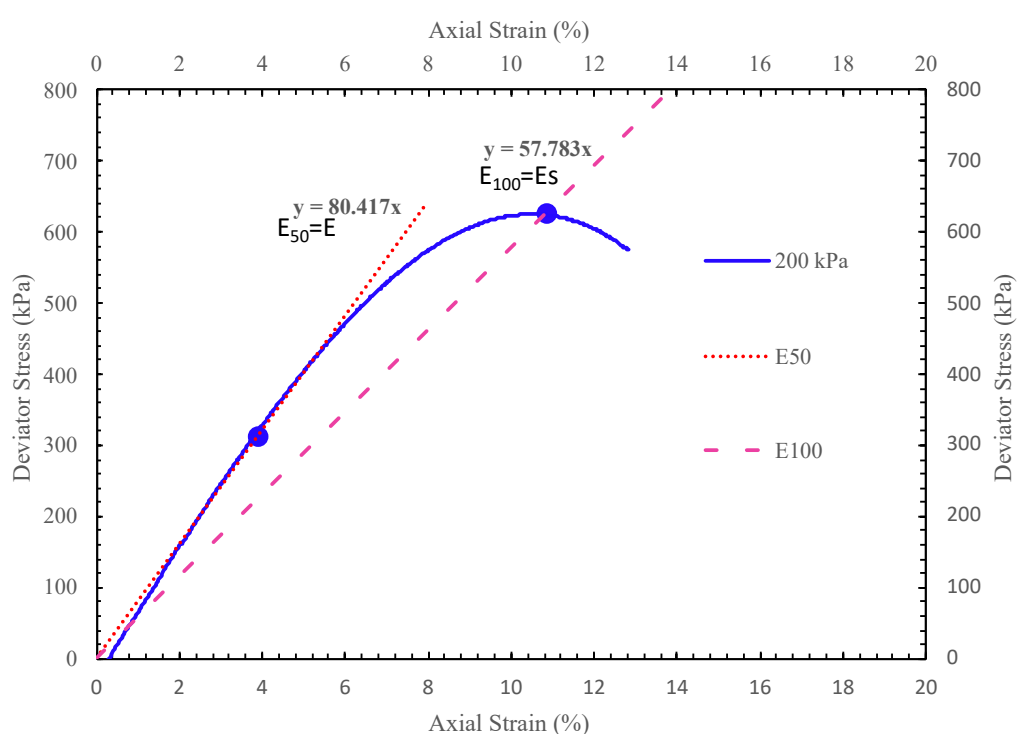


(a)

Chapter 5. Results and Discussion



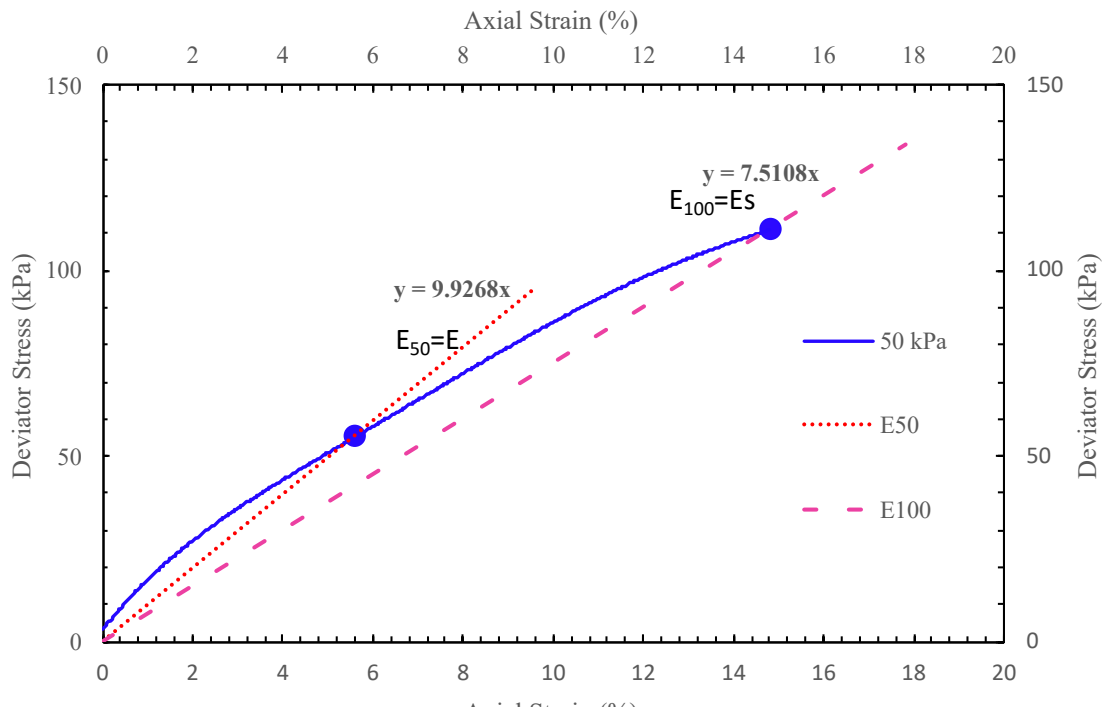
(b)



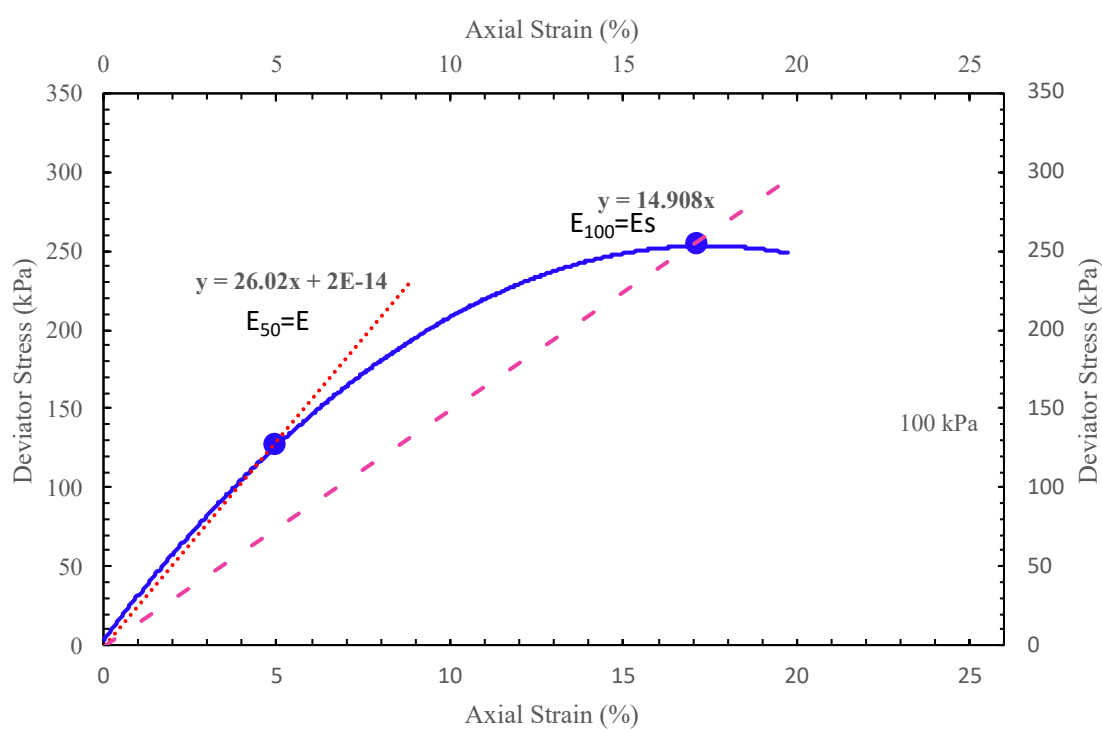
(c)

Figure 5.21: Evaluation of Young's modulus from strain vs. stress curve of HVDM treated samples-(a) 50 kPa, (b) 100 kPa, and (c) 200 kPa

Chapter 5. Results and Discussion



(a)



(b)

Chapter 5. Results and Discussion

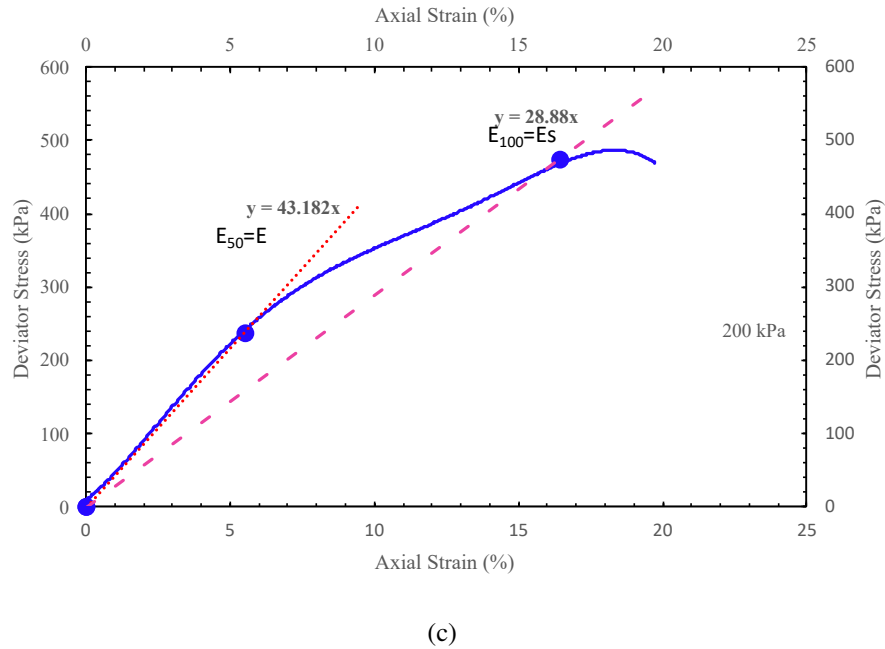
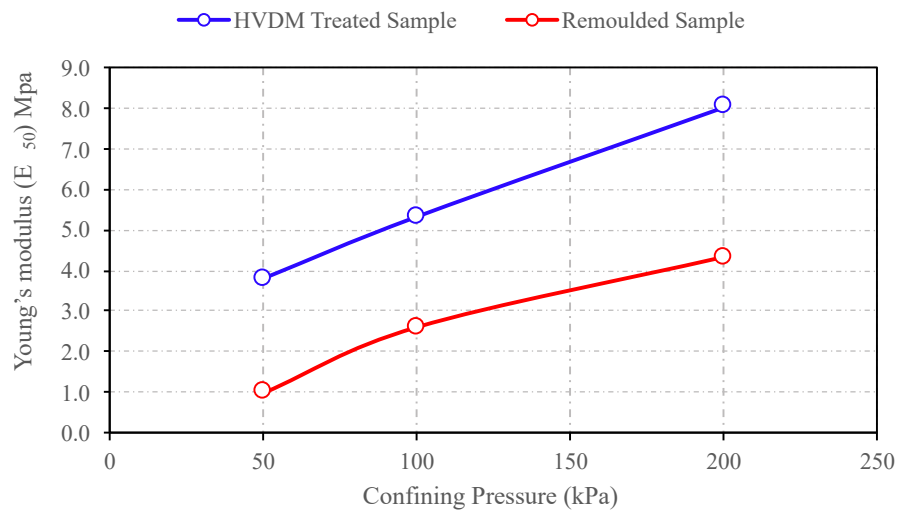


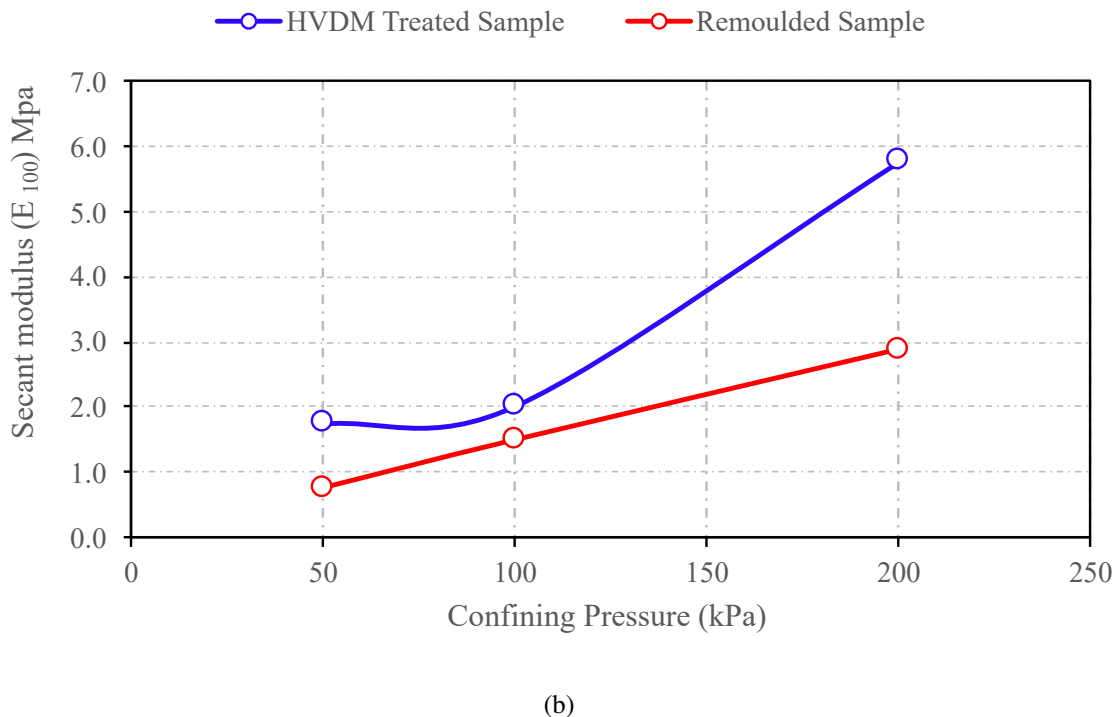
Figure 5.22: Evaluation of Young's modulus from strain vs. stress curve of remolded samples- (a) 50 kPa, (b) 100 kPa, and (c) 200 kPa

Table 5.7 presents the summarized and evaluated result of Young's modulus and Secant modulus at a different confining pressure of the HVDM treated and remolded sample.

Table 5.7: Summary of the evaluated result of Young's modulus and Secant modulus

Properties	HVDM Treated Sample			Remoulded Sample		
Confining Pressure (kPa)	50	100	200	50	100	200
Secant modulus (E_{100}) MPa	1.75	2.03	5.78	0.75	1.49	2.89
Young's modulus (E_{50}) MPa	3.80	5.33	8.04	0.99	2.60	4.32





(b)

Figure 5.23: Illustration of the comparative result of Confining pressure vs Young's modulus and Confining pressure vs Secant modulus relationship of HVDM treated and Remoulded samples-(a) Confining pressure vs Young's modulus relationship and (b) Confining pressure vs Secant modulus relationship

From Table 5.7 and Figure 5.23, it is clearly seen that the HVDM-treated sample has greater values of Young's modulus than the remoulded sample, which also indicates that the HVDM treated sample is stiffer than the remoulded sample.

5.6 Evaluation and Comparison of Consolidation Characteristics from 1D Consolidation Test on Remoulded and HVDM Treated Sample

The One dimensional Consolidation test aims to investigate the amount and rate of volume loss in a laterally constrained soil specimen as a function of applied vertical stress. One dimensional Consolidation tests are conducted on HVDM-treated and remoulded samples for this research. The details of soil sample preparation and testing procedure are described in Chapter 3 in section 3.5.7. In this section, the results and comparison of HVDM-treated and remoulded samples will be presented. Figure 5.24 shows the void ratio vs. effective stress curves for both HVDM-treated and remoulded samples. From Figure 5.24, compression index C_c and re-compression index C_r were evaluated for both samples. The preconsolidation pressure was estimated by the Casagrande method (Figure 5.25) for both samples.

Chapter 5. Results and Discussion

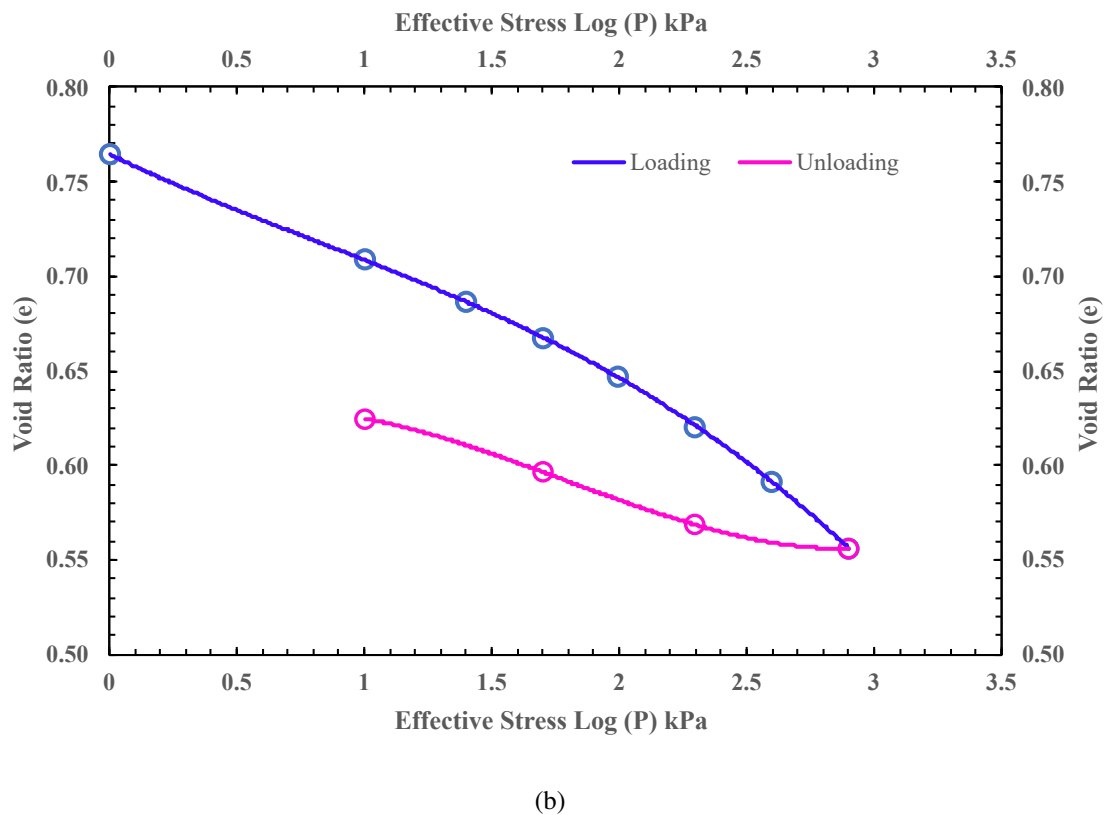
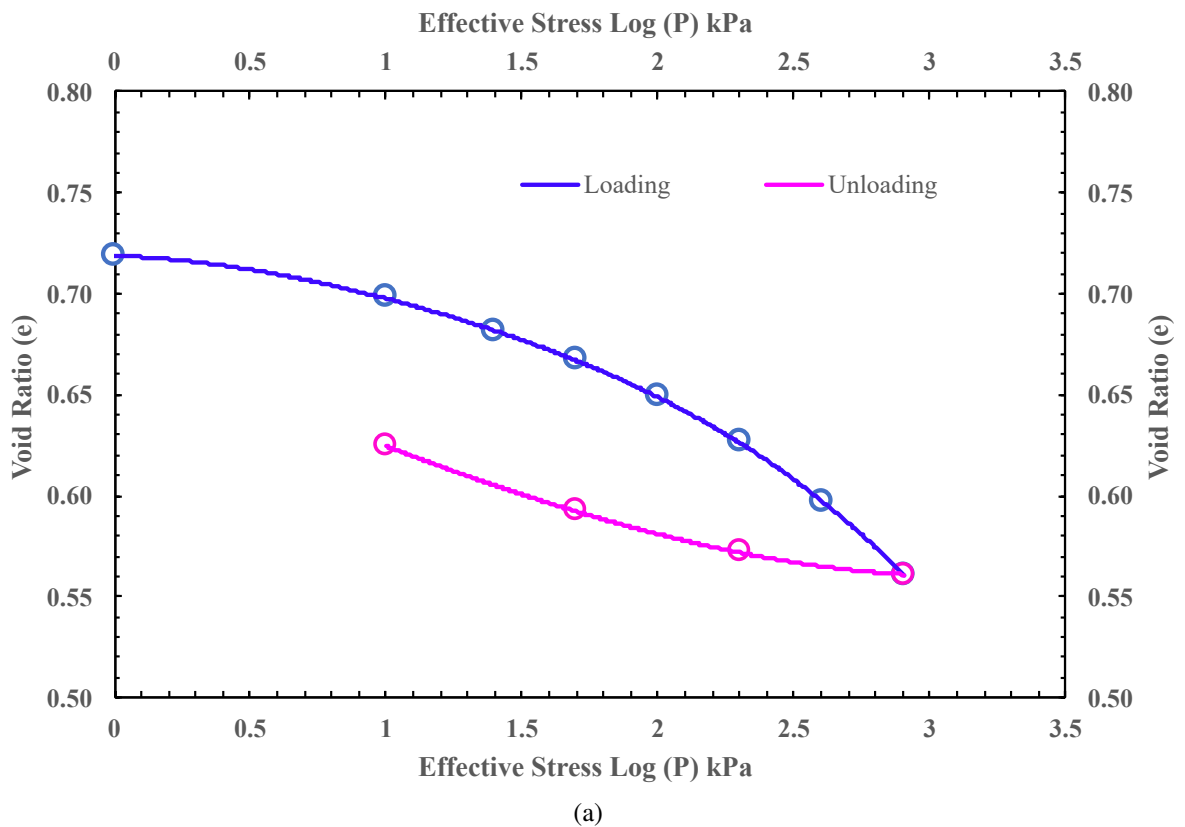


Figure 5.24: e vs $\log p$ curve for HVDM treated and remoulded sample; a) HVDM treated sample, b) Remoulded sample

Chapter 5. Results and Discussion

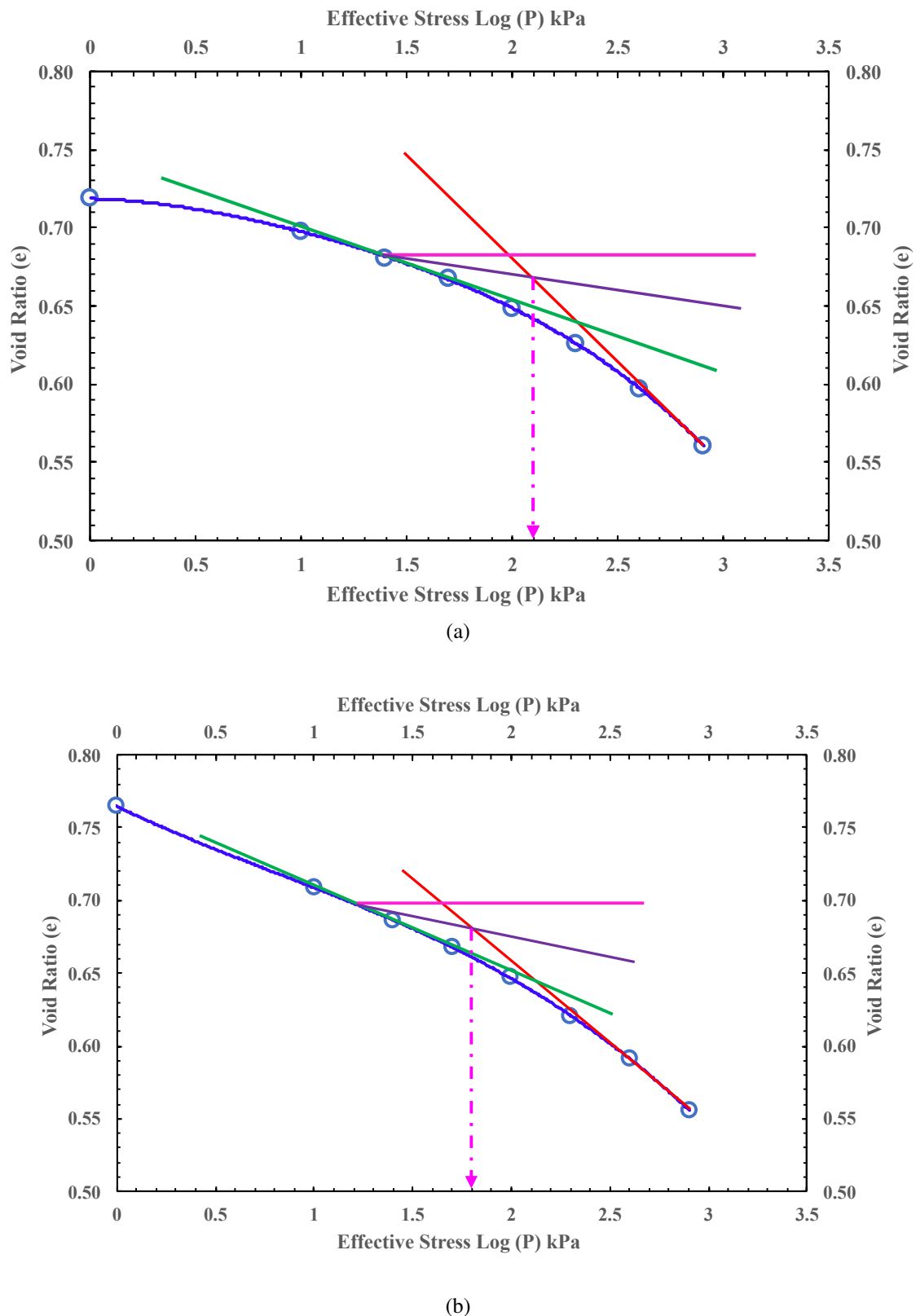


Figure 5.25: Evaluation of preconsolidation pressure from e vs $\log p$ curve-(a) HVDM Treated Sample and (b) Remoulded Sample

The summary of Consolidation test comparative results of HVDM treated and remoulded sample is presented in Table 5.8.

Chapter 5. Results and Discussion

Table 5.8: Summary of consolidation test results of HVDM treated and remoulded sample

Properties	HVDM Treated Sample	Remolded Sample
Bulk Desnity (g/cc)	1.89	1.88
Dry Density (g/cc)	1.58	1.56
Moisture Content (%)	21	20.23
Compression Index (C_c)	0.1199	0.0997
Swell Index (C_s)	0.03998	0.04349
Coefficient of Compressibility A_v (cm ² /kN)	4.5	9
Coefficient of Volume Compressibility M_v (cm ² /kN)	2.6	5.1
Initial Void Ratio (e_0)	0.72	0.76
Final Void Ratio (e_f)	0.54	0.56
Preconsolidation Pressure (kPa)	126	63

From Table 5.8, it is seen that the Compression index (C_c), Recompression index (C_r), Coefficient of Compressibility (A_v), Coefficient of Volume Compressibility (M_v), Initial Void Ratio (e_0) & the Final Void Ratio (e_f) of HVDM treated sample is smaller than remoulded sample which indicates the stiff soil characteristics of HVDM treated sample. Also, from the tests, preconsolidation pressure is estimated at 126 and 63 kPa for HVDM-treated and remoulded samples, respectively, which proves that HVDM-treated samples achieved larger effective vertical overburden stress during the HVDM experiment.

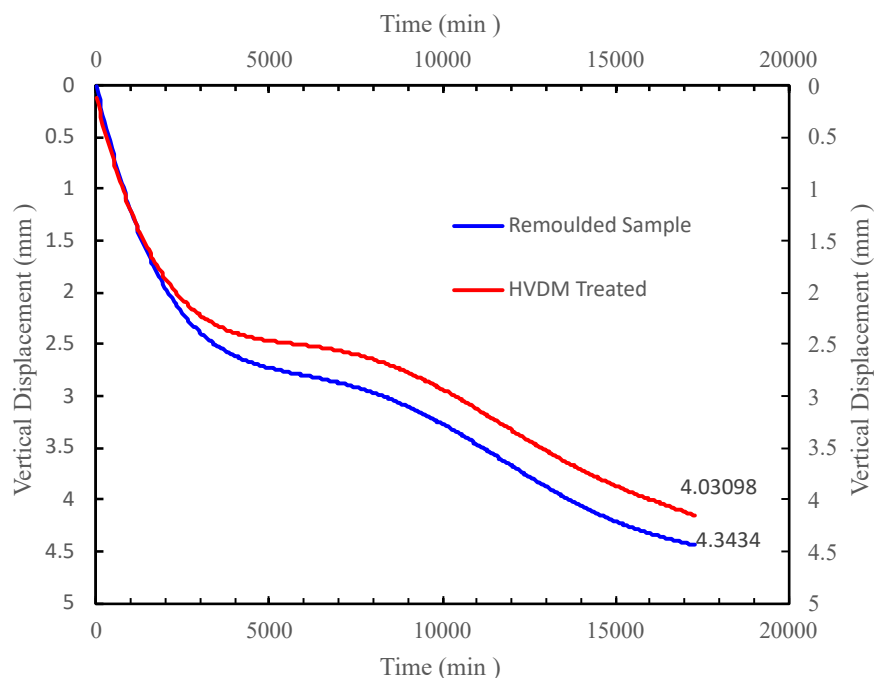


Figure 5.26: Time vs vertical displacement curves of entire consolidation test duration for both sample

Chapter 5. Results and Discussion

Figure 5.26 shows the time versus vertical displacement curves of the entire consolidation test duration for both samples. From this figure, it is seen that the remoulded sample has more settlement than the HVDM-treated sample at the same vertical effective stresses. Figure 5.27 shows the void ratio versus effective stress relationship curve for HVDM-treated and remoulded samples.

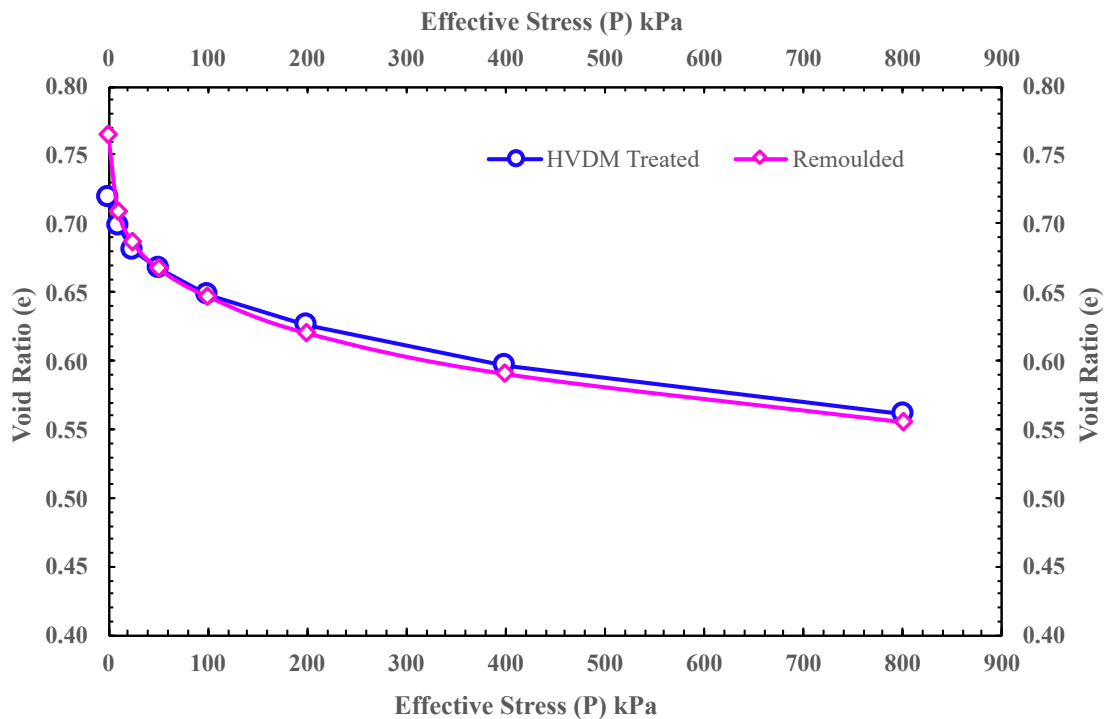


Figure 5.27: e vs P curves for HVDM treated and remoulded sample

To evaluate the C_v value from the consolidation test, Taylor's Square-root of time T_{90} Method was used. Appendix A.1 shows the Square-root of time versus Dial reading curves for both HVDM-treated and remoulded samples.

Table 5.9 summarizes the C_v evaluated results of the HVDM treated and Remoulded sample. From Table 5.9, it can be seen that the C_v value is less for the remoulded sample, indicating that the soil condition is soft, and the Higher C_v value of the HVDM-treated sample indicates the soil is stiff.

Chapter 5. Results and Discussion

Table 5.9: Summary of comparative results of Coefficient of Consolidation of HVDM treated and remoulded sample

Effective Stress (kPa)	Coefficient of Consolidation C_v (m^2/yr)	
	HVDM Treated Sample	Remoulded Sample
	Taylor's Method (t_{90})	Taylor's Method (t_{90})
25	11.11	0.74
50	5.57	0.65
100	6.53	0.52
200	3.37	0.56
400	3.26	0.60
800	3.21	0.48

Figure 5.28 shows the comparison of HVDM treated and Remoulded sample's obtained C_v values from Taylor's method.

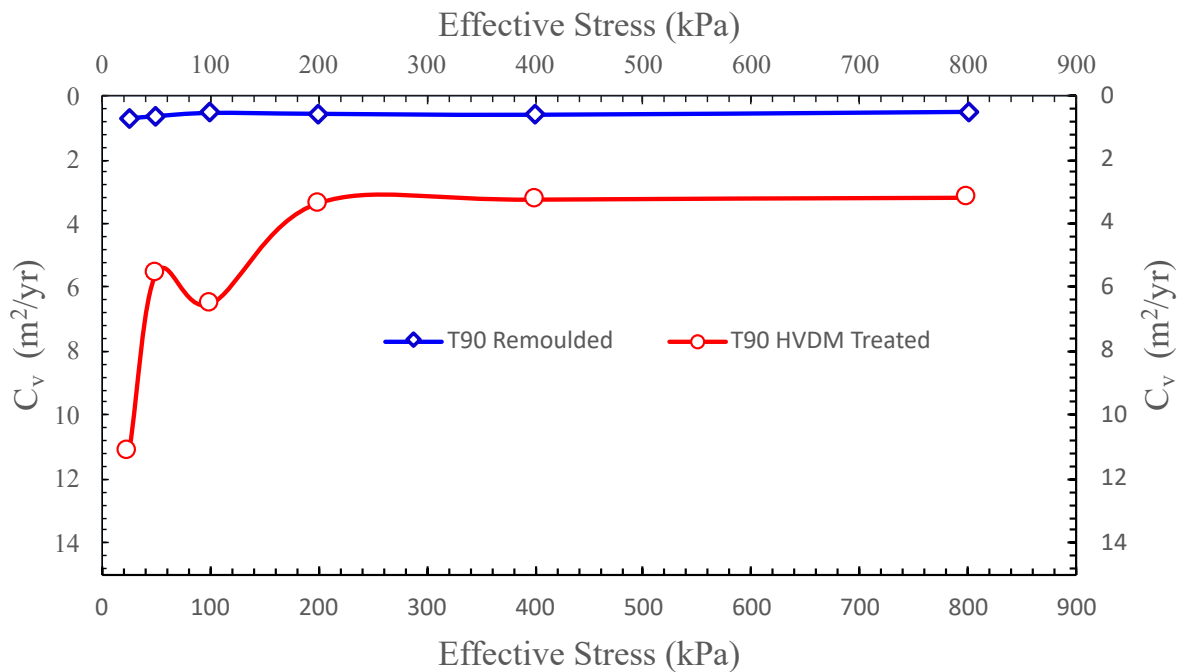


Figure 5.28: Comparison of C_v values from Taylor's T_{90} method for HVDM treated and remoulded samples.

Chapter 6

Conclusions and Recommendation

6.1 General

The main objective of this study was to investigate the High Vacuum Densification Method in a physical model. The current study starts with the field investigation and brings bulk soil samples from a site in Bangladesh where HVDM has been actually implemented. A physical model was developed to investigate and simulate the High Vacuum Densification Method . After several trials, it was found that the prototype was fully functional and ready for the final experiment. The prototype was prepared, and the HVDM was carried out successfully with a satisfactory outcome. This chapter presents the conclusions from this study, followed by recommendations for future work.

6.2 Conclusions

The following conclusions can be drawn based on the results obtained after investigating various aspects related to the High Vacuum Densification Method in the laboratory,

- A 1g physical model was developed, and HVDM was carried out successfully. In the 1g physical model, the vacuum consolidation and dynamic compaction were implemented with satisfactory outcomes.
- Approximately 25 mm settlement was recorded by sensors and manually after the successful execution of HVDM in the physical model. This amount of settlement for a small area in a short time is a remarkable achievement compared to other ground improvement methods.
- The measured excess pore water pressure from the experiment versus experiment run time curve shows the sign of rapid consolidation process.
- From the Proctor test and field density test after the execution of HVDM, it was found that the field compaction in the physical model was approximately 94 %. This percentage of field compaction is also the evidence of achieving maximum field density by HVDM.

- The evaluated values of shear strength properties from the Direct Shear test, UCS test, and Triaxial CD test proved that the HVDM-treated sample gained more strength than remolded samples and HVDM treated sample showed stiff soil characteristics.
- The evaluated values of consolidation properties from the 1D consolidation oedometer test proved that the HVDM-treated sample behaves like over consolidated soil compared to remould samples. Also, the estimated C_V Value indicates the HVDM treated sample as stiff soil.
- The experimental results were compared with the actual field HVDM results. The comparison shows that the small-scale HVDM simulation in the physical model was a successful experiment. The visual witness after and before the HVDM experiment, observed settlement and pore pressure dissipation pattern are the evidence of the success of the simulation of HVDM. It proved that HVDM is an effective ground improvement method for saving project time and improving very soft soil to stiff soil.

6.3 Recommendations for Future Study

Several developments throughout the course of this research have the potential to add new dimensions to future investigations and yield more in-depth findings. Some suggestions for further research to broaden the scope of the study are presented below.

- The physical model was built to investigate only one ground Improvement method called HVDM. However, after successfully execution HVDM, the prototype may be suitable to run the other ground improvement methods (Dynamic Compaction, Vacuum Consolidation without Preloading, Vacuum Consolidation with Preloading, preloading with surcharge, Prefabricated Vertical Drains (PVDs), Sand Drain, and others)
- The data collected from the data logger was huge because the data taken frequency was set to 1000 data per second. However, for a long-run experiment, it may be good practice to take 1 data per second.
- A two-dimensional or Three-dimensional numerical analysis can be performed to compare the results obtained from numerical analysis with this experiment.
- It may be possible to conduct other ground improvement methods in the physical model using this representative soil sample. This allows for comparing the execution time and total settlement with the experiment being conducted to identify a more cost-effective solution.

References

- Aklik, P., Idinger, G., and Wu, W. (2010). Tunnels modeling face stability of a shallow tunnel in a geotechnical centrifuge. In *Physical Modelling in Geotechnics, Two Volume Set*, pages 557–562. CRC Press.
- Al Heib, M., Emeriault, F., and Nghiem, H.-L. (2020). On the use of 1g physical models for ground movements and soil-structure interaction problems. *Journal of Rock Mechanics and Geotechnical Engineering*, 12(1):197–211.
- Alam, M. and Kabir, M. (2000). use of geonatural and geosynthetic technology in bangladesh. In *Proceedings of the 2nd Asian Geosynthetics conference - Geosynthetics Asia 2000*.
- Allersma, H. (1996). Simulation of subsidence in soil layers in a geotechnical centrifuge. In *International Journal of Rock Mechanics and Mining Sciences and Geomechanics Abstracts*, volume 7, page 331A.
- Ansary, M. and Doulah, I. (1993). Ground improvement-state of art report and application prospect in bangladesh. In *Proceedings of First Bangladesh-Japan Joint Geotechnical Seminar on Ground Improvement*, pages 1–25.
- Ansary, M., Siddique, A., and Hasan, K. (2003). A study of lime stabilization on soil of a selected reclaimed site of dhaka city. In *Proceedings of 12th Asian Regional Conf. on Soil Mechanics and Geotechnical Engineering*, volume 1, pages 439–442.
- Berthier, D., Boyle, P., Ameratunga, J., De Bok, C., and Vincent, P. (2009). A successful trial of vacuum consolidation at the port of brisbane. In *Coasts and Ports 2009: In a Dynamic Environment*, pages 640–647. Engineers Australia [Wellington, NZ].
- Chakraborty, S., Hore, R., Ahmed, F., and Ansary, M. (2018). Soft ground improvement at the rampal coal based power plant connecting road project in bangladesh. *Geotechnical Engineering Journal of the SEAGS AGSSEA*, 49.
- Chang, D. T.-T., Lou, X.-M., Xu, S.-L., Wang, J.-C., and Guo, L.-L. (2010). Innovative soft soil stabilization using simultaneous high-vacuum dewatering and dynamic compaction. *Transportation research record*, 2186(1):138–146.
- Chu, J., Yan, S., and Indraranata, B. (2008). Vacuum preloading techniques—recent developments and applications. *GeoCongress 2008: Geosustainability and Geohazard Mitigation*, pages 586–595.

REFERENCES

- Chu, J., Yan, S., and Yang, H. (2000). Soil improvement by the vacuum preloading method for an oil storage station. *Geotechnique*, 50(6):625–632.
- Cognon, J. (1991). Vacuum consolidation. rev. *French Geotechnique, Vol. 3, No.*, pages 37–47.
- Dam, L. T., Sandanbata, I., and Kimura, M. (2006). Vacuum consolidation method-worldwide practice and the latest improvement in japan. *Tokyo, Japan: Hazama Corporation*.
- Das, B. (2010). *Principles of Geotechnical Engineering*. PWS series in civil engineering. Brooks Cole/Thompson Learning.
- Deng, A. and Xu, S.-l. (2010). Consolidating dredge soil by combining vacuum and dynamic compaction effort. American Society of Civil Engineers.
- Dhar, A. S., Siddique, A., and Ameen, S. F. (2011). Ground improvement using pre-loading with prefabricated vertical drains. *ISSMGE International Journal of Geoengineering Case Histories*, 2(2):86–104.
- Feng, S.-J., Shui, W.-H., Gao, L.-Y., He, L.-J., and Tan, K. (2010). Field studies of the effectiveness of dynamic compaction in coastal reclamation areas. *Bulletin of engineering geology and the environment*, 69(1):129–136.
- Garnier, J., Gaudin, C., and Springman (2007). Catalogue of scaling laws and similitude questions in geotechnical centrifuge modelling. *International Journal of Physical Modelling in Geotechnics*, 7(3):01–23.
- Green, D. (2014). Modelling geomorphic systems: scaled physical models. *Geomorphological techniques (online edition)*.
- Guo, Mei Ling (2016). On high vacuum densification of soft foundation treatment. *MATEC Web Conf.*, 63:02014.
- Han, J. (1998). Ground modification by a combination of dynamic compaction, consolidation, and replacement. In *Proceedings of the 4th International Conference on case histories in geotechnical Engineering, St. Louis, Missouri*, pages 341–346.
- Holtz, R. D. and Wager, O. (1975). Preloading by vacuum: current prospects. *Transportation research record*, 548:26–29.
- Hore, R. and Ansary, M. (2020). Different soft soil improvement techniques of dhaka mass rapid transit project. *Journal of Engineering Science*, 11:37–44.
- Hore, R., Chakraborty, S., Shuvon, A. M., and Ansary, M. A. (2020). Effect of acceleration on wrap faced reinforced soil retaining wall on soft clay by performing shaking table test. *Proceedings of engineering and technology innovation*, 15:24.

REFERENCES

- Indraratna, B., Bamunawita, C., and Khabbaz, H. (2004). Numerical modeling of vacuum preloading and field applications. *Canadian Geotechnical Journal*, 41(6):1098–1110.
- Indraratna, B., Rujikiatkamjorn, C., and Sakr, M. (2007). Vacuum consolidation of soft clay via vertical drains and associated design charts. In *International Conference on Soil Mechanics and Geotechnical Engineering*, pages 1–15. International Society for Soil Mechanics and Geotechnical Engineering.
- Islam, M. R. and Ahmad, M. (2004). *Living in the coast: Problems, opportunities and challenges*. Program Development Office, Integrated Coastal Zone Management Plan.
- Jacob, A., Thevanayagam, S., and Kavazanjian, E. (1994). Vacuum-assisted consolidation of a hydraulic landfill. In *Proceedings of the Conference on Vertical and Horizontal Deformations of Foundations and Embankments. Part 2 (of 2)*, pages 1249–1261. Publ by ASCE.
- Jan E Alam, M., Hossain, M., Patowary, F., and Rana, M. (2018). Improvement of soft clay using stone columns and compaction techniques. *Journal of Geotechnical Studies*, 3:13–17.
- Ji-hong, C. (2014). Hvdm method application in a sandy clay ground. *Proceedings of Softsoils*, 21(23rd).
- Johnson, S. J. (1977). *State-of-the-Art applicability of conventional densification techniques to increase disposal area storage capacity*. US Waterways Experiment Station.
- Kjellman, W. (1952). Consolidation of clay soil by means of atmospheric pressure. In *Proc. of Conf. on Soil Stabilization, 1952*.
- Koirala, N., Soralump, S., and Phakdimek, S. (2022). Observations from ground improvement using vacuum consolidation method. *Civil Engineering and Architecture*, pages 771–783.
- Kumar, S. (2001). Reducing liquefaction potential using dynamic compaction and construction of stone columns. *Geotechnical & Geological Engineering*, 19(2):169–182.
- Kumar G., S., Sridhar, G., Radhakrishnan, R., Robinson, R., and Rajagopal, K. (2015). A case study of vacuum consolidation of soft clay deposit. *Indian Geotechnical Journal*, 45(1):51–61.
- Liang, R. and Xu, S. (2010). Innovative soft clay improvements using vacuum and dynamic compaction. In *Proc. Indian Geotechnical Conference-2010*, pages 133–141.
- Liang, R. and Xu, S. (2012). High vacuum densification method for soft soil improvement. In *GeoCongress 2012: State of the Art and Practice in Geotechnical Engineering*, pages 1928–1937.

REFERENCES

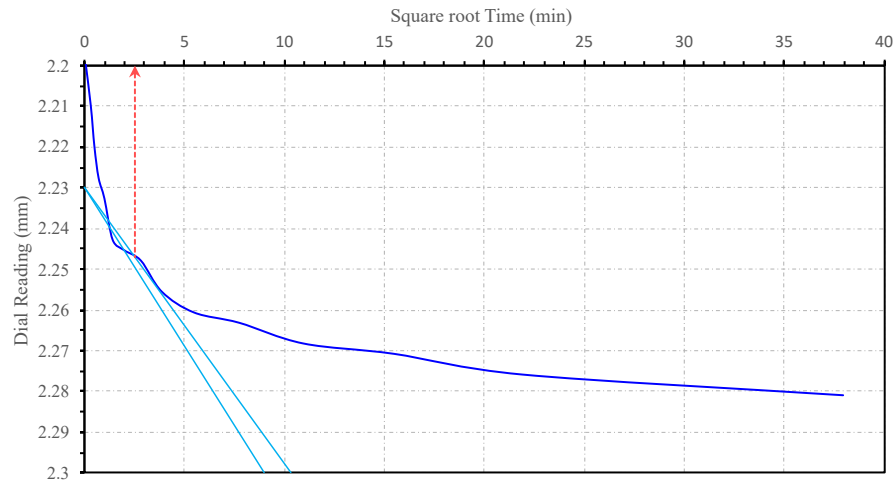
- Liang, R. Y. and Xu, S. (2011). Innovative soft clay improvement technique using vacuum and dynamic compaction (hvdm). In *2011 Pan-Am CGS Geotechnical Conference*.
- Liu, J.-h., Yuan, J.-b., Xiong, H., and Chen, W. (2008). Dynamic compaction treatment technology research of red clay soil embankment in southern mountains. *Journal of Central South University of Technology*, 15(2):50–57.
- Liu, X. (1996). Application and experience of vacuum preloading method. In *Proc. of Int. Workshop on Technology Transfer for Vacuum-Induced Consolidation*.
- Lukas, R. et al. (1995). Geotechnical engineering circular no. 1-dynamic compaction. Technical report, United States. Federal Highway Administration. Office of Technology Applications.
- Lukas, R. G. (1986). Dynamic compaction for highway construction, volume 1: design and construction guidelines.
- Mayne, P. W., Jones Jr, J. S., and Dumas, J. C. (1984). Ground response to dynamic compaction. *Journal of Geotechnical Engineering*, 110(6):757–774.
- Menard, L. and Broise, Y. (1975). Theoretical and practical aspect of dynamic consolidation. *Geotechnique*, 25(1):3–18.
- Mitchell, J., Jardine, F., Research, C. I., Association, I., of Trade, G. B. D., and Industry (2002). *A Guide to Ground Treatment*. CIRIA publication. CIRIA.
- Rahman, M. M., Rabbi, A. T. M. Z., and Siddique, A. (2011). Strength and deformation characteristics of cement treated soft bangladesh clays. *International Journal of Nanoelectronics and Materials*.
- Sandiford, R., Ludewig, N., and Dunlop, P. (1996). Evaluation of enhanced consolidation for dredged material disposal newark bay confined disposal facility. In *International Workshop on Technology Transfer for Vacuum-Induced Consolidation: Engineering and Practice, Los Angeles, California*, pages 31–37.
- Selby, J. P. A. (2002). Simulation of dynamic compaction of loose granular soils. *Advances in Engineering Software (Thomson Reuters) 2002-jul vol. 33 iss. 7-10*, 33.
- Shang, J., Tang, M., and Miao, Z. (1998). Vacuum preloading consolidation of reclaimed land: a case study. *Canadian Geotechnical Journal*, 35(5):740–749.
- Shi, Y. and Chai, J. (2017). Application of high vacuum densification method to soft soil foundation treatment engineering at pingtan comprehensive experimental area. *Journal of Engineering Geology*, 25(1):11–18.

REFERENCES

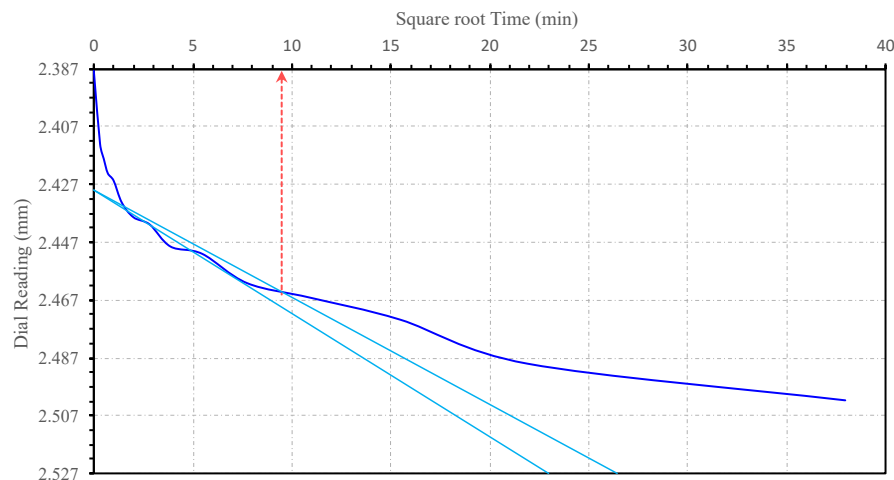
- Shiau, J., Sams, M., and Lamb, B. (2016). Introducing advanced topics in geotechnical engineering teaching - tunnel modelling. *journal of GEOMATE*, 10:1607–1614.
- Shinsha, H. (1991). Improvement of very soft ground by vacuum consolidation using horizontal drains. *GEO-COAST, Yokohama, 1991*, pages 3–6.
- Siddique, A., Dhar, A. S., and Ameen, S. F. (2023). *Ground Improvement Using Prefabricated Vertical Drains with Preloading for Port Park Area at Chittagong, Bangladesh*, pages 5–20. Springer Nature Singapore, Singapore.
- Siddique, A., Safiullah, A., and Ansary, M. (2002). Characteristic features of soft ground engineering in bangladesh. *Coastal Geotechnical Engineering in Practice, Nakase and Tsuchida (eds), Swets and Zeithinger, Lisse*, pages 231–248.
- Tang, M. and Shang, J. (2000). Vacuum preloading consolidation of yaoqiang airport runway. *Geotechnique*, 50(6):613–623.
- Wang, R., Zhu, C., Wang, J., and Yang, M. Z. (2000). Improvement of soft clays by dynamic compaction with puds. In *Advances in Grouting and Ground Modification*, pages 311–324.
- Wood, D. M. (2004). *Geotechnical modelling(1st ed.)*. CRC press.
- Yin, D., Zhang, B., and Tao, Y. (2013). On the basis of high vacuum densification method in dalian coastal soft soil analysis. In *Applied Mechanics and Materials*, volume 256, pages 1903–1907. Trans Tech Publ.
- Zhou, Y.-G., Sun, Z.-B., and Chen, Y.-M. (2018). Zhejiang university benchmark centrifuge test for leap-gwu-2015 and liquefaction responses of a sloping ground. *Soil Dynamics and Earthquake Engineering*, 113:698–713.

Appendix A

Appendix

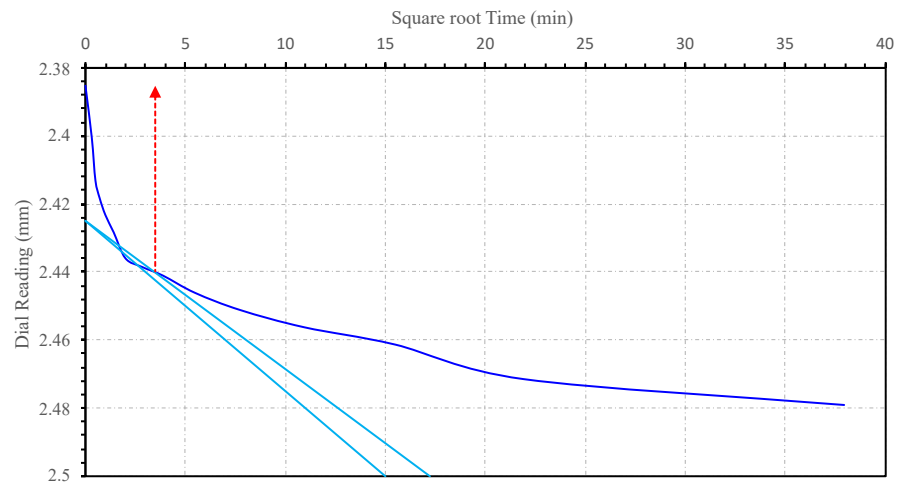


(a)

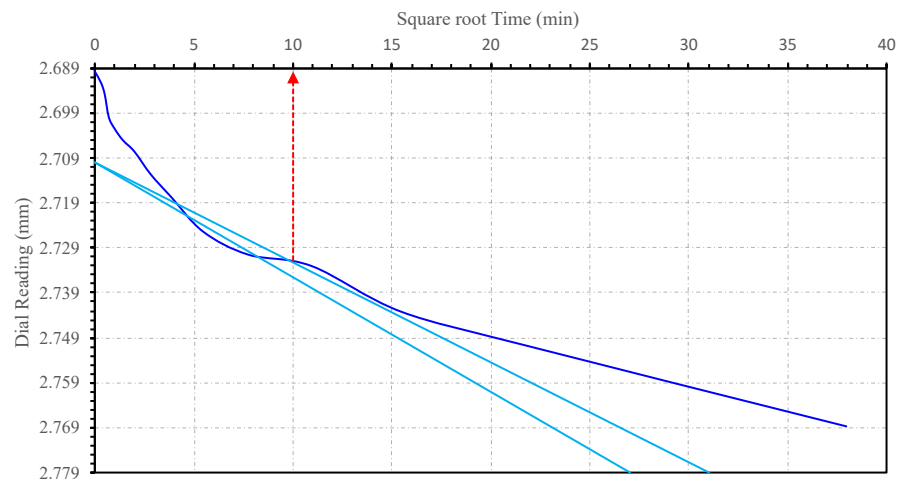


(b)

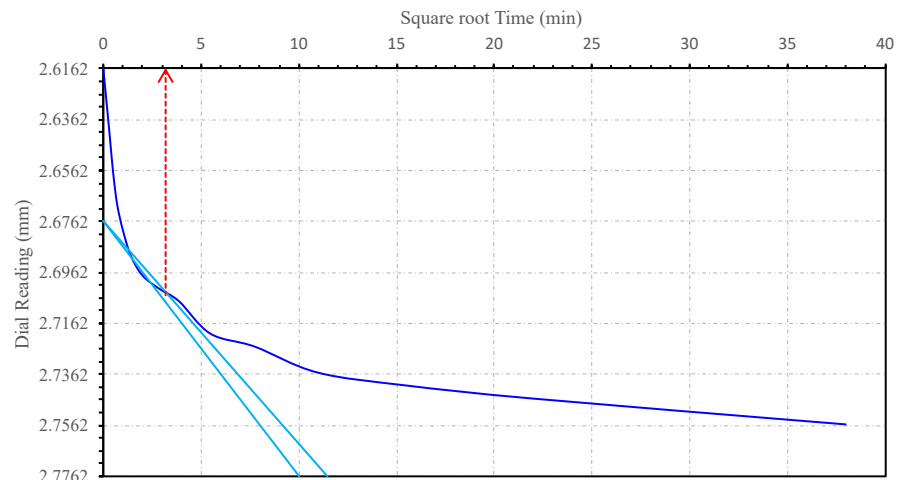
Chapter A. Appendix



(c)

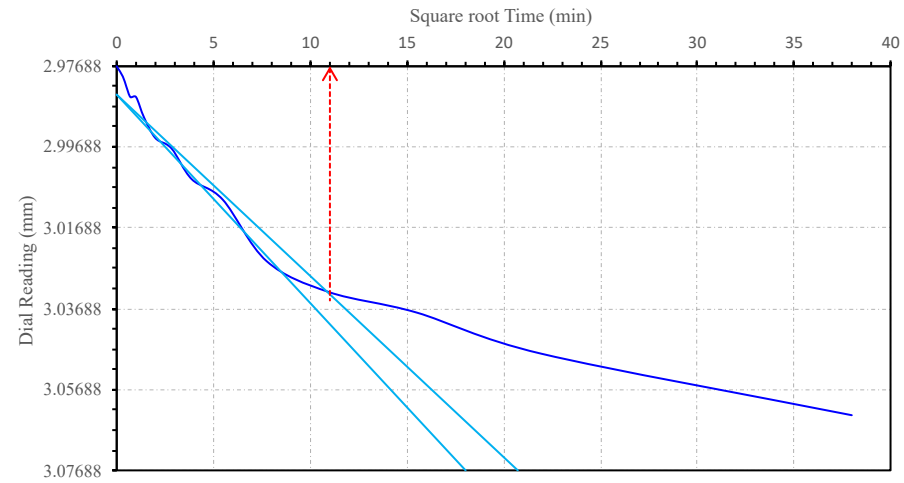


(d)

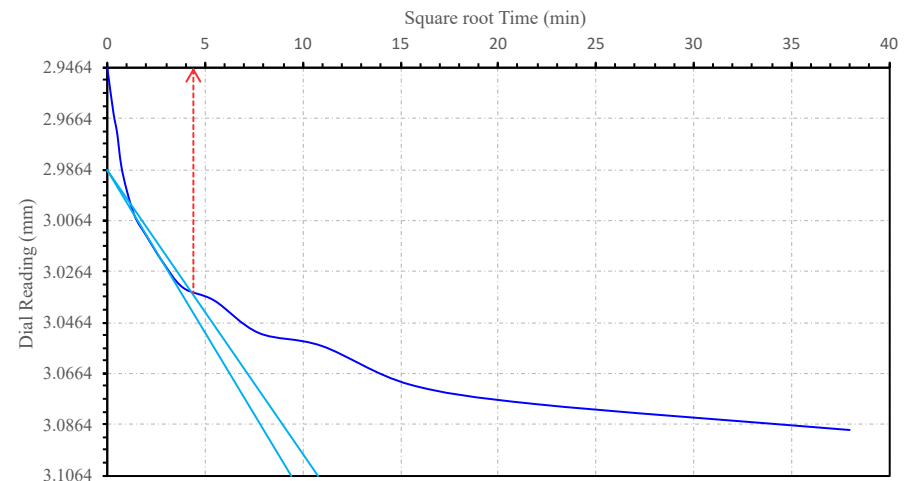


(e)

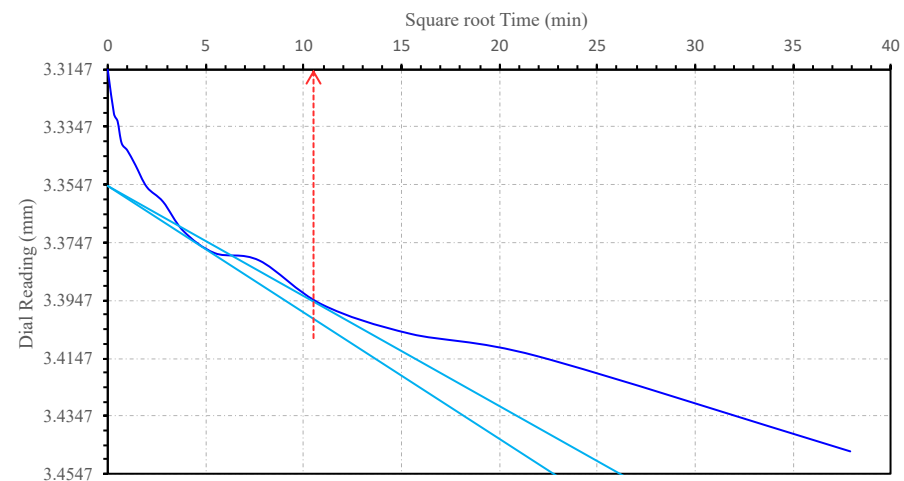
Chapter A. Appendix



(f)

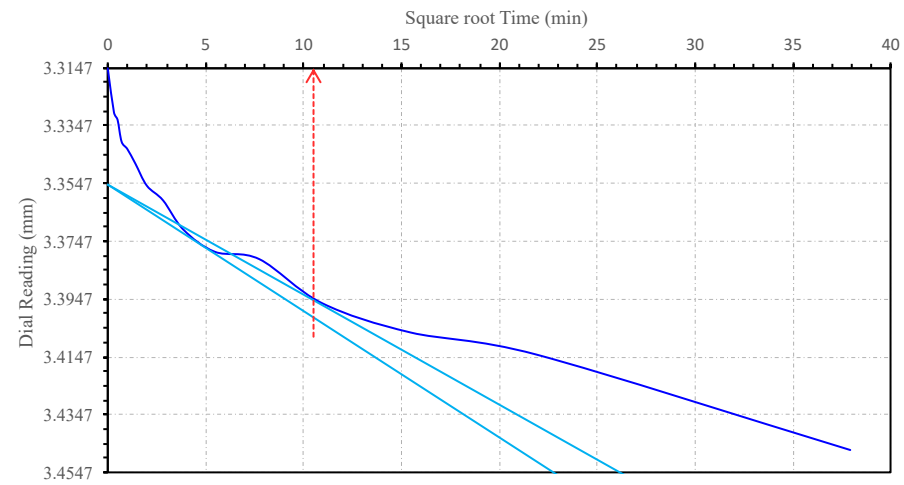


(g)

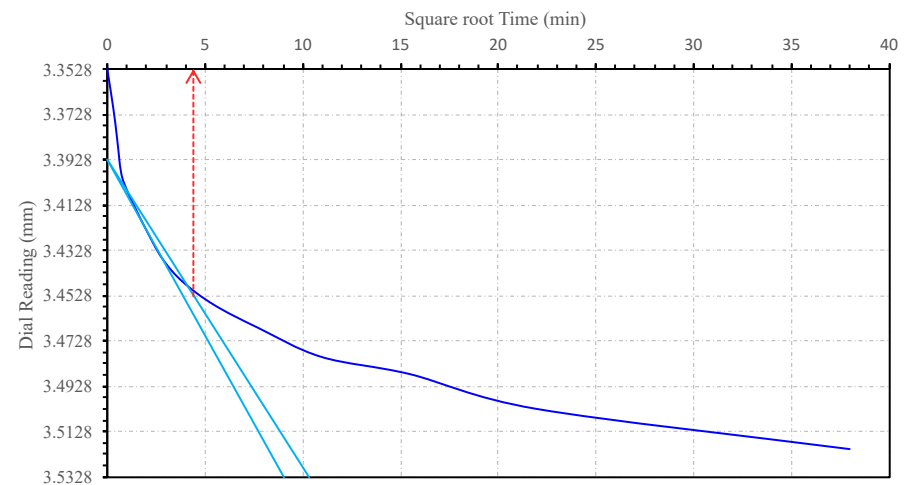


(h)

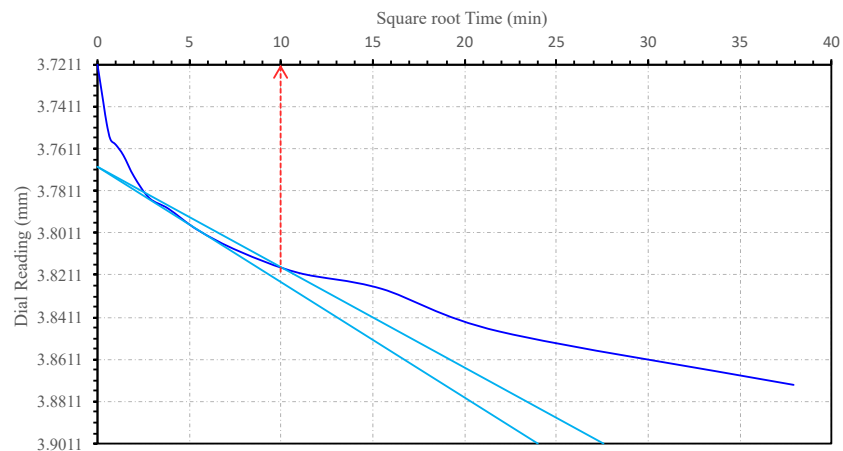
Chapter A. Appendix



(i)

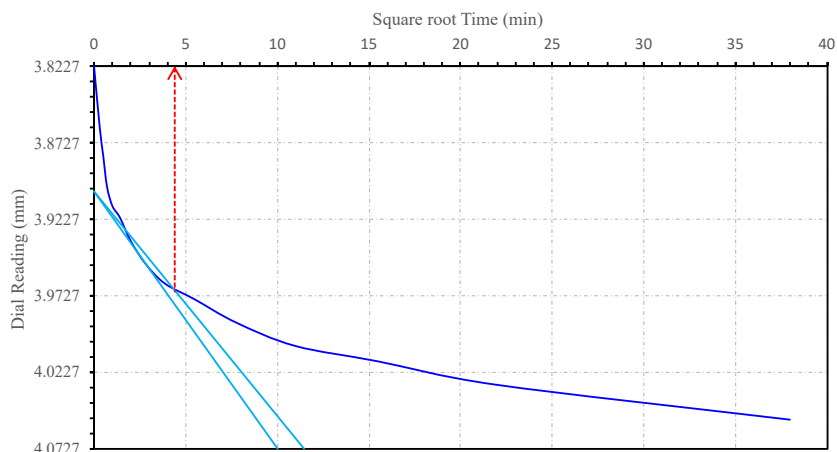


(j)

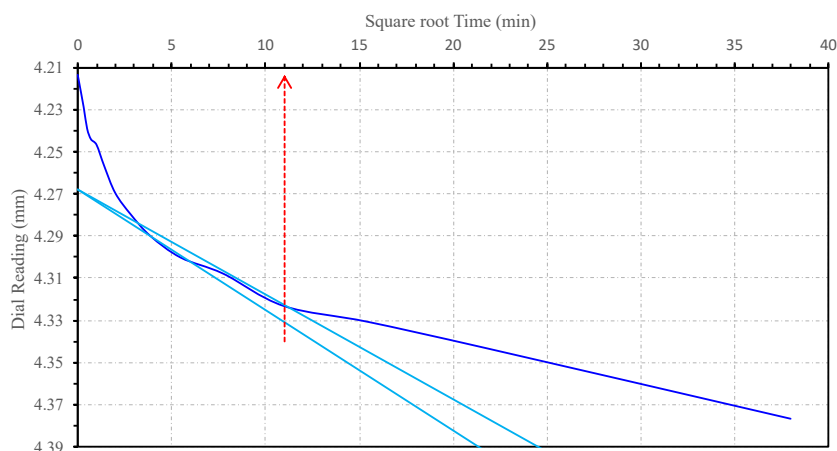


(k)

Chapter A. Appendix



(l)



(m)

Figure A.1: Square-root of time vs Dial reading plot for both HVDM treated and remoulded sample-a) 25 kPa HVDM Sample, (b) 25 kPa Remoulded Sample, (c) 50 kPa HVDM Sample, (d) 50 kPa Remoulded Sample, (e) 100 kPa HVDM Sample, (f) 100 kPa , (g) 200 kPa HVDM Sample, (h) 200 kPa Remoulded Sample, (i) 200 kPa Remoulded Sample, (j) 400 kPa HVDM Sample, (k) 400 kPa Remoulded Sample, (l) 800 kPa HVDM Sample, and (m) 800 kPa Remoulded Sample